

**Nanotechnology enabled
drug delivery
of proteins and peptides to the lung**

DISSERTATION

zur Erlangung des Grades des Doktors der Naturwissenschaften
der Naturwissenschaftlich-Technischen Fakultät III
Chemie, Pharmazie, Bio- und Werkstoffwissenschaften
der Universität des Saarlandes

von

Sarah Barthold

Saarbrücken

2016

Die vorliegende Arbeit wurde in der Zeit von Oktober 2012 bis September 2015
an der Universität des Saarlandes in Saarbrücken angefertigt.

Tag des Kolloquiums:	13. Juni 2016
Dekan:	Prof. Dr.-Ing. Dirk Bähre
Vorsitzender:	Prof. Dr. Gerhard Wenz
Berichterstatter:	Prof. Dr. Claus-Michael Lehr Jun.Prof. Dr. Thorsten Lehr
Akad. Mitarbeiter:	Dr. Stefan Böttcher

*Dass ich erkenne, was die Welt
Im Innersten zusammenhält.*

Johann Wolfgang von Goethe

This thesis was conducted as part of the project “Collaboration on the Optimization of Macromolecular Pharmaceutical Access to Cellular Targets (COMPACT)”, financially supported by the Innovative Medicines Initiative (IMI) Joint Undertaking under grant agreement n°115363.

Für Oma und Opa

TABLE OF CONTENTS

Summary	1
Kurzzusammenfassung.....	2
1. State of the Art	3
1.1 Proteins and peptides as active pharmaceutical ingredients	3
1.1.1 The structure of proteins and peptides	3
1.1.2 Protein and peptide therapeutics.....	4
1.1.3 Needs in protein delivery	6
1.2 Nanoparticles for medical applications	7
1.2.1 A pharmaceutical perspective on nanotechnology	7
1.2.2 Advantages of nanoparticles and their market situation	9
1.2.3 Route of administration	12
1.3 The pulmonary route of administration	13
1.3.1 The human lung and its clearance mechanisms	13
1.3.2 Particle design	16
2. Aim of the work	18
3. Starch derivatives as excipients for nanotechnology enabled pulmonary drug delivery systems: polymer characterization, improvement of synthesis and purification.....	20
3.1 Introduction	21
3.2 Materials and Methods	22
3.2.1 Materials.....	22
3.2.2 Starch oxidation – synthesis of negatively charged starch.....	22
3.2.3 Coupling of ethylenediamine with DCC/HOBt	23
3.2.4 Coupling of ethylenediamine with DMTMM	23
3.2.5 Synthesis of fluorescently labeled positively charged starch.....	24
3.2.6 Characterization of synthesized starch derivatives	25

3.3 Results and Discussion	25
3.3.1 Oxidation of potato starch	25
3.3.2 Conjugation of ethylenediamine with DCC/HOBt	26
3.3.3 Conjugation of ethylenediamine with DMTMM	28
3.3.4 Characterization of starch derivatives	28
3.3.5 α -starch derivatives, used for nanoparticle preparation	32
3.4 Conclusion	33
4. Starch vs. chitosan nanoparticles – preparation and physicochemical characterization ...	35
4.1 Introduction	36
4.2 Materials and Methods	37
4.2.1 Materials	37
4.2.2 Preparation and loading of chitosan nanoparticles	37
4.2.3 Preparation and loading of starch nanoparticles.....	38
4.2.4 Characterization of nanoparticles	39
4.3 Results and Discussion	40
4.3.1 Preparation of chitosan nanoparticles.....	40
4.3.2 Characterization of chitosan nanoparticles.....	45
4.3.3 Preparation of starch nanoparticles	52
4.3.4 Preparation of labeled starch nanoparticles	54
4.3.5 Characterization of starch nanoparticles	54
4.4 Comparison of chitosan and starch nanoparticles	62
4.5 Conclusion	63
5. Aerosol delivery of nanoparticles to the deep lung – nanoparticles embedded in microparticles	64
5.1 Introduction	65
5.2 Materials and Methods	66
5.2.1 Materials	66
5.2.2 Preparation of microparticles	67

5.2.3 Nanoparticle release from microparticles.....	67
5.2.4 Morphology	68
5.2.5 Particle size distribution	68
5.2.6 Powder crystallinity.....	68
5.2.7 Localization of nanoparticles in microparticles	69
5.2.8 Aerodynamic properties	69
5.2.9 PADD OCC deposition	70
5.3 Results and Discussion	70
5.3.1 Preparation of microparticles	70
5.3.2 Release of nanoparticles from microparticles	73
5.3.3 Morphology	75
5.3.4 Particle size and particle size distribution	77
5.3.5 Powder crystallinity.....	79
5.3.6 Localization of nanoparticles in microparticles	80
5.3.7 Aerodynamic properties	82
5.3.8 PADD OCC deposition	83
5.4 Conclusion	86
6. <i>In vitro</i> biopharmaceutical evaluation of the novel carriers.....	88
6.1 Introduction	89
6.2 Materials and Methods	90
6.2.1 Materials.....	90
6.2.2 Cell culture	91
6.2.3 Cell viability	91
6.2.4 Immunogenicity	92
6.2.5 EndoLISA.....	93
6.2.6 Uptake studies	93
6.3 Results and Discussion	94
6.3.1 Cytotoxicity screening.....	94

6.3.2 Immunogenicity screening	100
6.3.3 EndoLISA.....	105
6.3.4 Uptake studies	106
6.4 Conclusion	110
7. Summary and outlook	112
8. List of abbreviations.....	114
9. Bibliography.....	117
Scientific Output	127
Curriculum Vitae.....	130
Acknowledgments	132

SUMMARY

In addition to the so-called *small molecule drugs*, proteins and peptides are of increasing interest for pharmacotherapy, due to several advantageous properties. In general, those compounds are administered parenterally. However, non-invasive routes of administration represent a great part of research. Amongst others is the pulmonary application of proteins and peptides for local delivery in the case of pulmonary diseases, such as idiopathic pulmonary fibrosis, where the alveolar epithelium is affected.

To ensure an intracellular delivery, nanoparticles in a size range of 150 nm were prepared *via* charge-mediated coacervation, characterized for their physicochemical properties and loaded with several model-proteins and -peptides. The material used for nanoparticle preparation was chosen to be positively and negatively charged starch derivatives, which were synthesized from potato starch.

Although nanoparticles in that size range are known to show an increased cell uptake, they do not show a high deposition in the deep lung. Thus, an advanced carrier system consisting of a fast dissolving microparticle matrix with embedded starch nanoparticles was developed and characterized. Due to its aerodynamic properties, that carrier system was able to deposit a high fraction of the applied dose in the deep lung (~50%), while at the same time demonstrating (in *in vitro* models) the ability to facilitate uptake of starch nanoparticles into cells of the alveolar epithelium after fast dissolution of the microparticle matrix.

KURZZUSAMMENFASSUNG

Aufgrund zahlreicher Vorteile, stellen Proteine und Peptide eine vielversprechende Erweiterung der Pharmakotherapie dar, weg von sogenannten *small molecule drugs*. Die nicht-invasive Applikation solcher Wirkstoffe steht heutzutage im Fokus der Forschung. Unter anderem zählt hierzu die pulmonale Applikation von Proteinen und Peptiden für die lokale Gabe bei bestimmten Lungenerkrankungen wie z.B. der idiopathischen pulmonalen Fibrose, bei der vor allem das Alveolarepithel betroffen ist.

Um ein intrazelluläres Delivery zu gewährleisten wurden Nanopartikel durch ladungsvermittelte Koazervation im wässrigen Medium mit einem Größenbereich um die 150 nm hergestellt und charakterisiert. Im Anschluss wurden die Nanopartikel mit verschiedenen Modell-Proteinen und -Peptiden beladen. Das Material für die Nanopartikel bestand dabei aus negativ und positiv geladenen Stärkederivaten, welche aus Kartoffelstärke synthetisiert wurden.

Da Nanopartikel in diesem Größenbereich zwar eine Aufnahme in die Zelle erleichtern, allerdings keine hohe Depositionsrate in der tiefen Lunge erreichen, wurde im Rahmen dieser Arbeit ein spezielles Drug Delivery System, bestehend aus einer sich schnell auflösenden Mikropartikel Matrix mit eingebetteten Nanopartikeln, entwickelt und charakterisiert. Durch seine aerodynamischen Eigenschaften ist das Drug Delivery System fähig einen Großteil der applizierten Dosis in der tiefen Lunge zu deponieren (~50%), als auch, nach der schnellen Auflösung der Mikropartikel Matrix, die Aufnahme der Nanopartikel in das Lungenepithel (*in vitro*) zu gewährleisten.

1. STATE OF THE ART

1.1 PROTEINS AND PEPTIDES AS ACTIVE PHARMACEUTICAL INGREDIENTS

Historically speaking, active pharmaceutical ingredients (APIs) such as acetylsalicylic acid or paracetamol have been commonly characterized by a small molecular weight. However, modern drug discovery approaches most often lead to drugs with a hydrophobic character and a high molecular weight, resulting in poor water solubility and low permeability over epithelial barriers, respectively.^{1, 2} In recent times, the use of so-called biopharmaceuticals, including nucleic acid- and protein- based APIs with complex chemical structures have begun to find favor in therapeutic settings; such entities have shown faster and higher success rates in phase two and three clinical trials compared to conventional APIs.^{3, 4} This is especially important for pharmaceutical industry with clinical trials being the most expensive part of development.

Due to the fact that this thesis is about drug delivery systems (DDS) for protein and peptide delivery, the focus of this chapter lies on protein- and peptide-based APIs. Nucleic acid based APIs will not be explained, so the reader is referred to several literature reviews about this topic.⁵⁻⁸

1.1.1 THE STRUCTURE OF PROTEINS AND PEPTIDES

Proteins and peptides are biomacromolecules consisting of amino acid residues. The main difference between proteins and peptides is their size, represented by different numbers of constituent amino acids. While peptides in general consist of a linear chain of 20-30 amino acid monomers (primary structure), proteins generally have more than 100 residues, also showing different protein folding and resulting higher levels of structure (secondary, tertiary, quaternary structure), as can be seen in Figure 1.1.

Proteins and peptides in the human body are mainly composed of 22 different amino acids. Amino acids consist of an amine group (-NH₂) and a carboxyl group (-COOH) that are both linked to a carbon atom which is also bound to a hydrogen atom and a variable moiety. The primary structure is constructed of so-called peptide bonds between the carboxyl group of one amino acid and the amine group of another.⁹ The secondary structure is mainly formed by two motifs: the α -helix and the β -sheet. Additionally, random coils with no clear spatial arrangements occur (displayed as turquoise strands in Figure 1.1). For the formation of a tertiary or quaternary structure, several peptide chains building multiple subunits are combined to form the final protein, *e.g.* in enzymes. The process of folding is highly complex

and cannot be done easily by chemical synthesis. As a result, biotechnology-based methods are often used as manufacturing tools.⁹

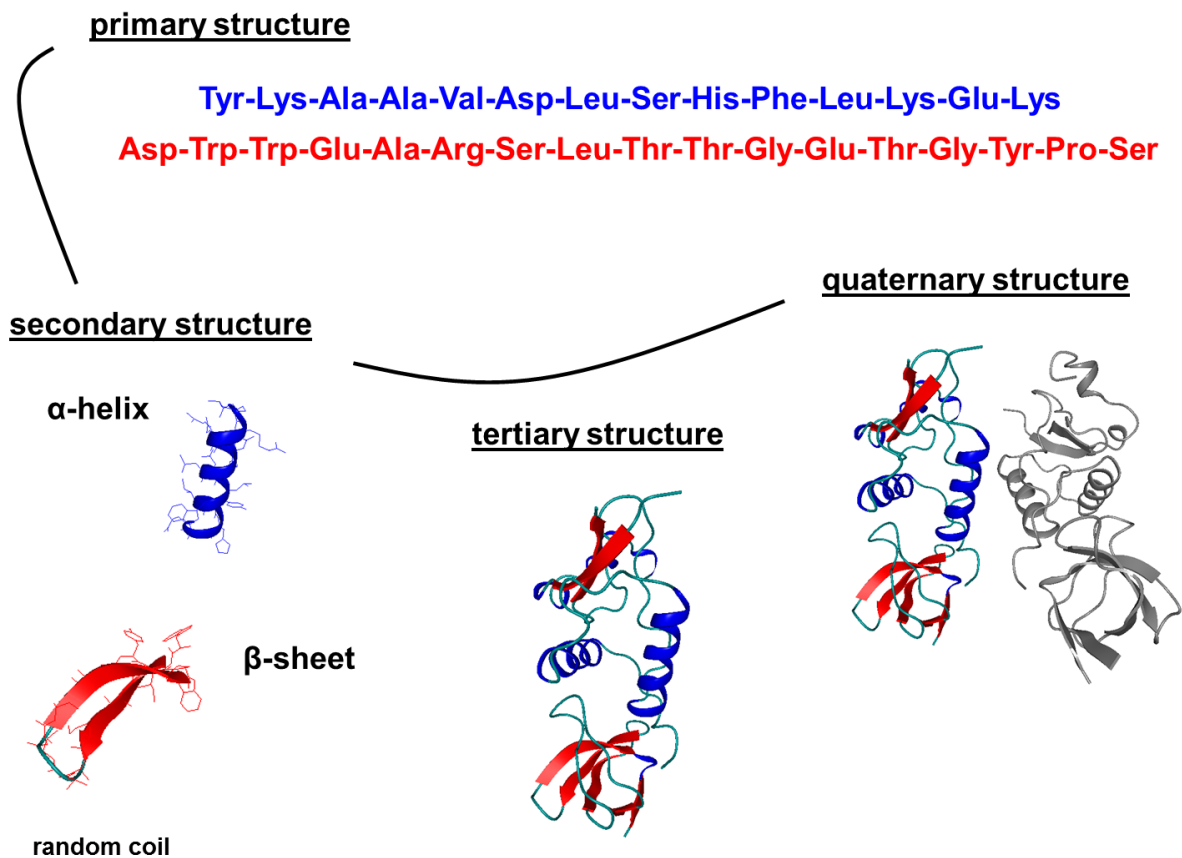


Figure 1.1: Different protein folding, shown by the example of the HIV-1 NEF protein, a non-receptor tyrosine-protein kinase that plays a role in many biological processes.

Unlike proteins, peptides mostly only possess a primary structure. Due to disulfide bond formation, they sometimes express a secondary structure,⁹ as known from vasopressin (antidiuretic hormone) or insulin.

1.1.2 PROTEIN AND PEPTIDE THERAPEUTICS

Proteins fulfil various functions in the human body, ranging from stabilizing tissues and organs (*e.g.* collagens), to transport, storage of molecules, mediation of receptors, and catalysis of metabolic reactions (enzymes). As a result, they often exhibit post-translational modifications, such as phosphorylation, acetylation or glycosylation, which activates the protein and allow it to carry out its specific function. In contrast, most peptides work as signaling agents and are classified as hormones.⁹

In many cases, diseases are the result of missing or malfunctioning proteins. The idea of protein- or peptide-based APIs is often therefore to replace these compounds. Currently, proteins and peptides represent a large fraction of compounds in drug development pipelines, due to their predictable activity profiles and their highly selective mode of action. Additionally, several formulations incorporating protein or peptide APIs are already on the market, as illustrated in the following.

Insulin is the oldest example of a peptide-based API, used for the treatment of diabetes mellitus type 1 - a metabolic disorder resulting from an absolute insulin deficiency, caused by either defects in insulin action, secretion, or both. Before the discovery of insulin by Banting and Best in the 1920s, this disease in its most severe form often led to death.¹⁰ Today, insulin is usually administered *via* subcutaneous injection. Different modifications of the molecule, resulting in long-acting and short-acting insulin derivatives, allow for mimicry of the physiological secretion of insulin by the pancreas.¹⁰

The small peptide-derivative leuporelin is a luteinizing hormone-releasing hormone (LH-RH) agonist which was first synthesized by Takeda Chemical Industries in 1974,¹¹ being 80 times more potent than natural LH-RH.¹² It is used today in the treatment of *e.g.* advanced and metastatic prostate cancer - as part of androgen deprivation therapy (ADT), acting to suppress testicular steroidogenesis - when administered continuously. This first formulation, which was associated with the need for frequent dosing *via* subcutaneous or intramuscular administration, was soon replaced by a depot formulation, allowing for dosing at one-month intervals. Further developments, using various DDS allow for application at a three-monthly or even six-monthly (Eligard® 45mg; Atrix Laboratories) intervals.¹³ ADT in general and the advanced depot leuporelin medication in particular, replaced orchiectomy, an irreversible surgical castration, which was one of the rare and unpleasant treatment options in the 1940s.

With the progress in biotechnology, the use of monoclonal antibodies for the treatment of various inflammatory diseases has seen a rapid increase in popularity. One example is adalimumab (Humira®), a recombinant fully humanized monoclonal antibody, used for the treatment of moderately to severely active rheumatoid arthritis (an immune-mediated, chronic inflammatory disease characterized by chronic synovitis). Adalimumab binds specifically to the pro-inflammatory cytokine TNF- α , neutralizing cytokine activity. It can either be used as monotherapy or in combination with so-called disease-modifying anti-rheumatic drugs (DMARDs) such as methotrexate.¹⁴

It can therefore be seen that in a wide range of diseases with diabetes, cancer and inflammatory diseases representing just a few examples - proteins and peptides are

successfully used as API. The use of proteins and peptides in such contexts may act to provide a treatment where none was available before, or to further improve the outcome of existing therapy options, considered inefficient from a modern perspective. However, the delivery of proteins and peptides is a complicated task, as discussed further below.

1.1.3 NEEDS IN PROTEIN DELIVERY

Parenteral application is the typical route to deliver proteins and peptides and is the least expensive and quickest strategy for commercialization, however owing to their complex structure, proteins and peptides are susceptible to degradation. Degradation results in protein unfolding and thus a loss of function,¹⁵ which may also be accompanied by an unwanted immune response *in vivo*. The maintenance of the spatial structure of proteins is therefore of great importance. For peptides, besides their short half-life, the most important property to either maintain or enhance is their ability to gain intracellular access, as they often have their target inside the cell. One strategy employed to overcome stability or pharmacokinetic issues associated with proteins or peptides is to chemically modify the molecular structure, as known for example from the use of protein analogs¹⁵ or *via* acylation¹⁶⁻¹⁸ or PEGylation.^{19, 20} However, care must be taken during modification not to reduce efficacy or to cause immunogenicity. As an alternative to changing the chemical structure, the use of DDS based on micro- or nanoparticles could be applied for protein and peptide delivery. Here, the protein can be used in its original form, and will be protected during storage and delivery by the DDS. The application of nanotechnology in the form of DDS ('nanotechnology enabled DDS') could even enhance protein uptake into or permeation over epithelial barriers, allowing for non-invasive administration and avoiding the requirement for injection. Nevertheless, as high salt concentrations, heat, shear stress or extreme pH values during preparation might be detrimental to the protein/ peptide structure, mild manufacturing processes have to be chosen, that do not degrade the protein or peptide during DDS preparation and loading.

In summary, the successful formulation of proteins and peptides requires a thorough understanding of the physicochemical and biological properties of the protein-/peptide-based API. This includes knowledge of physical and chemical stability, as well as of the characteristic pharmacokinetic profile.

1.2 NANOPARTICLES FOR MEDICAL APPLICATIONS

The following section gives an overview on the topic of nanotechnology, as background to further discussion on nanotechnology enabled DDS.

1.2.1 A PHARMACEUTICAL PERSPECTIVE ON NANOTECHNOLOGY

Although the concept of *nanotechnology* was defined by Taniguchi in the 1970s, a universally agreed upon interpretation of this term is still unavailable. Typically, a material can be considered as ‘nano’ if it exists in a size range of 1 nm to 100 nm, with special physical and chemical properties or biological effects that differ from its larger-scale counterpart. In the field of pharmacy the definition is even broader, including particles up to 1000 nm in size.

A broad range of industrial sectors apply nanotechnology and nanoparticles: From food agriculture²¹ to electronics,^{22, 23} renewable energy,^{24, 25} and health care²⁶⁻²⁹ to just mention a few.

However, there is also a public fear of nanotechnology, with toxicity arising from materials in the nano-size range being an important concern to be addressed.³⁰ Worst case scenarios from *e.g.* studies on combustion particles and their effect on the environment or human health are indeed important for risk assessment but should never be extrapolated to nanoparticles with a deliberate use in humans as for the field of nanomedicine. Here, nanotechnology is applied for medical purposes in order to produce the safest possible product, manufactured from high quality raw materials by the best manufacturing processes, and regulated by a quality control of the highest standards. The European Technology Platform on NanoMedicine has defined nanomedicine as: “The application of nanotechnology in health care, exploiting the improved and often novel physical, chemical, and biological properties of materials at the nanometric scale”.³¹ Figure 1.2 demonstrates the specific position of nanomedicine within the broad field of nanoparticles and illustrates the diversity of such nanoparticles.

In general, there are two main groups of nanoparticles used for medicinal applications. The first group basically consists of plain nano-sized API particles, so-called nanocrystals. The second group is based on DDS. Here, the API is incorporated into a carrier matrix of excipient(s), usually made up of polymers or lipids. The latter can vary considerably – from simple structures, to highly complex systems, such as core-shell and also multilayer structures. In the following, when the term *nanoparticle* is used, it refers to these kind of nanoparticles used within the field of nanomedicine.

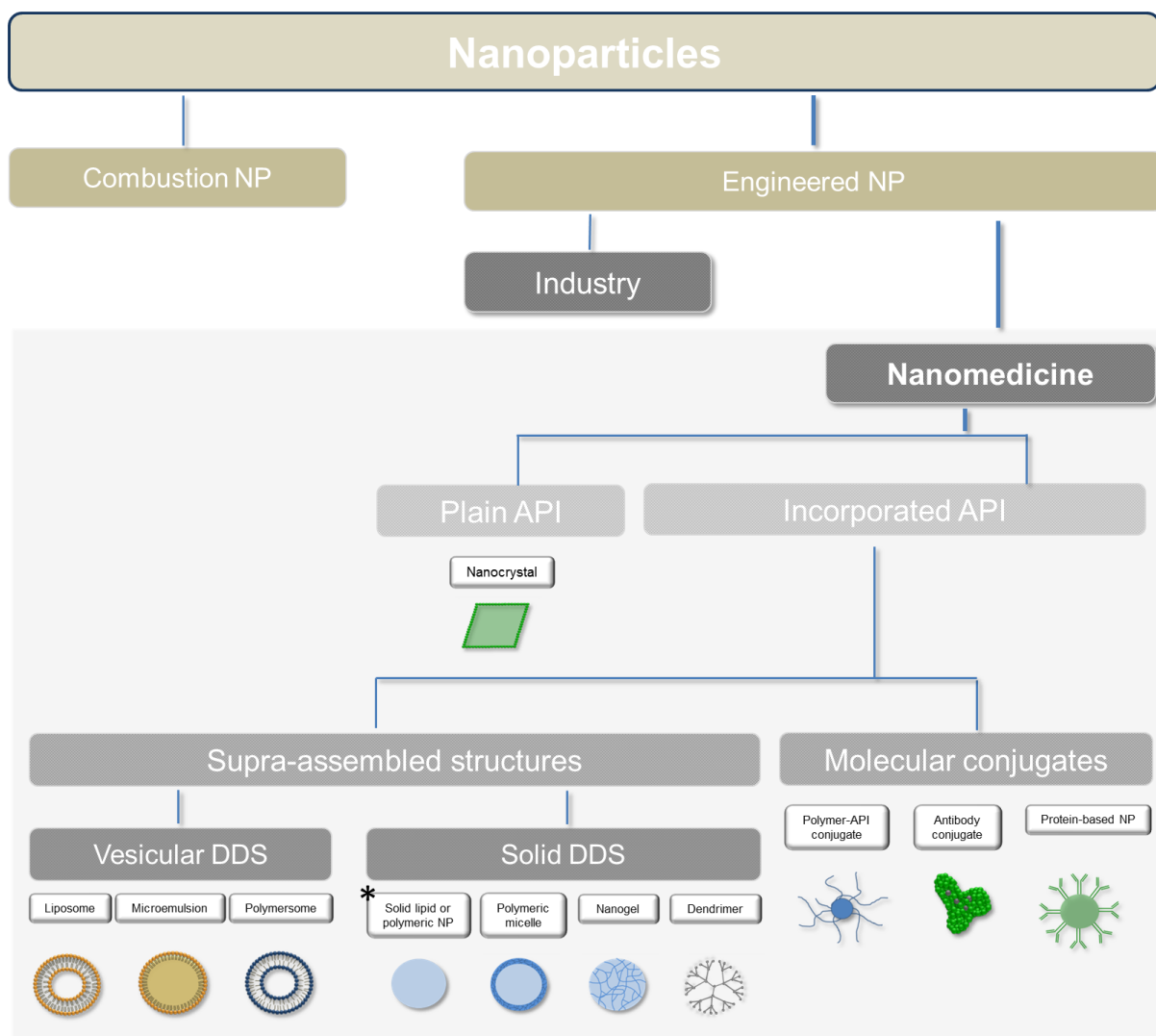


Figure 1.2: Overview of nanoparticles with different origins and with a focus on nanomedicine. NP: nanoparticle; API: active pharmaceutical ingredient; DDS: drug delivery system. NP type used in this thesis (*); modified with permission from Barthold *et al.*³²

As safety is a huge issue, the material chosen for nanoparticle preparation generally must have pharmaceutical acceptance, meaning that it is of high purity, and is biocompatible and biodegradable (if necessary). Such properties provide a good starting point for evaluating the safety profile of the final formulation. Materials which fulfil these criteria generally have GRAS (Generally Recognized As Safe) status, if not already used as excipients in FDA- (US Food and Drug Administration) or EMA- (European Medicines Agency) approved products. Materials with a high toxicity are not considered for nanoparticle preparation. One approach that may help in the evaluation of safety of future nano-products was introduced by Lehr and Groß.³³ Here, the intrinsic toxicity of the nano-product compounds is evaluated as a first parameter, followed by consideration of their solubility and biodegradability as second parameter. According to those parameters, a product can be classified into classes from I to

IV, with class I representing non-toxic bulk materials with high solubility/ biodegradability. By comparison, class II also represents non-toxic bulk materials, but with low solubility/ biodegradability. A product that belongs to class III or IV shows a toxic behavior in its bulk form being highly soluble/ biodegradable (III) or not (IV). For class I materials, additional safety testing could be set aside, whereas additional testing might be advisable for class II and class III products. Class IV products, however, require exhaustive safety testing.

An earlier system for the risk assessment of final nanoparticle formulation was proposed by Keck *et al.* in 2013.³⁴ The Nanotoxicology Classification System (NCS) is designed to categorize formulations based firstly on size and biodegradability, and secondly on biocompatibility. Again, there are four categories of increasing risk. Particles above 100 nm in size that are biodegradable are in class I, whereas particles which are not biodegradable belong to class II. Class III and IV deal with particles below 100 nm. To differentiate here, class III particles are again biodegradable, whereas particles in class IV are not. While the NCS considers characteristics such as formulation size and biodegradability, the initial toxicity of material is not considered – here therefore, the further developed system of Lehr and Groß may find application as a complementary tool.

1.2.2 ADVANTAGES OF NANOPARTICLES AND THEIR MARKET SITUATION

The first nanoparticles for pharmaceutical applications, at that stage called *nanoparts*, were synthesized by Birrenbach and Speiser in the 1970s.³⁵ However, materials and preparation as well as analytical techniques used at that time, had to be optimized or even newly developed to suit the high demands of a pharmaceutical application. Nevertheless, from the 1990s onwards, various nanoparticulate formulations have been approved by the FDA or the EMA and are currently on the market.^{36, 37} In the following section a number of selected examples will be discussed; further information about nanoparticle formulations on the market can be found in literature.³⁶

APIs are not always ideal drug candidates showing a high solubility and permeability, and an excellent safety profile. Using nanoparticles for drug delivery may therefore improve the performance of non-ideal APIs in several ways.³⁶ Most modern drugs in fact show low water solubility. Nanoparticles show increased dissolution kinetics, which can lead to higher bioavailability of the API.³⁸ The issue of poor API solubility has mainly been overcome by using Nanocrystal® technology, where the size of API particles is reduced *via* wet-milling into the nano-size range, leading to improved water solubility of the product and hence bioavailability.³⁹⁻⁴¹ The first marketed drug, developed with the Nanocrystal® technology was

Sirolimus (Rapamune®) in 1999.^{40, 42} Sirolimus, a potent immunosuppressive agent used for the prevention of graft rejection in organ transplantation is highly hydrophobic, shows low water solubility, and hence has a low bioavailability. However, an orally administered nanoparticle formulation, based on the Nanocrystal® technology, shows fast dissolution kinetics and an improved bioavailability.

Another issue that can be addressed by using nanoparticles is the possibility of tuning release kinetics of an API *via* encapsulation into a carrier matrix (a DDS).³⁷ A prolonged release of drug over a certain period of time can be achieved, meaning a reduction in dose frequency. A further benefit could lie in reduced side effects, which are dose dependent, as has been shown by Bawa:³⁷ adverse effect, seen for traditional formulations, can be reduced by adjusting the release kinetics *via* tunable sizes and surfaces of nanoparticles, as has been seen for the liposomal formulation of AmBisome®,⁴³⁻⁴⁵ which was approved by the FDA in 1997. A bottleneck preventing widespread use of the drug amphotericin B is its toxicity which further compromises its fungicidal activity. However, the encapsulation into liposomes lowers the toxic effects and improves drug therapeutic efficacy.⁴³⁻⁴⁵

The importance of DDS is also derived from their targeting potential and ability to overcome biological barriers. Some DDS for example are able to cross the blood-brain-barrier,^{46, 47} although practically all macromolecules and most of the small-molecule drugs are not able to cross. An indirect targeting mechanisms of nanoparticles has also been described by Maeda and Matsumara:⁴⁸ a higher endothelial fenestration and architectural anarchy compared to healthy tissue has been found for tumor capillaries, making a passive tumor-targeting of nanoparticles possible. This phenomenon has been called the EPR (enhanced permeation and retention) effect. Liposomes of up to 400 nm have been shown to be able to permeate tumor vessels.⁴⁹ Such observations have led to the conclusion that injected agents of the right size are able to accumulate in tumor tissue, if not previously recognized and cleared by the immune system. This point addresses another important aspect of surface characteristics of nanoparticles: nanoparticles with a hydrophilic surface (*e.g.* conferred *via* PEGylation) have a higher chance of escaping immune cell detections⁵⁰ allowing for circulation for a longer period of time in the bloodstream. An example for this delivery strategy is the marketed and previously mentioned formulation Doxil®/Caelyx®. Doxil/Caelyx®, is a formulation of the API doxorubicin, which is an intercalating agent used in cancer therapy. The formulation is based on PEGylated liposomes, also known as STEALTH® liposomes.⁵¹ STEALTH® liposomes are not recognized by the immune system, therefore showing a prolonged blood

circulation time.⁵² Further, the formulation has shown a decreased toxicity compared to free doxorubicin.⁵³

A similar effect based on passive targeting is called ELVIS, “Extravasation through Leaky Vasculature and the subsequent Inflammatory cell-mediated Sequestration”, introduced by Yuan *et al.* with respect to rheumatoid arthritis.⁵⁴ It can be suspected that such effects are also applicable in other inflammatory tissue, when several pathophysiological features such as vascular leakage and activated inflammatory cells are shared - indeed an accumulation of particles in inflamed areas of the intestinal epithelium has also been observed.^{55, 56} In contrast to passive targeting, active targeting *via* modification of the carrier’s surface with appropriate ligands binding to specific pathological sites in the body is also possible.

To summarize, nanoparticles offer several advantages including enhanced solubility of drug compounds, reduced side effects, and passive/active targeting possibilities. They can not only serve as delivery agents but also protect the drug from degradation and can furthermore control drug release and enhance permeation through cell membranes.⁵⁷

Although there are only a few formulations on the market yet, the impact of reformulated or novel nanoparticle-based formulations on medicine and health care is more than promising. It should be emphasized, however, that the bench to bed-side process is a long and slow one. Although liposomes have been widely studied since the 1960s, the first liposomal formulation only reached the market in the 1990s (AmBisome®). Solid nanoparticles were studied later, and are currently in clinical trials, but are still some way from reaching the market.⁵⁸ Obviously, nanoparticle-based formulations that are currently on the market are quite simple, compared to what nanoparticle-based DDS can offer (multicomponent systems). However, the full characterization that is required from FDA and EMA in the case of nanoparticles is still quite challenging. Nanoparticles do not yet count as well-established formulations (as do tablets, inhalables, creams, *etc.*), due to their special properties conferred by their nano-size. As mentioned, people are inherently concerned of nano-toxicity. It is of no help that there are no clear regulatory and safety guidelines directly related to nanoparticles for medicinal applications. Responsible institutions are thus very careful in selecting the right analytical tools for every formulation as repetition of the Contergan® scandal is absolutely not wanted. Contergan® was primarily prescribed as a sedative drug, however, after it became an over-the-counter API it was later also used against morning sickness in pregnant women. Shortly after, thousands of infants were born with phocomelia, severe malformations of the extremities. Unfortunately, at that time, pharmacovigilance was still in the early stages of development. Only after that scenario, people began to think carefully about the safety of medicines leading

to the development of more precise drug regulations and control over drug use and development. Therefore, successful nanoparticulate formulations should be based on a sound knowledge of the API (in the context of this project, the protein/peptide), the excipients, their biocompatibility, biodegradability and toxicity.⁵⁹ Further, consistent quality must be ensured by appropriate manufacturing processes and a sound characterization of the formulation.

1.2.3 ROUTE OF ADMINISTRATION

Biodistribution is guided by the application route, as are parameters including onset of action, efficacy and elimination. A first step in the development of a formulation for administration *via* a specific route is to decide whether local or systemic delivery is preferable. Usually local delivery is favored, although not always the easiest choice as the target can be hard to reach. So far, nanoparticles for medicinal use are administered parenterally, including *via* intravenous (*i.v.*) application. This route has the advantage of always demonstrating a 100% bioavailability as no absorption *via* an epithelial barrier is necessary. This route is most famously employed for cancer therapy, as nanoparticles are able to accumulate in tumor tissue due to their passive targeting (EPR effect). However, the drawbacks of this route of administration are the invasive character, the need of medical personnel for application and the assurance of sterility for the applied medicine, which makes production usually quite expensive.

By contrast, the most well-renowned non-invasive route of administration is the oral route. Production is cheap, and people are usually quite eager to swallow tablets/ capsules or liquids compared to receiving an injection. Unfortunately, there are drawbacks such as variations in pH, sometimes to extreme levels (*e.g.* in the stomach), the potential for variation in drug absorption depending on whether dosing is performed in a fed or fasted state (food effect), the mucus layer, which acts as a barrier to oral absorption, and the enzymatic environment. Often, sensitive drugs are destroyed in that environment and nanoparticles are often not able to cross the mucus barrier, meaning no or only low absorption into the circulation. Nanoparticles with special properties, however, are able to show some penetration.⁶⁰ Additionally, some therapeutically interesting formulations based on nanoparticles could be used for the treatment of inflammatory bowel disease (IBD)⁶¹ or for uptake *via* M-cells for vaccination.⁶²

Another non-invasive route of administration is the skin. As its purpose is to prevent unintentional permeation, delivery *via* the intact skin is not that easy. Microneedles for vaccination⁶³, however, or needle-free vaccination through the use of nanoparticles have been reported recently.⁶⁴

Furthermore, the lungs are an interesting target for drug delivery *via* nanoparticles, for both local and systemic delivery. This is discussed in more detail below.

1.3 THE PULMONARY ROUTE OF ADMINISTRATION

Diseases like Chronic Obstructive Pulmonary Disease (COPD), asthma, lung cancer, cystic fibrosis (CF), and also idiopathic pulmonary fibrosis (IPF) locally affect the lung. To achieve here a maximum effect with at the same time reducing side effects, a direct and local application to the lung is favored (*air-to-lung-delivery*). Moreover, pulmonary delivery to obtain a systemic effect is of increasing interest (*lung-to-blood-delivery*). A few drug candidates delivered *via* the lung have already been selected for clinical trials: dihydroergotamine as non-oral treatment of migraine⁶⁵ is one of them. As patients with migraine often suffer from nausea, a formulation for oral delivery is difficult; inhalation of the API is therefore preferred under this condition.

Regarding non-invasive delivery of proteins and peptides, the lung and especially the deep lung (also called alveolar region), consisting of a very thin layer of tissue for high efficiency gas exchange⁶⁶, is an important epithelial barrier. Due to a low level of resident degrading enzymes, drug delivery directly to the lung or *via* the lung into the circulation can occur without much enzymatic or metabolic loss (as is well-known to occur for example for the oral route of administration), making administration *via* this route very attractive. One famous example of a protein formulation pulmonary delivery is the inhalable insulin formulation called Afrezza[®] from Mannkind Inc., that was approved by the FDA in June 2014.⁶⁷

1.3.1 THE HUMAN LUNG AND ITS CLEARANCE MECHANISMS

With around 100 m² of surface area, the lung represents one of the biggest exchange interfaces of the human body with its surrounding environment.⁶⁸ The large surface area on the one hand enables efficient gas exchange (oxygen uptake *vs.* carbon dioxide excretion), but on the other hand also provides a gateway for microorganisms and particles contained within the inhaled air. Therefore, to protect this area, several barriers are prominent in the lung. The most prominent are the respiratory epithelia (cellular barrier), together with the mucus (conducting airways) and the pulmonary lining fluid (deep lung) as non-cellular barriers.⁶⁹ Both types of barriers vary along the respiratory tract in terms of structure and composition. The fate of an inhaled particle after deposition in the lung is illustrated in Figure 1.3.

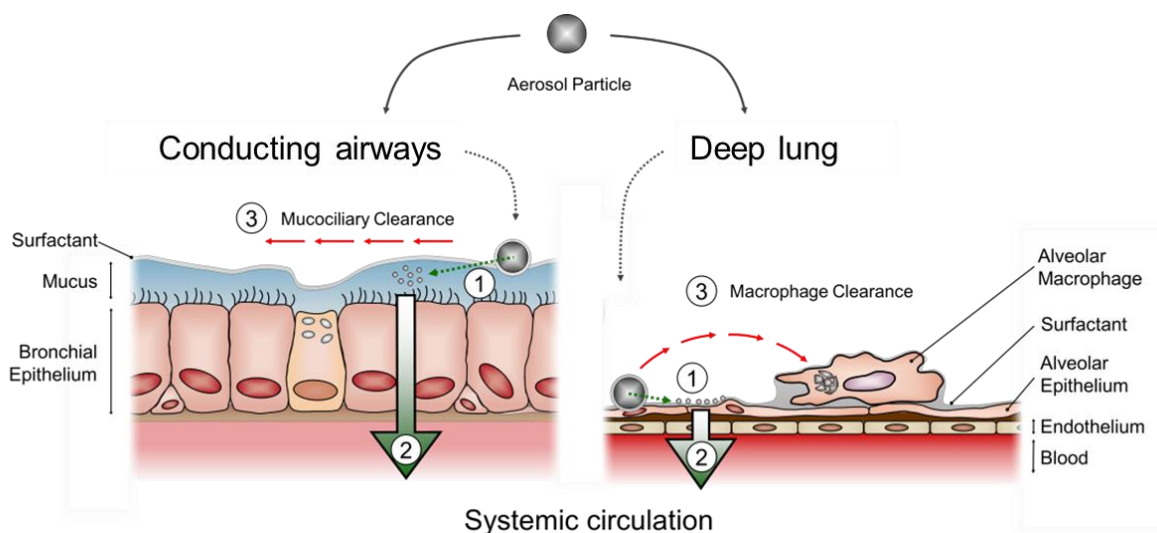


Figure 1.3: Fate of a particle after deposition in the lung; (1) first contact with the lung lining fluids; (2) uptake into / across the pulmonary epithelium; (3) clearance; modified with permission from Ruge *et al.*⁶⁹

Depending on the specific pulmonary location, different clearance mechanisms exist. In the conducting airways, the mucociliary clearance is most prominent, whereas in the deep lung it is macrophage clearance.⁷⁰ Mucociliary clearance has the ability to entrap particulates within the mucus and propel them out of the human lungs at rates between 3 and 25 mm/min.^{71, 72} This speed varies according to pulmonary condition⁷³ and airway caliber, but a maximum lung-residence time of about 6 h can be predicted.⁷⁴ In the deep lung, the clearance depends on the phagocytic stimuli elicited by deposited particulates, which in turn is a function of their shape, surface chemistry and size. Between 50 and 75% of inhaled particulates are cleared within 2-3 h after deposition, and nearly 100% are removed after 25 h.⁷⁰ The alveolar clearance rate, however, may be influenced by a number of pulmonary conditions. Thus, a time frame of up to 6 h could be estimated for non-biodegradable nanoparticles to deliver their cargo.

Conducting airways

The mucociliary clearance is an effective system to entrap and remove particulates contained in inhaled air. Cellular and non-cellular barrier elements again cooperate, to allow for operation of this system. A pseudo-stratified columnar epithelium is formed by ciliated, secretory and basal cells that build the bronchial airway epithelium.⁶⁶ The apical membranes of such cells are further joined by tight junctions, giving the epithelium its barrier properties.⁷⁵ The pulmonary mucus (pulmonary lining fluid of this particular region) on top of the epithelial cells is made of 90-95% water, mucins (glycoproteins), lipids, proteins, DNA and

cells.^{76, 77} It consists of two different layers:⁶⁶ the lower layer shows aqueous sol-like characteristics. It allows the cilia to beat and recover so that the thick viscous upper layer can be propelled towards the proximal airways in a continuous way. Subsequently, the mucus can be transferred to the digestive tract for further gastric metabolism and elimination.^{66, 78} The upper layer is a viscous gel layer containing mucins that form a complex mesh-like structure with a high capacity to entrap particulates.^{76, 77} These mucins are built of a polypeptide backbone, with high levels of O-glycosylated tandem repeats, leading to a negative charge at physiological pH.^{79, 80} There are five major mucins expressed in the respiratory tract: MUC1, MUC4 and MUC16 (cell-membrane tethered mucins), as well as MUC5AC and MUC5B (main gel-forming mucins), which are secreted by submucosal glands and goblet cells onto the luminal surface of the airways.^{81, 82} The latter two mucins are primarily responsible for the viscous mesh-like size structure of the pulmonary mucus.⁸³ The pore size of the mucus is highly heterogeneous and ranges between small pores of just 100 nm up to large voids of several μm in size.⁸⁴ Thus, water, ions and small molecules are able to diffuse through the mucin mesh, whereas larger particulates at some point are hindered due to steric interactions with the rigid walls. Additionally to the size filtering effect, electrostatic and hydrophobic filtering effects enable the immobilization and clearance of particulates, even smaller than the pore size of the mucus mesh. These effects are based on the interactions of negatively charged mucins⁸⁵ and hydrophobic regions located in the non-glycosylated regions of the mucins,⁷⁹ with particulates.

Deep lung

The alveolar region represents a major target of many inhaled therapeutic agents. Two epithelial cell types constitute the alveolar epithelium: due to their flattened shape (approximately 0.2 to 0.3 μm thick in the cell periphery⁷⁸), Alveolar Type I (AT-I) cells provide an exceptional platform for gas exchange and cover about 90% of the entire alveolar surface. Alveolar Type II (AT-II) cells are cuboidal in shape and are responsible for the synthesis and release of pulmonary surfactant (composed of a complex mixture of lipids and proteins that reduce the surface tension in the alveoli, preventing their collapse).^{86, 87} They further serve as progenitors for ATI cells and are important for cell renewal. Both cell types are able to form tight junctions^{88, 89} and represent a significant barrier, although nanoparticles smaller than 100 nm may efficiently cross the alveolar epithelium.⁹⁰ Endocytic pathways provide an opportunity for bigger particles to be internalized.⁹¹ Another cell type present in the deep lung are the macrophages, which patrol on top of the epithelium, having the ability to

engulf and degrade particles in a size range of 1-5 μm .⁸³ Nanoparticle uptake by alveolar macrophages (mediated by hydrophilic proteins contained in the pulmonary surfactant) has also been described, showing different absorption patterns depending on the nanoparticle coating.^{92, 93} When considering the prospect of delivery to the lung, it is important to keep in mind that these described aspects of barrier function and clearance must be preserved, as they are of the highest importance for maintaining human health. Thus, the aim is to design a system with the ability to avoid clearance and penetrate or pass barriers without significant interference with such clearance mechanisms and barrier integrity.

1.3.2 PARTICLE DESIGN

It can be seen that the biological barriers within the lung represent a challenge for pulmonary drug delivery. However, a better understanding and characterization of the pulmonary barriers in recent years has given the opportunity to enhance and improve drug delivery to the lung.⁹⁴ Nanotechnology enabled DDS in particular have the potential to improve pulmonary drug delivery. This can be achieved through the ability to rationally design nanoparticles with optimal surface chemistry, size and shape for overcoming those barriers.

Designing mucus penetrating particles, which are able to escape the mucus entrapment by means of a hydrophilic polymer coating (PEGylation) which results in particles with a neutral or slightly negative charged surface,^{77, 95, 96} has helped in improving particle uptake in the lung. Gulturonate oligomers have been shown to alter the network architecture in mucin matrices, thus leading to an enhanced nanoparticle mobility in both native and highly purified mucus matrices.⁹⁷ These strategies could for example be most suitable for drug delivery to the lung in diseases with increased or pathologically thickened mucus.

In the alveolar region, the clearance of particles occurs mostly by way of alveolar macrophages.⁹⁸ Furthermore, it is known that the macrophage clearance is faster for microparticles than for nanoparticles.⁹⁹ Therefore, nanoparticles could be designed in different sizes that might help to avoid macrophage clearance.

Traditionally, the focus of pulmonary drug delivery has been on improving lung deposition of inhaled therapeutics. Thus, most of the factors influencing particle size during aerosol generation and subsequent drug inhalation have been well-described.^{77, 78} In this respect, a dramatic improvement of deposition can be achieved with most modern aerosol delivery devices.¹⁰⁰ The design of particles additionally plays an important role in such effective deposition – particles with a certain shape or in an acceptable size range for sufficient aerodynamic properties may enable deposition in the alveolar region. However, nanoparticles

in a pharmaceutically relevant size range of approximately 100-200 nm are not suitable for a high deposition in the deep lung.¹⁰¹ Thus, a carrier system with optimum aerodynamic properties (generally in the lower μm size range) is necessary to improve the delivery of nanoparticles to the alveolar region. Several investigations have been made in that context, in which the delivery of nanoparticles *via* dry powder carriers seems to be the most promising. One approach is to combine the high alveolar deposition of microparticles with the slower clearance by alveolar macrophages of nanoparticles. For example, Ely *et al.* used an active release mechanism of nanoparticles from carrier particles by an incorporated effervescent technology.¹⁰² Another concept is utilized by so-called large porous Trojan particles, introduced by Tsapis *et al.* Also here, nanoparticle-in-microparticle systems are formed and administered. Upon deposition, the microparticles quickly dissolve, releasing the incorporated nanoparticles again.¹⁰³

Although nanoparticles represent a great chance for improved pulmonary delivery (*e.g.* enhanced cell uptake, avoidance of macrophage clearance), they cannot be administered as such but need an advanced carrier system, necessary for high deposition in the deep lung.

2. AIM OF THE WORK

Biopharmaceuticals, such as proteins and peptides, currently represent a large fraction of compounds in drug development pipelines, due to their highly selective mode of action and predictable activity profiles. Nevertheless, a widespread application of potential protein therapeutics is restricted due to limitations in both drug disposition and pharmacokinetic properties. Their success, amongst other factors, will depend on formulation and delivery strategies that can address these limitations.

This thesis was part of a joint research program entitled COMPACT (Collaboration on the Optimization of Macromolecular Pharmaceutical Access to Cellular Targets), which is a European project funded by the Innovative Medicines Initiative (IMI) and the European Federation of Pharmaceutical Industries and Associations (efpia). COMPACT focuses on two major aims: first of all, the identification and characterization of transport pathways across biological barriers and across cell membranes (work packages (WPs) 4-7), and secondly the construction and characterization of DDS for proteins and peptides (WP 1) or nucleic acids (WP 2). Within the COMPACT consortium, the motivation of this thesis was the development and characterization of a nanotechnology enabled, novel and safe DDS for pulmonary protein and peptide delivery.

One of the most important points to be addressed in this respect is the excipient used for the DDS. The material should be biocompatible, biodegradable, and easily accessible. Furthermore, the material should be suitable for the nanoparticle preparation process. Charge-mediated coacervation in aqueous medium was chosen as the preparation procedure for nanoparticle formation. This process is mild, fast, straight-forward and easy to upscale, *e.g.* by using microfluidics. Further, no additional excipients, such as stabilizers, are necessary. As the alveolar epithelium seems to play a major role in diseases such as IPF, this site of action was chosen as target in this project. Due to the low deposition of NPs in the deep lung, the final pulmonary formulation should be based on a delivery system, consisting of microparticles with embedded nanoparticles, suitable for a high deposition in the alveolar region. The microparticle matrix should further be highly water soluble to ensure a fast release of the nanoparticles, which are then ready for cell uptake.

The major aims and corresponding work of this thesis can subsequently be divided into four sections:

Chapter 3 Starch derivatives as excipients for nanotechnology enabled pulmonary drug delivery systems: polymer characterization, improvement of synthesis and purification

Chapter 4 Starch vs. chitosan nanoparticles – preparation and physicochemical characterization

Chapter 5 Aerosol delivery of nanoparticles to the deep lung – nanoparticles embedded in microparticles

Chapter 6 *In vitro* biopharmaceutical evaluation of the novel carriers

3. STARCH DERIVATIVES AS EXCIPIENTS FOR NANOTECHNOLOGY ENABLED PULMONARY DRUG DELIVERY SYSTEMS: POLYMER CHARACTERIZATION, IMPROVEMENT OF SYNTHESIS AND PURIFICATION

The author of the thesis made the following contribution to this chapter:

Planned, designed and performed all experiments, analyzed all data from the mentioned studies, interpreted all experimental data and wrote the chapter, if not stated otherwise.

The XRPD studies were kindly performed by Dr. Robert Haberkorn at the Department of Inorganic Solid State Chemistry.

The synthesis of the two α -starch polymers, used for nanoparticle preparation, was kindly performed by Dr. Carolin Thiele.

3.1 INTRODUCTION

DDS (shown in Figure 1.2) are prepared from a wide range of different materials. The most common ones are polymers of synthetic or natural origin, with both types showing advantages and disadvantages.¹⁰⁴ The most studied synthetic polymers are polyesters, such as poly (ϵ -caprolactone) (PCL), poly (lactic acid) (PLA), poly (lactide-co-glycolide) (PLGA) and their derivatives.¹⁰⁵ PLGA is a well-known material. Being biocompatible, with GRAS status for some applications, and offering a controlled release of its cargo, it is an ideal material for DDS preparation. The delivery of proteins, however, requires special care and attention. The release of the cargo at the desired site of action is one point, but with particular respect to proteins and peptides the DDS should further be able to protect the complex structure from degradation during DDS preparation and loading, storage and on exposure to physiological conditions following application. In the latter context, PLGA is mainly degraded by hydrolysis *in vivo*, leading to acidic degradation products that could be detrimental to the encapsulated cargo.¹⁰⁶

The importance of new natural or semi-synthetic polymers as DDS components is increasing in line with the considerable current interest in material sustainability. Natural polymers, especially polysaccharides are among the most studied polymers as components of DDS for biopharmaceuticals.^{107, 108} Within this group, dextran-,¹⁰⁹⁻¹¹¹ alginate-,¹¹² and chitosan-based systems have all been well-explored.¹¹³⁻¹¹⁷ In addition, starch is an excellent bio-polymer for nanotechnology enabled DDS. It is a commonly employed excipient in pharmaceutical industry, used for example in tableting processes,¹¹⁸⁻¹²¹ as well as an excipient in novel DDS for nasal¹²² and other site-specific^{123, 124} applications. Regarding its toxicity, starch consists of linear amylose and branched amylopectin - both polysaccharides consisting of α -(D)-glucose units, which have been evaluated as safe and without the need for restrictions on daily intake.¹²⁵ Starch is further GRAS listed and included in the FDA Inactive Ingredients Database. Its excellent biocompatibility is further underlined by its biodegradability not only by hydrolysis, but also by α -amylase, an enzyme commonly present in the human body.

Additionally, the molecular structure of starch allows for different chemical derivatizations, due to the presence of a high amount of hydroxyl groups; this in turn leads to the possibility for numerous new applications. Santander-Ortega *et al.* previously prepared NPs from propyl starch for the dermal application of small molecule drugs.¹²⁶ However, as this starch derivative was not water soluble, ethyl acetate had to be used as a solvent for particle preparation. Further, the use of a high speed homogenizer makes the utilized preparation method challenging for the encapsulation of proteins. The synthesis of a water soluble,

negatively charged starch derivative for complex formation with cationic cyclodextrins as targeted cancer therapy was investigated by Thiele *et al.*¹²⁷ Another study, using positively charged, water soluble starch-derivatives for better pDNA transfection was carried out by Yamada *et al.*¹²⁸

The properties of the excipient for DDS preparation is of great importance in order to ensure a good quality of the used material as well as compatibility with a protein or peptide cargo. As charge-mediated coacervation in aqueous medium was the method of choice for NP preparation, the focus was set on water soluble starch derivatives. Thus, negatively and positively charged α -starch-derivatives that were used for nanoparticle preparation were characterized for their degree of substitution, purity, and their weight average molecular weight. Additionally, different syntheses were carried out to optimize both the synthesis procedure and purification method; the products of this optimization work were also characterized.

3.2 MATERIALS AND METHODS

3.2.1 MATERIALS

Potato starch, partially hydrolyzed with a molecular weight (Mw) of 1 300 000 g/mol and an amylose content of approximately 33% was a kind gift from AVEBE (Netherlands). (2,2,6,6-tetramethylpiperidin-1-yl)oxidanyl (TEMPO), N,N'-dicyclohexylcarbodiimide (DCC), 1-hydroxybenzotriazole (HOBt) and 4-(4,6-Dimethoxy-1,3,5-triazin-2-yl)-4-methylmorpholinium chloride (DMTMM) were obtained from Sigma Aldrich (USA). Ethylenediamine was purchased from Acros Organics (USA). All other reagents were of analytical grade.

3.2.2 STARCH OXIDATION – SYNTHESIS OF NEGATIVELY CHARGED STARCH

Potato starch was oxidized to produce a negatively charged starch derivative, in the following referred to as NegSt. Briefly, 20 g of dried potato starch was weighed into a 1 L glass beaker, suspended in 800 mL of purified water and heated at 95 °C for 1 h. After cooling down to room temperature (RT), the catalyst TEMPO was added to the suspension (4 mg/g potato starch). Adequate volumes of sodium hypochlorite solution (12%) were then added (1 mL/min). The pH was kept at 8.5 during the reaction by adding 1 M sodium hydroxide solution. Sodium borohydride (0.5 molar equivalents relative to sodium hypochlorite) was then slowly added to stop the reaction. The resulting solution was stirred overnight. After filtration the next day, the solution was extensively purified by ultrafiltration (Vivaflow 200;

5 kDa Hydrosart membrane, Sartorius Stedim Biotech GmbH, Germany) and lyophilized for two days (Alpha 2-4, Martin Christ GmbH, Germany) before storing at RT until usage.

3.2.3 COUPLING OF ETHYLENEDIAMINE WITH DCC/HOBT

To obtain the positively charged starch derivative (PosSt), NegSt was coupled with ethylenediamine. To achieve this, 13 g of the free acid form of NegSt, obtained by ion exchange, was first dissolved in 650 mL DMSO at 50 °C under a reflux condenser overnight, with stirring. The coupling agents DCC and HOBT (each 1.5 molar equivalents relative to the degree of oxidation of NegSt) were then added and stirred for 24 h. Afterwards, ethylenediamine was slowly added (10 molar equivalents relative to the degree of oxidation of NegSt) and the reaction was allowed to proceed for another 48 h (end product termed PosSt α) or 72 h (end product termed PosSt β). After filtration, the solution was either lyophilized, subsequently dissolved in 1% acetic acid (HOAc), extensively ultrafiltered (Vivaflow 200; 5 kDa Hydrosart membrane, Sartorius Stedim Biotech GmbH, Germany) and lyophilized for two days (PosSt α and PosSt β) or precipitated with ethanol (EtOH), washed and then lyophilized (PosSt γ and PosSt δ). PosSt was stored at RT until further use. An overview of the different materials and their synthesis specifications can be found in Table 3.1.

Table 3.1

Different PosSt derivatives and details of their synthesis. Coupling was performed with DCC/HOBT.

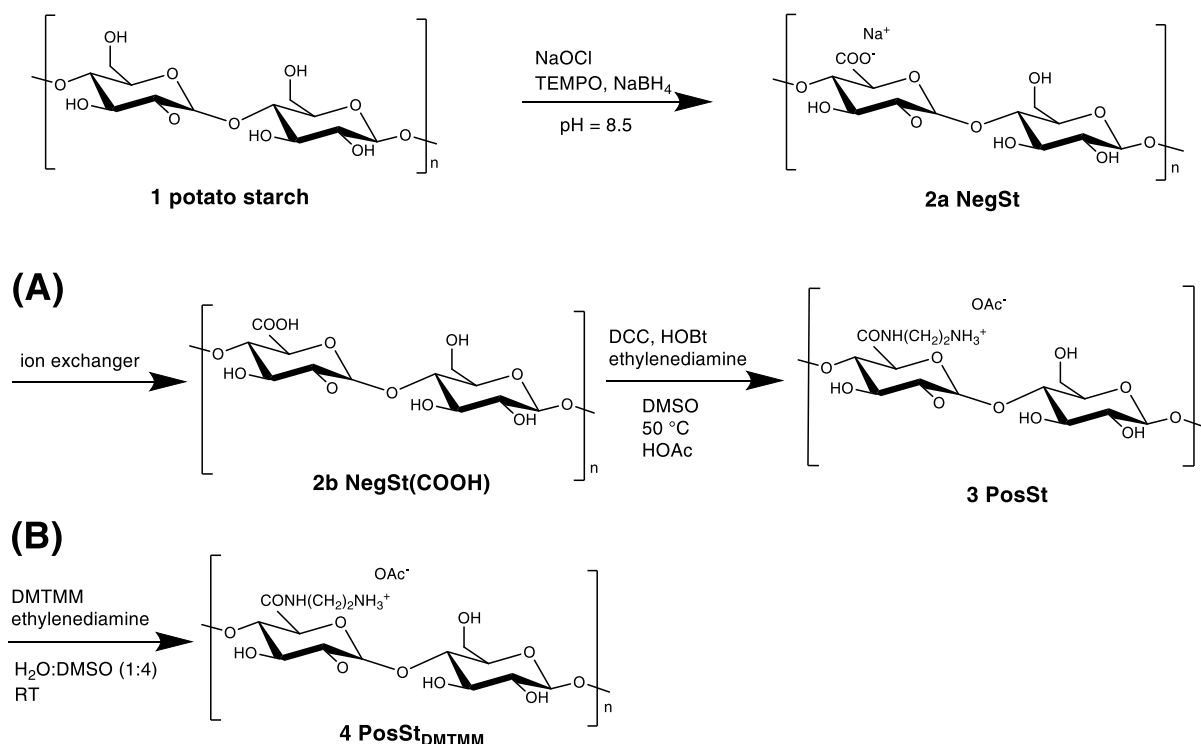
<i>PosSt</i>	<i>NegSt</i> [<i>D_{ox}</i>]	<i>Reaction time</i> [<i>h</i>]	<i>Method of purification</i>
α	36	48	ultrafiltration
β	52	72	ultrafiltration
γ	25	48	precipitation
δ	21	48	precipitation

3.2.4 COUPLING OF ETHYLENEDIAMINE WITH DMTMM

As a second coupling reaction, the coupling of ethylenediamine to NegSt *via* DMTMM was carried out, according to Kunishima *et al.*¹²⁹ Here, 250 mg of NegSt was first dissolved in 6.25 mL milliQ water. Afterwards, 18.75 mL of DMSO was added, to obtain a solvent mixture of 1:4 (water:DMSO). Further, 0.68 mmol DMTMM (conjugation reagent, adapted from Yamada *et al.*¹²⁸) was added under stirring and the resulting mixture was further stirred

for 30 min to activate the carboxylate groups. After 30 min, 10 equivalents of ethylenediamine relative to the degree of oxidation of NegSt were added and the reaction was allowed to proceed for another 72 h at RT. The mixture was then filtered and precipitated with EtOH. The resulting product, termed PosSt_{DMTMM} was then lyophilized for two days. PosSt_{DMTMM} was stored at RT until usage.

An overview of all syntheses can be found in Scheme 3.1.



Scheme 3.1: Synthesis of negatively charged starch (NegSt) and positively charged starch (PosSt); (A) coupling reaction with DCC/HOBt (PosSt); (B) coupling reaction with DMTMM (PosSt_{DMTMM}); potato starch is illustrated as amylose.

3.2.5 SYNTHESIS OF FLUORESCENTLY LABELED POSITIVELY CHARGED STARCH

For later characterization and cell interaction studies, PosSt was labeled with green Bodipy[®] FL-C5 NHS Ester. Briefly, 30 mg of polymer was dissolved in 5 mL purified water and diluted slowly with 5 mL of methanol. A 2 mL volume of Bodipy[®] FL-C5 NHS Ester solution in methanol (0.5 mg/mL) was then added slowly to obtain a molar ratio of 50:1 (starch:dye). The sample was stirred for 1 h at RT under light protection, and then precipitated with 1 M sodium hydroxide and ethanol. Washing was performed with ethanol:methanol (1:1) until the supernatant was fluorescence free. Labeled positively charged starch, referred to as PosSt_F, was then dissolved in purified water, freeze dried and stored in the fridge under light protection until usage.

3.2.6 CHARACTERIZATION OF SYNTHESIZED STARCH DERIVATIVES

The degree of oxidation of NegSt was determined with the Blumenkrantz assay, a colorimetric method based on detection of uronic acid content.¹³⁰ The degree of oxidation was calculated as follows:

$$\text{Degree of oxidation [\%]} = \frac{\frac{A}{\epsilon * d} * 1\,000\,000}{m(\text{NegSt}) \text{ in } 50\,\mu\text{L}} * 100$$

A: absorbance; ϵ : extinction coefficient (26700 [Lmol⁻¹cm⁻¹]); d: cuvette length (1 [cm]); m: mass [mg].

¹H-NMR spectra were collected at RT on a Bruker Biospin spectrometer NMR Magnet System 400 MHz Ultrashield plus (Bruker, USA) in D₂O (64 scans). Fourier transform infrared (FT-IR) measurements were carried out in solid state with a Spectrum 400 FT-IR/FT-NIR spectrometer (PerkinElmer, UK) between 700 and 3600 cm⁻¹. The weight average molecular weights of starch derivatives were analyzed by gel permeation chromatography (GPC, HLC-8320 GPC, Tosoh, Japan), equipped with online viscometer (ETA-2010, PSS, Germany) on SUPREMA 1000 and 30 columns (NegSt) or SUPREMA-MAX 1000 and 30 columns (for PosSt; PSS, Germany) at a flow rate of 1 mL/min at 35 °C in 1 M sodium nitrate (NegSt) or 1% formic acid (PosSt). The calibration was done with Pullulan and PVP standards, respectively.

For X-ray powder diffraction (XRPD), samples were analyzed by a diffractometer of the type Bruker D8 Advance, equipped with a 1D-detector 'Lynxeye' using variable divergence slit and Cu K α radiation.

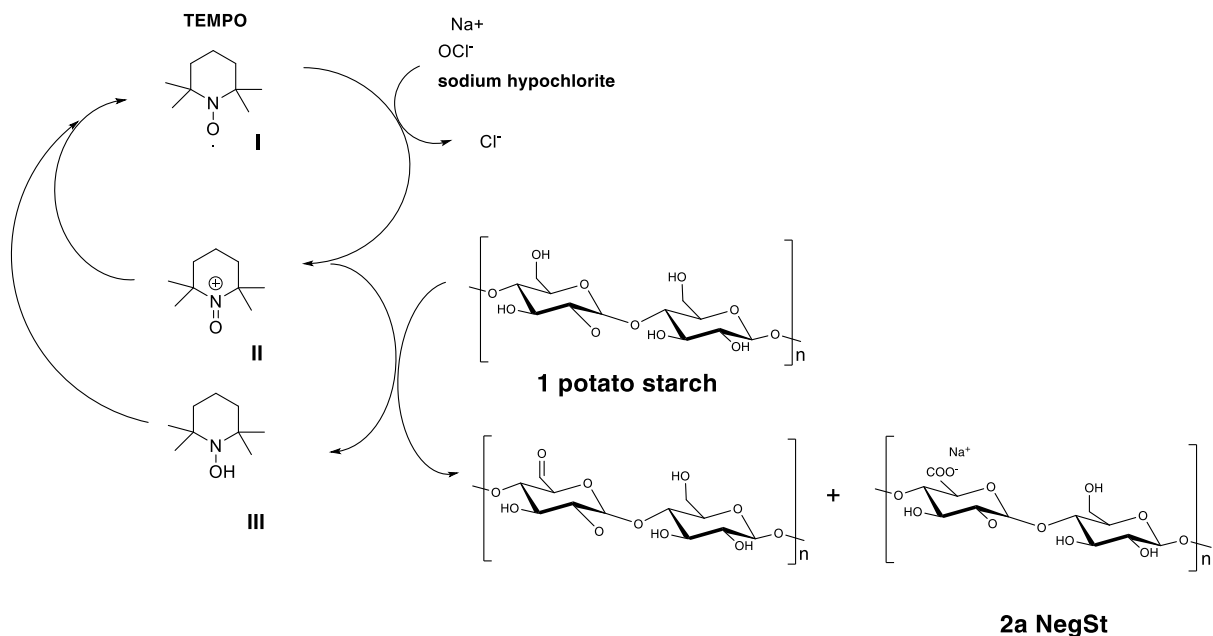
3.3 RESULTS AND DISCUSSION

3.3.1 OXIDATION OF POTATO STARCH

The raw material used for the oxidation was a partially hydrolyzed potato starch with an amylose content of approximately 33% and a molecular weight of 1 300 000 g/mol. For the synthesis, a TEMPO-mediated system was used, which enabled the selective C6-oxidation (primary hydroxyl group) of potato starch.¹³¹

TEMPO (I) is a stable radical, which is oxidized to the nitrosonium ion (II), the actual oxidizing species, under the influence of hypochlorite. During the oxidation process of potato starch, the hydroxyl group is oxidized *via* an aldehyde to the carboxylate, while the nitrosonium ion (II) is reduced to the hydroxylamine (III). The regeneration of the

nitrosonium takes place *in situ* with the help of the oxidant hypochlorite.¹³¹ Here, the hydroxylamine reacts with another nitrosonium ion to reform the stable TEMPO radical. This process is shown in Scheme 3.2.



Scheme 3.2: Mechanism of TEMPO-mediated oxidation of potato starch.

For the synthesis, a ratio of 4 mg of TEMPO per 1 g of starch was chosen, as a higher amount probably leads to the degradation of the polymer (as suggested by Thiele¹³²). For the oxidation of the hydroxyl group to the aldehyde, as well of the aldehyde to the carboxylate, 1 molar equivalent of hypochlorite is required. Different molar ratios of sodium hypochlorite were used (1.5, 1.25, 1, 0.75) to obtain a product with different degrees of oxidation.¹³² A degree of oxidation below 100% was expected, as some of the primary alcohol groups are necessary for formation of the α -1,6-glycosidic bond in amylopectin.

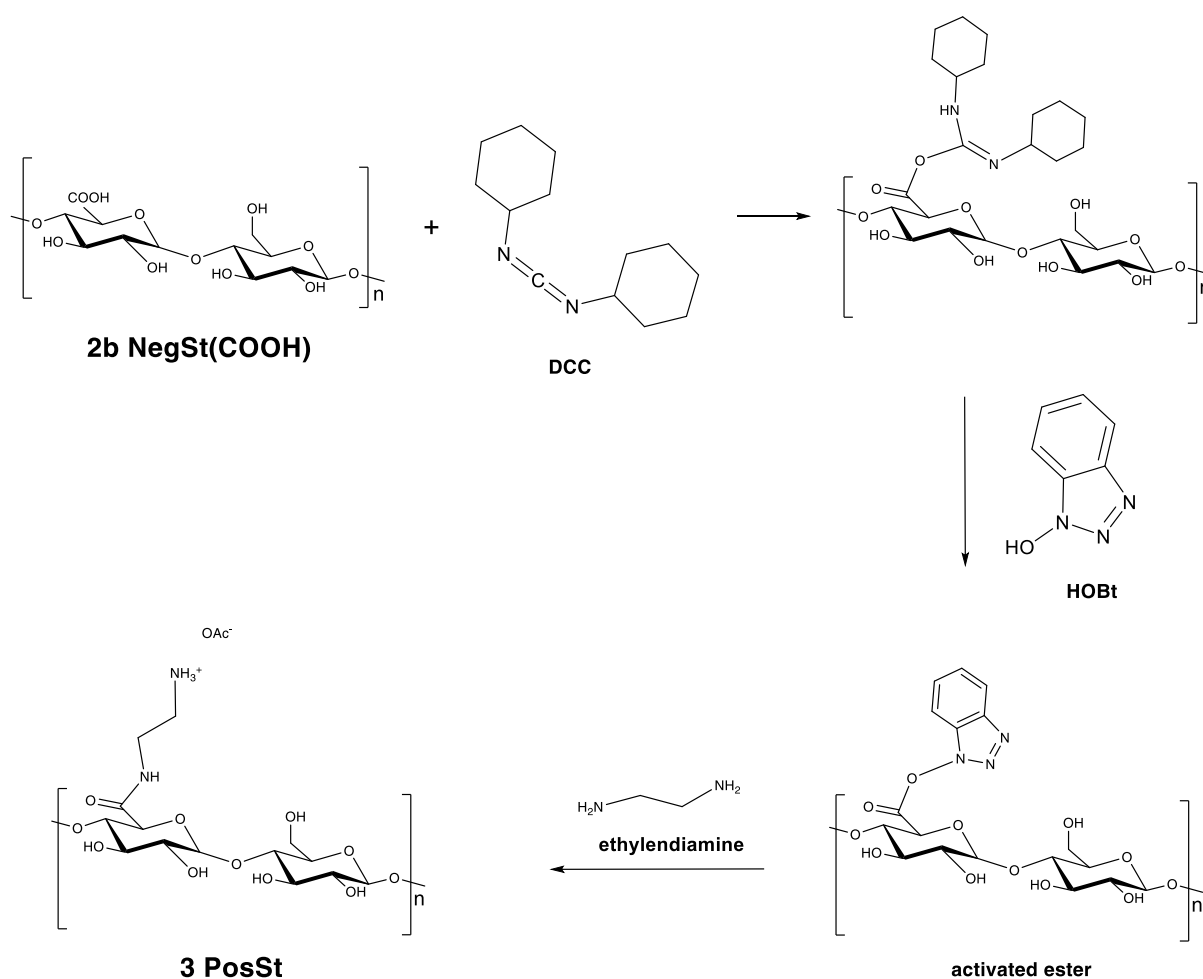
After the reaction, sodium borohydride was slowly added to selectively reduce aldehyde groups back to hydroxyl groups, without reducing the carboxyl groups.

3.3.2 CONJUGATION OF ETHYLENEDIAMINE WITH DCC/HOBT

The oxidation of potato starch was carried out as a first step for two reasons. One reason is the need for a negatively charged starch derivative for the further development of a nanotechnology enabled DDS prepared *via* charge-mediated coacervation in aqueous medium. Additionally, the use of NegSt as a precursor for modification with ethylenediamine allows for a selective coupling reaction between carboxyl groups of NegSt and amine groups

of ethylenediamine, meaning that protection of hydroxyl groups is unnecessary. Conversion of the carboxyl group *via* an activated ester to an amide (as possible for example with the DCC/HOBt system - Scheme 3.3) also does not lead to toxic side products or impurities, as usually known from paper industry, where the synthesis of cationic starches is usually performed with epoxyalkylamines^{133, 134} or halogenalkylamines.¹³⁵

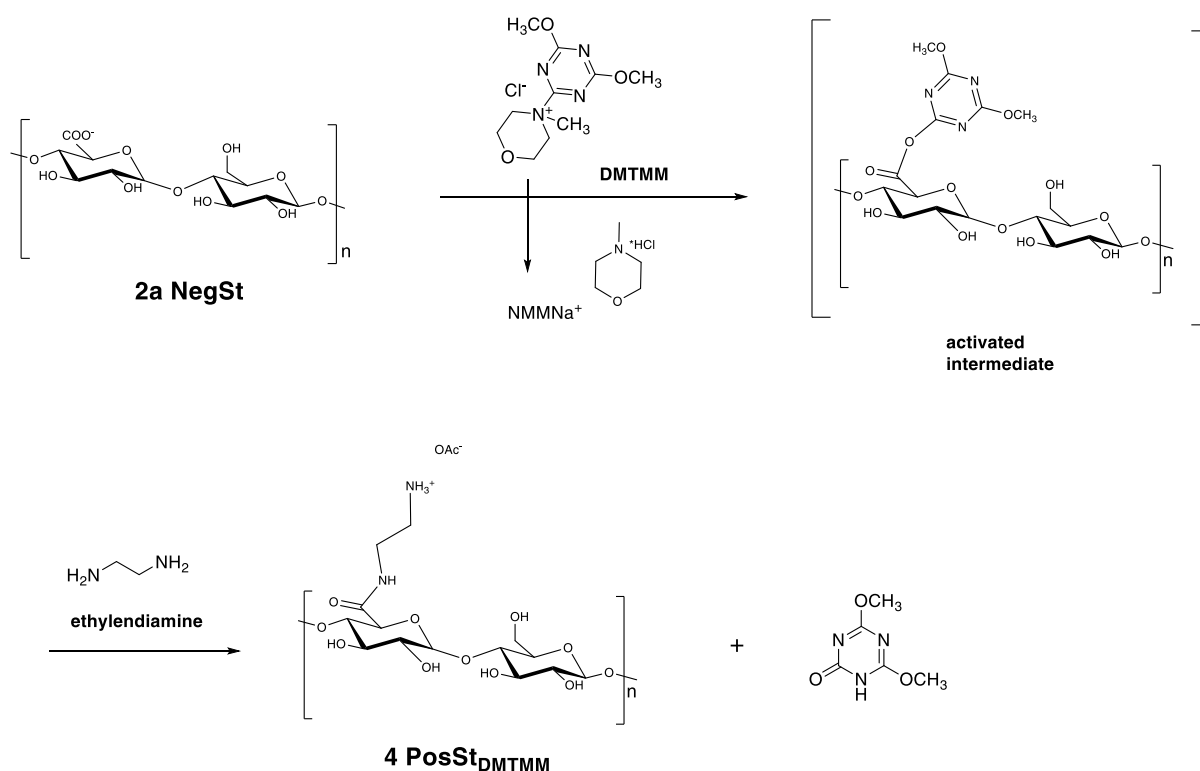
The conjugation of ethylenediamine with DCC/HOBt in DMSO was adopted from Sheehan¹³⁶ and König,¹³⁷ who have used the reaction for peptide bond formation. Furthermore, this method was used by Thiele for the synthesis of amino-functionalized pteroates (folic acid salt) and for their coupling with oxidized starch.¹³² As a free carboxylic group is necessary for the reaction, the carboxyl group was transferred into the free acid form with the help of an ion exchanger (Dowex 50 WX2-200). Successful coupling could already be observed during synthesis, by the formation of the non-water soluble dicyclohexylurea (not shown in Scheme 3.3).



Scheme 3.3: Mechanism of coupling: ethylenediamine with DCC/ HOBt.

3.3.3 CONJUGATION OF ETHYLENEDIAMINE WITH DMTMM

An alternative coupling reaction between carboxyl groups of NegSt and amine groups of ethylenediamine was performed using DMTMM (adopted from Kunishima¹²⁹) instead of DCC/HOBt. The conjugation with DMTMM is shown in Scheme 3.4. In a first step, an activated ester is produced by the reaction of a NegSt carboxylate anion with DMTMM. In order to achieve this, the reaction mixture was stirred for 30 min to activate the sodium carboxylate groups. The formed activated ester is then subjected to attack by the amine group of ethylenediamine, forming an amide bond. Reaction conditions, such as solvent choice, reaction time and molar ratio of DMTMM:NegSt were extracted from Yamada *et al.*,¹²⁸ who used this technique for coupling s-PEI to oxidized starch. The advantage of the DMTMM conjugation is the mild reaction condition at RT as compared to the DCC/HOBt system, which takes place at 50 °C – such an elevated temperature could result in an accelerated degradation of the polymer.



Scheme 3.4: Mechanism of coupling: ethylenediamine with DMTMM.

3.3.4 CHARACTERIZATION OF STARCH DERIVATIVES

Proof of successful reaction

The reaction was followed by conduction of FT-IR spectroscopy (shown for β -starch derivatives synthesized with DCC/HOBt in Figure 3.1 (A), and for δ -starch derivatives synthesized with DMTMM in Figure 3.1 (B). The typical peaks of the C=O stretching of the

carboxyl anion COONa at 1600 cm^{-1} , and of the C=O stretching from the COOH group (after ion exchange) at 1732 cm^{-1} , disappeared for $\text{PosSt}\beta$, and were replaced by two peaks at 1660 cm^{-1} and at 1550 cm^{-1} . These correspond to the amide bond formation: the amide I peak (1660 cm^{-1}) is mainly associated with the C=O stretching vibration, while the amide II (1550 cm^{-1}) results from the N-H bending vibration and from the C-N stretching vibration. This is in principle also true for the reaction with DMTMM, however the stretching of the C=O arising from the carboxyl anion at 1594 cm^{-1} is still visible in the FT-IR spectrum, indicating a lower amount of amide bond formation for the $\text{PosSt}\delta_{\text{DMTMM}}$ -derivative.

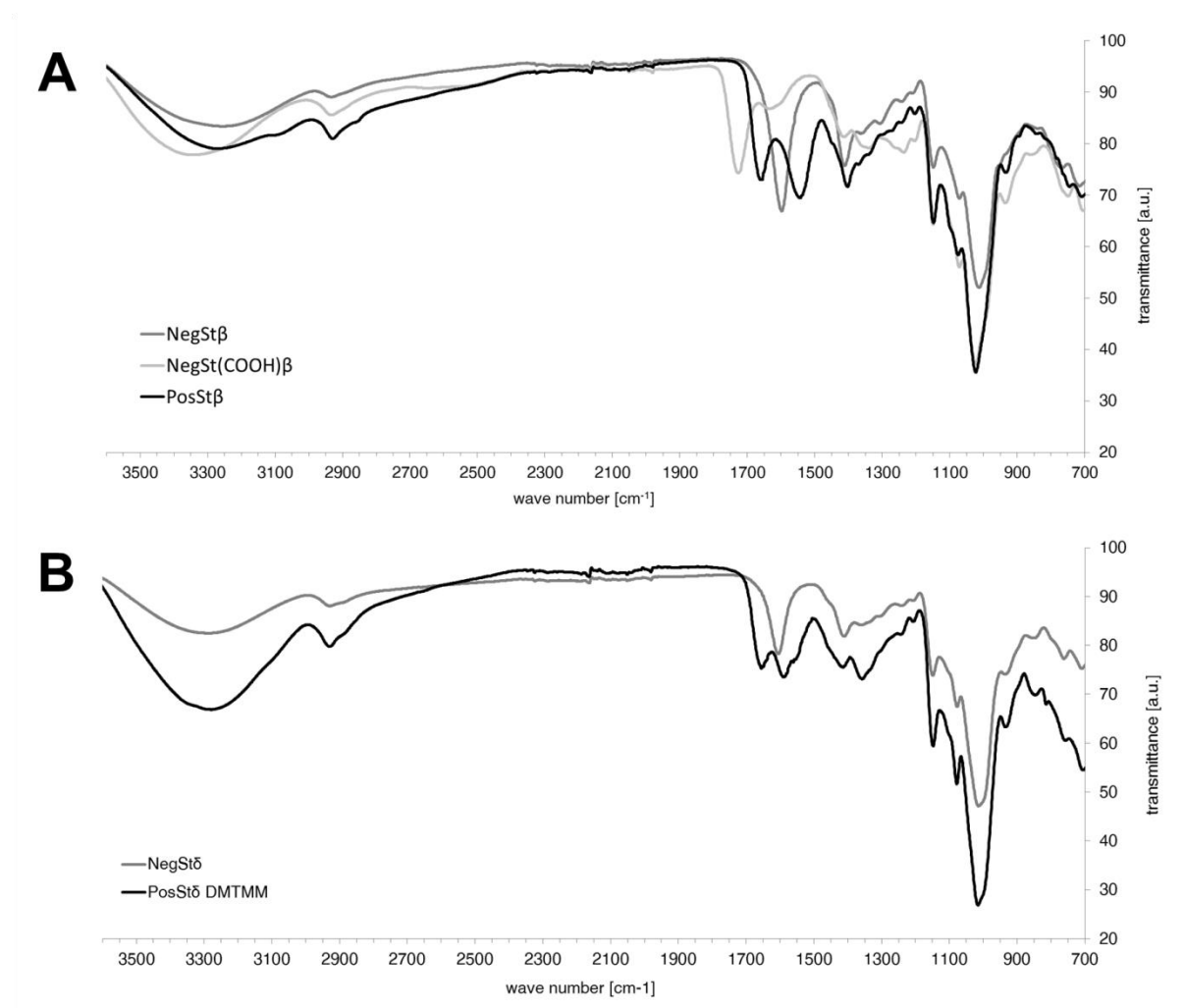


Figure 3.1: FT-IR spectra of β -starch derivatives (A) and δ -starch derivatives (B).

Further, ^1H -NMR spectra were collected to analyze the purity of the samples and to determine the degree of substitution with ethylenediamine. NegSt (shown for NegSt α in Figure 3.2 (A)) showed δH values between 5.28 – 5.58 ppm that were assigned to the anomeric 1H atom, whereas the signals from 3.20 – 4.20 ppm were ascribed to the ring protons 2H , 3H , 4H , 5H , 6H .^{127, 138}

NegSt was afterwards coupled with ethylenediamine, which could also be observed by ^1H -NMR (shown for PosSt α in Figure 3.2 (B)). PosSt showed the typical pattern between 5.10 – 5.62 ppm of the anomeric ^1H atom. The ring protons were visible between 3.30 – 4.30 ppm.

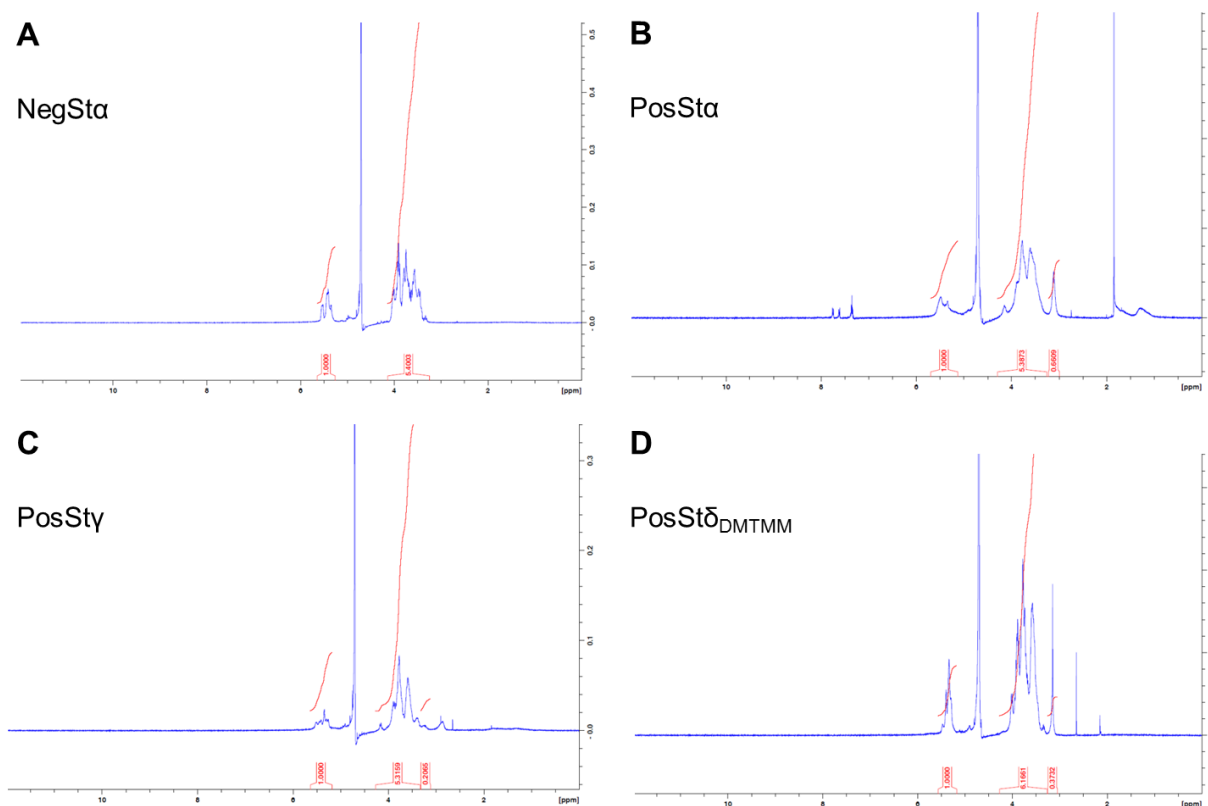


Figure 3.2: ^1H -NMR spectra of synthesized starch derivatives in D_2O : Oxidized starch (NegSt α , (A)) and coupled with ethylenediamine using DCC/HOBt (B and C). PosSt γ was precipitated with EtOH rather than lyophilized followed by tangential flow filtration (PosSt β). PosSt δ_{DMTMM} was produced from NegSt δ coupled with ethylenediamine using DMTMM, and was precipitated with EtOH (D).

Further, the value between 3.00 – 3.22 ppm was ascribed to the coupled ethylenediamine ($\text{NH-CH}_2\text{-CH}_2\text{-NH}_2$). HOAc, used to protonate the synthesized PosSt, can be seen in the spectrum as an intense peak at 1.8 ppm. The peaks at 7.4, 7.6 and 7.8 ppm were ascribed to small impurities arising from the coupling reagents DCC/HOBt. Therefore, for the synthesis of PosSt γ , the purification method was changed from lyophilization/tangential flow filtration to precipitation with ethanol. As DCC and HOBt are both soluble in ethanol, whereas starch derivatives are not, they can be separated through precipitation. This method was successful, as can be found in the ^1H -NMR of PosSt γ , shown in Figure 3.2 (C). Although the degree of substitution is less compared to PosSt α , the previously noted peaks between 7 and 8 ppm were not visible. However, some traces of free ethylenediamine remained, suggesting that the washing after precipitation could still be improved. The same holds true for the product synthesized with DMTMM (Figure 3.2 (D)).

Degree of substitution

The degree of oxidation of NegSt was determined by a colorimetric assay, according to Blumenkrantz *et al.*,¹³⁰ as this information is important for the following coupling reaction. Briefly, the Blumenkrantz assay detects the uronic acid content (carboxyl groups arising from the TEMPO C6-oxidation) by building a chromogen when heated in concentrated sulfuric acid/tetraborate and treated with m-hydroxybiphenyl. The degree of substitution of PosSt samples was calculated from ¹H-NMR spectra. Both the degree of oxidation of different NegSt syntheses as well as the degree of substitution of PosSt is shown in Table 3.2.

Table 3.2

Degree of substitution of starch derivatives. Degree of oxidation of NegSt was determined with the Blumenkrantz assay (mean \pm SD; n = 3), while the degree of substitution of PosSt was calculated from ¹H-NMR spectra.

	<i>degree of oxidation (NegSt) / substitution (PosSt) [%]</i>				
	α	β	γ	δ	δ_{DMTMM}
NegSt	36 \pm 1	52 \pm 5	25 \pm 2	21 \pm 2	21 \pm 2
PosSt	33	47	10	11	19

It can be seen that for different syntheses, the degree of oxidation varied. NegSt α showed a degree of oxidation of 36 \pm 1%, whereas NegSt β showed an increased degree of substitution of 52 \pm 5%. The γ - and δ -samples showed a lower degree of oxidation between approximately 25% and 20%. The degree of oxidation depended on the equivalent amount of NaOCl used for the synthesis. This is in accordance with Thiele,¹³² who described the degree of oxidation in relation to the equivalent amount of NaOCl - the more equivalents of NaOCl per starch monomer, the higher the degree of oxidation. For approximately 52% oxidation, 1.5 equivalents of NaOCl were used, for 36% 1.25 equivalents were used, and for 25% and 21% oxidation, 1 and 0.75 equivalents were used respectively.

For the substitution, 10 equivalents of ethylenediamine according to the degree of oxidation of NegSt were used. It can be seen that, the lower the degree of observed oxidation, the correspondingly lower the degree of coupling with ethylenediamine. Compared to the coupling with DCC/HOBt, the coupling with DMTMM was more efficient, showing a degree of substitution of 19%.

Molecular weight

GPC measurements of α -starch derivatives showed a weight average molecular weight of around 76000 ± 4300 for PosSt (Table 3.3), which is in the same range as that of NegSt, showing a weight average molecular weight of $87\,000 \pm 1\,800$. However, for the synthesis of PosSt β , the weight average molecular weight decreased almost by half – this showed values of $43\,000 \pm 2\,000$, compared to NegSt β which had a weight average molecular weight of $82\,000 \pm 1\,900$. It is likely that the elevated temperature of 50 °C combined with an increased reaction time led to degradation of the polymer backbone, leading to such a decrease.

Table 3.3

Mean average molecular weight of starch derivatives, determined with GPC (mean \pm SD, n = 2).

	α	β	γ	δ
NegSt	$86\,799 \pm 1\,806$	$81\,791 \pm 1\,889$	n.a.	n.a.
PosSt	$75\,753 \pm 4\,282$	$43\,402 \pm 2\,014$	n.a.	n.a.
PosSt_{DMTMM}	n.a.	n.a.	n.a.	n.a.

Unfortunately, the weight average molecular weights of the other polymers could not be determined, due to irreparable malfunction of the GPC. It is expected that at least for the PosSt samples, synthesized with DMTMM, the weight average molecular weight would be maintained, as the reaction was taking place at RT.

3.3.5 α -STARCH DERIVATIVES, USED FOR NANOPARTICLE PREPARATION

In the following chapter, “*Starch vs. chitosan nanoparticles – preparation and physicochemical characterization*”, α -starch derivatives were used for the preparation of nanoparticles *via* charge complexed coacervation in aqueous medium. Therefore, material properties will shortly be summarized in this paragraph.

The yield of the oxidation was 80.6% for NegSt α and the reaction yield for the coupling with ethylenediamine was found to be 59.6%. Negatively and positively charged α -starch derivatives showed approximately the same weight average molecular weight, being 87 000 for NegSt α and 76 000 for PosSt α . NegSt α showed a degree of oxidation of around 36%, whereas the coupling reaction with ethylenediamine was found to be around 33%. Both polymers showed a stable amorphous solid state after lyophilization, which can be seen in

Figure 3.3. In comparison, the starting material of the synthesis, potato starch, showed a semi-crystalline state, which is known to be characteristic of starch material.¹³⁹

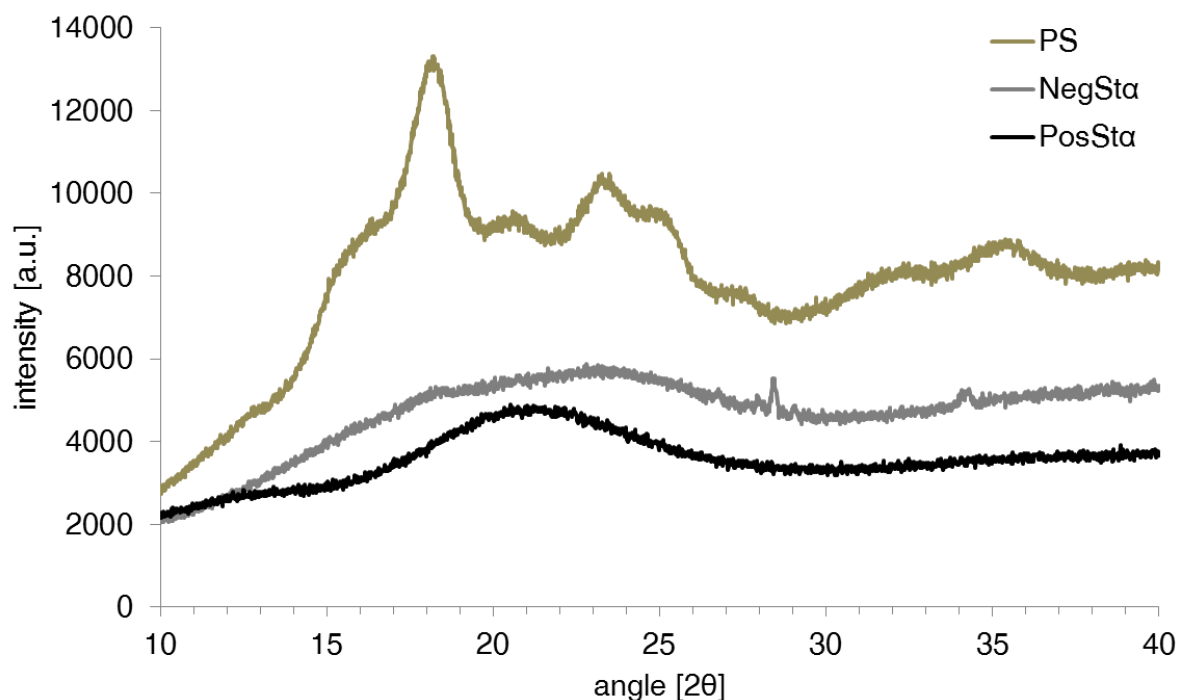


Figure 3.3: XRPD pattern of potato starch (PS) and α -starch derivatives (NegSt α , PosSt α).

For further characterization of the formulation as well as for cell interaction studies, PosSt was labeled with the fluorescent dye Bodipy[®] FL-C5 NHS Ester. The resulting polymer was orange in appearance as a dry powder with maximum fluorescence intensity at an excitation wavelength of 488 nm.

3.4 CONCLUSION

The NP formation via charge-mediated coacervation in aqueous medium requires water soluble materials. The synthesis and characterization of positively and negatively charged, water soluble starch derivatives was successfully carried out. Although the oxidation of potato starch was straight-forward, the conjugation of ethylenediamine with DCC/HOBt had some drawbacks. The medium for the coupling reaction consisted of 100% DMSO, which made purification using the Vivaflow 200 system challenging, as the Hydrosart[®] membrane (a stabilized cellulose-based membrane) is incompatible with DMSO. A pre-lyophilization step before the purification step was therefore necessary, which additionally proved to be both challenging (due to the high sublimation point of DMSO) and time consuming. An alternative

strategy to the pre-lyophilization step and purification with Vivaflow 200 was therefore found, namely the precipitation of PosSt with EtOH. With this time saving method, even the small amount of impurities arising from DCC/HOBt that were visible in the ^1H -NMR spectrum could be removed. However, further improvement of the precipitation is necessary to remove residual free ethylenediamine. A more thorough washing procedure is suggested in this respect. Another drawback of the DCC/HOBt method is the elevated temperature of 50 °C that is necessary for the coupling reaction. GPC measurements showed a decrease in the mean average molecular weight between PosSt α and PosSt β from 76 000 to 43 000, respectively, indicating that the elevated temperature in combination with the prolonged reaction time of 72 h could result in an accelerated degradation of the polymer backbone. As a result, NegSt was coupled to ethylenediamine instead using DMTMM. Here, the reaction is taking place at RT in a mixture of water:DMSO. The product can be purified by precipitation with EtOH as solvent of choice.

An important aspect for future work would be the testing of reproducibility of the synthesis to ensure a product of constant quality. Also scalability would be a variable to be explored.

4. STARCH VS. CHITOSAN NANOPARTICLES – PREPARATION AND PHYSICOCHEMICAL CHARACTERIZATION

The author of the thesis made the following contribution to the current chapter:

Planned and designed all experiments, performed experiments related to particle preparation and characterization, analyzed all data obtained from the mentioned studies, interpreted all experimental data and wrote the chapter, if not stated otherwise.

Greta Magnano, an Erasmus student, who was instructed by the author of the thesis, contributed to the chapter by performing parts of the CS nanoparticle preparation and characterization.

Julian Taffner, a ten week internship student was instructed by the author of the thesis and contributed to the chapter by performing parts of the starch nanoparticle preparation and characterization.

4.1 INTRODUCTION

The use of NPs as DDS for protein delivery is well-established, as they can offer protection during both storage, and administration, and are known to facilitate an enhanced permeation through epithelial barriers.^{140, 141}

The selection of an appropriate NP preparation method depends on both the carrier material as well as the drug (in this case the protein) to be encapsulated. There are several methods which can be utilized for NP preparation. In principle, they can all be described as either top-down or bottom-up methods.^{142, 143} The first case employs material on a large scale and involves the reduction of its lateral dimensions (that is, its particle size) with *e.g.* wet milling techniques. However, these methods involve a great amount of energy input and are highly inefficient.¹⁴⁴ On the other hand, bottom-up methods start with the material in a dissolved form, upon which nano- and microstructures are built up. Several approaches can be assigned to the bottom-up method, such as spray drying,¹⁴⁵ supercritical fluid processes,¹⁴⁶ nanoprecipitation,^{147, 148} and emulsion solvent evaporation.¹⁴⁹⁻¹⁵¹ Each preparation method has its advantages and disadvantages. Most of these processes necessitate input of energy, by heating, sonication, or vortexing. Further, the use of organic solvents may be necessary, for example when DDS are prepared from polymers that are not water soluble. All such factors could potentially damage the structure of the DDS protein cargo, as the secondary, tertiary and quaternary levels of protein structure are very sensitive to the application of energy. Although often preparation methods for DDS are emulsion based, this approach can additionally lead to unfolding of the protein, as protein molecules migrate to the phase interface, arranging their hydrophilic domains to the water side and their lipophilic domains to the hydrophobic side.

To avoid these issues and to ensure protein integrity, a preparation method for DDS was chosen that only applies the use of aqueous media, with no organic solvents and no harsh mixing conditions. Therefore, water soluble polymers were evaluated. Polysaccharides are among the most studied polymers for drug delivery applications.¹⁰⁷ Amongst these, chitosan (CS) was chosen as reference material, as chitosan-based DDS are widely explored^{114-116, 152} and can be prepared in aqueous solution by virtue of interaction of CS with a small ionic crosslinker tripolyphosphate (TPP).¹⁵²

Working in an aqueous environment, it should, however be noted that some proteins degrade under extreme pH conditions – and some even when their surrounding pH differs only a little from physiological pH - while others are sensitive to ionic strength. DDS preparation and loading with protein could be carried out in a buffered system; however, the presence of

buffer salts also has the potential to change the chemical properties of the DDS, as its formation is based on electrostatic interaction.

The aim of this chapter was to compare the preparation and characterization of NPs composed of two different carbohydrate-based materials. CS NPs introduced by Calvo *et al.* in 1997 and often used for protein delivery¹⁵² acted as an evaluation tool for the preparation process, and as a guide to help establish appropriate analytical methods for the newly developed starch NPs. The synthesized water soluble anionic and cationic α -starch derivatives were used in order to enable NP formation *via* charge-mediated coacervation; these NPs were compared to CS NPs, prepared also *via* charge-mediated coacervation with TPP, which is also called ionic gelation in this special case.

4.2 MATERIALS AND METHODS

4.2.1 MATERIALS

Protasan UPCL 113 (chitosan, CS) with a weight average molecular weight of 61268 ± 406 and a degree of deacetylation of $\sim 83\%$ was bought from Novamatrix, Norway. Sodium tripolyphosphate (TPP) was purchased from Merck KGaA, Germany. Negatively (NegSt) and positively (PosSt) charged starches were synthesized in house. IgG1 and insulin were kindly donated by Boehringer Ingelheim (Germany) and Sanofi (France), respectively. Vancomycin hydrochloride (vanco), Ribonuclease A from bovine pancreas (RNase A), α -amylase from porcine pancreas, chitosanase from *Streptomyces* (chitosanase), albumin from chicken egg white (OVA), albumin from bovine serum (BSA), and lysozyme from chicken egg white (Lyso) were bought from Sigma Aldrich (USA). The Nrf2 peptide¹⁵³ (peptide sequence: (LQL)DEETGEFLPIQ) was bought from Selleck Chemicals, U.S.A.

Purified water was produced by a milliQ water purification system (Merck Millipore, USA). All other reagents were of analytical grade.

4.2.2 PREPARATION AND LOADING OF CHITOSAN NANOPARTICLES

CS NPs were prepared by ionic gelation of positively charged amine groups of CS with negatively charged phosphate groups of TPP in aqueous solution, in a procedure adapted from Calvo *et al.*¹¹³ Besides material concentration, the molar ratio of components, as well as the stirring speed (500 rpm, 1000 rpm) and injection rate (5 mL/min, 10 mL/min, 20 mL/min) for particle preparation using a syringe pump were investigated, as parameters potentially influencing the characteristics of resulting NPs. Further, the impact of the preparation medium

was explored, by utilizing either purified water, or 10 mM HOAc/OAc⁻ buffer pH 5.0 with and without different amounts of NaCl (5 mM, 10 mM, 50 mM). Briefly, materials were dissolved in aqueous medium to obtain solutions of 1 mg/mL, 0.5 mg/mL and 0.25 mg/mL and filtered. Different molar ratios (20:1, 10:1, 2:1 and 0.5:1) of CS:TPP were studied by adding adequate volumes of TPP solutions (1, 0.5, 0.25 mg/mL) to CS solutions (1, 0.5, 0.25 mg/mL) under gentle stirring at RT. NPs formed spontaneously and were analyzed after 10 min of stirring for equilibration. The final pH value of all tested formulations was 5.0.

In order to assess the use of CS NPs as DDS for proteins, five proteins varying in size and net charge, were chosen for loading experiments. These proteins were IgG1 (Mw: 150 kDa, isoelectric point (IEP): 8.5), BSA (Mw: 66 kDa, IEP: 4.7), OVA (Mw: 44 kDa, IEP: 4.5), Lyso (Mw: 14 kDa, IEP: 11.4) and Nrf2 (Mw: 1.3 kDa, IEP: 3.5). For the loading experiments, each protein sample was prepared as 5 mg/mL stock solution in purified water and added in various concentrations to the NP suspension to obtain final protein concentrations of 10.4 µg/mL, 20.7 µg/mL, and 41.3 µg/mL.

4.2.3 PREPARATION AND LOADING OF STARCH NANOPARTICLES

Starch NPs were prepared by charge-mediated coacervation between negatively charged carboxylate groups (NegSt) and positively charged amine groups (PosSt) of α -starch derivatives in aqueous solution. Briefly, materials were dissolved in purified water to obtain solutions of 1 mg/mL, 0.5 mg/mL, and 0.25 mg/mL, and filtered. Different molar ratios (3:1, 1:1, 1:3) of PosSt and NegSt solutions were studied by adding adequate volumes of NegSt (1, 0.5, 0.25 mg/mL) solution to PosSt solution (1, 0.5, 0.25 mg/mL) under gentle stirring at RT. NPs formed spontaneously and were analyzed after 10 min of stirring for equilibration. The final pH value was 7.4 for all tested formulations.

For later characterization studies of the formulation as well as uptake studies, labeled starch NPs were prepared from solutions of 0.25 mg/mL and a molar ratio of 1:1 of PosSt:NegSt. Instead of PosSt alone, different mass ratios of PosSt:PosSt_F (100:0, 50:50, 10:90, 5; 95) were used for particle preparation.

Four proteins varying in net charge and size were chosen for loading experiments, in order to assess the use of starch NPs as DDS. In detail, these proteins were vanco (Mw: 1.5 kDa, IEP: 7.5), insulin (Mw: 6 kDa, IEP: 5.3), RNase A (Mw: 14 kDa, IEP: 9.6), and IgG1 (Mw: 150 kDa, IEP: 8.5). Each protein sample was prepared as 5 mg/mL stock solution in purified water (except insulin, which was dissolved in 0.01 N NaOH) and added to the NP suspension to obtain final protein concentrations of 17.2 µg/mL, 34.2 µg/mL, and 51.2 µg/mL.

4.2.4 CHARACTERIZATION OF NANOPARTICLES

Physicochemical properties (particle size, PDI, and ζ -potential) of NPs in preparation medium were determined using the Zetasizer Nano ZSP (Malvern Instruments, UK) with a scattering angle of 173°. Particle sizes were intensity based z-average values and standard deviation was of at least 3 measurements. Storage stability of CS NPs was assessed by monitoring NPs for size, PDI and ζ -potential for 7 days. Samples were stored in the fridge (4 °C). Physicochemical stability of starch NPs was monitored for size, PDI and ζ -potential for 14 days. Samples were stored either in the fridge (4 °C) or at RT (20 °C). Morphology of CS NPs was analyzed by scanning electron microscopy (SEM, JSM 7001F Field Emission SEM (Jeol, Japan)). Samples were placed on a silicon wafer on top of a carbon disc and sputtered with gold (layer thickness approx. 10 nm) prior to scanning. The accelerating voltage was 5 kV with a focal distance of 15 mm. Further, transmission electron microscopy (TEM) using a JEOL JEM 2011 microscope (Oxford Instruments, UK) was used for morphology analysis of CS and starch NPs. A 20 μ L volume of sample was incubated on a copper grid for 30 min. After staining with 1% (w/v) of phosphotungstic acid (PTA) for 30 s, samples were dried overnight (excess fluid was directly removed with filter paper) and analyzed.

To study the biodegradation of CS NPs, 10 mL of NP suspension was incubated at 50 °C with 0.5 μ L or 5 μ L of chitosanase solution (0.1352 units/ μ L) for 2, 4, 6, 8, or 24 h under gentle stirring. As control, 10 mL of CS NP suspension was incubated at 50 °C under gentle stirring without enzyme. The biodegradation of starch NPs was studied by incubating 10 mL of NP suspension with 25 μ L α -amylase solution (36.37 units/ μ L) at 37 °C for 2, 4, 6, or 8 h under gentle stirring. As a control in this case, 10 mL of starch NP suspension was incubated at 37 °C under gentle stirring in the absence of α -amylase. Particle concentrations were then analyzed at several time points by nanoparticle tracking analysis (NanoSight LM 10, Malvern Instruments, UK). For these measurements, 0.5 mL was taken from each sample. Described results are the particle concentration (after correction for the dilution factor needed for valuable measurement) of treated and non-treated samples (each n=3).

To study the stability of CS NPs and starch NPs upon aerosolization, they were nebulized with the Aeroneb®Lab nebulizer (Aerogen Ltd., Ireland) and collected to be analyzed for size, PDI and ζ -potential with the Zetasizer Nano ZSP (Malvern Instruments, UK).

For the determination of protein encapsulation efficiency (EE) and loading rate (LR) in each case, NPs were separated from the dispersing medium containing non-encapsulated protein, after 15 min equilibration, by ultracentrifugation (45.000 x g for 90 min (CS NPs) or 60 min (starch NPs), 20 °C; Optima L-XP, Beckman Coulter, UK). The amount of free protein in the

supernatant was determined with the BCA (bicinchoninic acid) Assay Kit (Sigma Aldrich, USA). This assay relies on the formation of Cu²⁺-protein complexes with reduction of Cu²⁺ to Cu¹⁺ under alkaline conditions. Bicinchoninic acid then forms a purple complex with the Cu¹⁺ in alkaline conditions that can be detected by measuring the absorbance at 562 nm. EE and LR of proteins/peptides were defined and calculated according to following equations:

$$EE[\%] = \frac{mass(protein)_{total} - mass(protein)_{free}}{mass(protein)_{total}} * 100$$

$$LR[\%] = \frac{mass(protein)_{total} - mass(protein)_{free}}{mass_{NP}} * 100$$

For determination of the particle yield (mass NP), washing of the particles was performed with Vivaflow[®] 50 (100 kDa MWCO, PES (Polyethersulfone) membrane, Sartorius, Germany). A 50 mL (CS) or 40 mL (starch) volume of NP suspension was washed with 150 mL or 120 mL of purified water, respectively, concentrated to 10 mL, freeze dried and weighed.

4.3 RESULTS AND DISCUSSION

The well-known system of CS NPs was chosen to get an idea of the preparation process and to establish analytical tools for the newly developed starch NPs. Further, the CS NP system was designated as a bench-mark for starch NPs.

CS NPs were chosen, due to the abundance of literature available describing such systems, as well as the ability to prepare CS and starch-based NPs using a similar aqueous-based preparation process. CS is a well-known material and was a good starting point for the evaluation of analytical tools. It was designated as the 1st generation DDS for the COMPACT consortium to be replaced by starch NPs as a 2nd generation DDS once all characterization methods had been developed.

4.3.1 PREPARATION OF CHITOSAN NANOPARTICLES

CS is prepared *via* partial deacetylation from the natural polymer chitin, consisting of N-acetylated glucosamine residues, occurring widely in nature as a structural polysaccharide present in the integument of crustacea and insects.¹⁵⁴ Further, there is a vegetarian source of CS, obtained by extracting chitin from cell walls of fungi.¹⁵⁵

CS NPs were prepared by adding different amounts of the highly negatively charged small molecule TPP to a CS solution under stirring. Both solutions always had the same mass concentration.

Particle preparation by manual injection

First of all, the influence of the molar ratio and concentration of components on the physicochemical properties of formed CS NPs was investigated (Figure 4.1). It can be seen that NP formation depended highly on the molar ratio of the two components: a molar ratio of CS:TPP 20:1 led to a particle size between 182.1 ± 29.2 nm and 395.4 ± 36.1 nm, with corresponding PDI values at these sizes of 0.25 and 0.23, respectively. A molar ratio of 10:1 was also shown to give good results with particle sizes ranging from 155.5 ± 2.7 nm to 395.8 ± 6.8 nm and PDIs between 0.15 and 0.36. In contrast, molar ratios of 2:1 and 0.5:1 resulted in aggregation of the material, with particle sizes between 800 and 4000 nm and high PDI values observed. This is in accordance with the determined ζ -potential values for these formulations, which are close to zero, indicating that an electrostatic stabilization of the NPs was not possible. However, this was possible for the formulations of molar ratios 20:1 and 10:1, with ζ -potential values around +45 mV and +35 mV, respectively. As a first result, it can therefore be concluded that the molar ratio of CS:TPP is important for NP formation, and should be between 20:1 and 10:1. A higher amount of negatively charged TPP leads to a loss in the ζ -potential, resulting in an unstable system.

As second parameter, the influence of material concentration was explored. Therefore, CS and TPP concentrations of 1, 0.5, and 0.25 mg/mL were investigated. For a molar ratio of 20:1, it can be seen that particle size increased with increasing material concentration: a particle size of 182.1 ± 29.2 nm was obtained for 0.25 mg/mL concentrations, whereas a particle size of 290.6 ± 52.2 nm and 395.4 ± 36.1 nm was found for 0.5 mg/mL and 1 mg/mL concentrations, respectively. Similar results were obtained for a molar ratio of 10:1: the particle size for the lowest concentration was 155.5 ± 2.7 nm, whereas a particle size of 261.8 ± 0.2 was obtained for 0.5 mg/mL and a particle size of 395.8 ± 6.8 nm was obtained for 1 mg/mL. The ζ -potential was not affected by the material concentration. The values rather depended on the molar ratio of CS:TPP, with ζ -potentials of around +45 mV for 20:1 and +30 - +35 mV for a molar ratio of 10:1. It can be concluded that particle size depends chiefly on material concentration, with a lower concentration leading to a smaller particle size. The ζ -potential, however, was mostly influenced by the molar ratio of components. This is in accordance with Calvo *et al.*, who obtained similar results.¹¹³

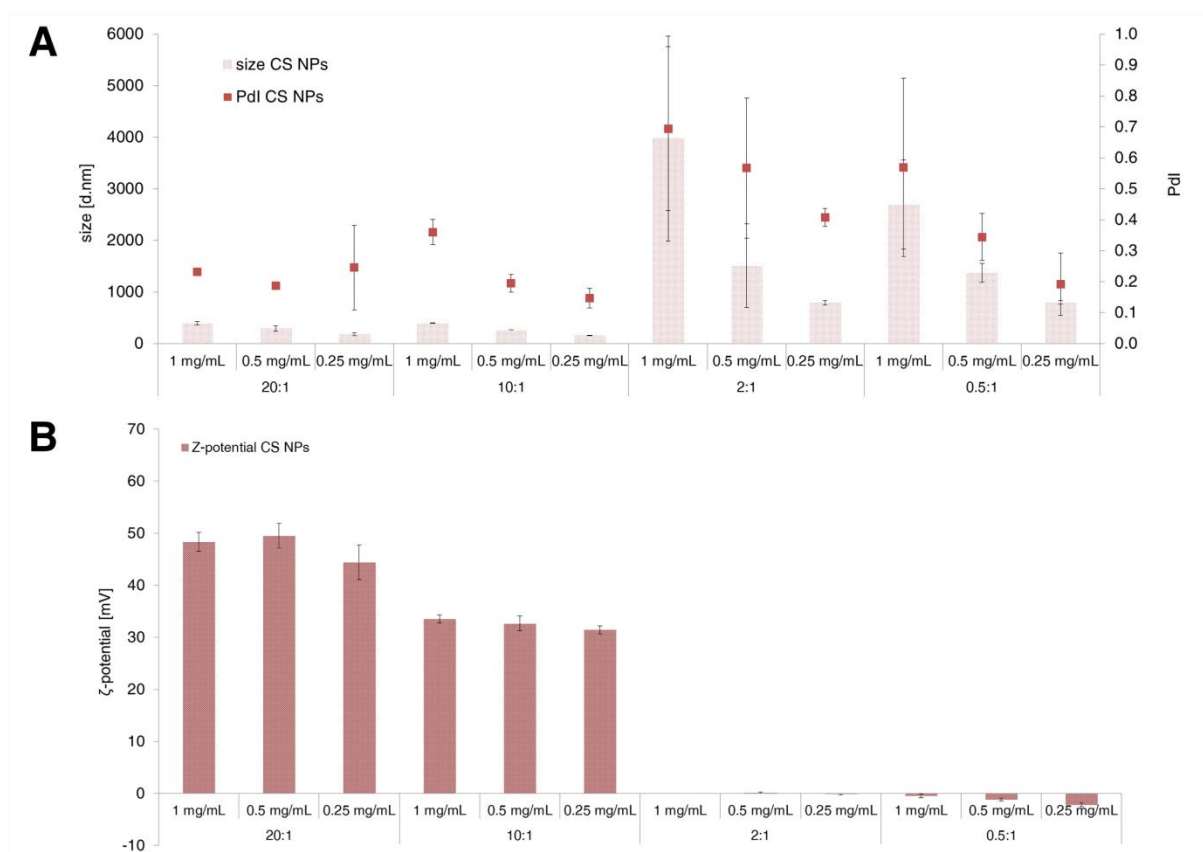


Figure 4.1: Preparation of CS NPs with different material concentrations (1, 0.5, 0.25 mg/mL), and molar ratios (20:1, 10:1, 2:1, 0.5:1 CS:TPP). (A) size (bar) and PDI (squares); (B) ζ-potential; TPP solution was applied by manual injection.

Particle preparation with a syringe pump

It could be seen that NP results obtained by manual injection were not always reproducible. To reduce the high standard deviations and to further improve reproducibility, the use of a syringe pump (Harvard Apparatus PHD ULTRA, Harvard Apparatus Inc., Holliston, USA) was explored. When using such a pump, the pressure, the added volume and the injection rate can be adjusted and controlled, which may lead to more reproducible results. For these experiments, a material concentration of 0.25 mg/mL of CS and TPP and two different molar ratios, 20:1 and 10:1, were chosen. Parameters such as stirring speed (500 rpm, 1000 rpm) and injection rate (5 mL/min, 10 mL/min, 20 mL/min) were varied and their effect on physicochemical properties of CS NPs studied. The results can be found in Figure 4.2.

In comparison to the experiments performed with manual injection, the PDI of NPs formed using a syringe pump was always below 0.2, indicating a narrow particle size distribution. The particle size, however, did not depend on stirring speed or injection rate. For a molar ratio of 20:1, particle sizes were between 180 nm and 210 nm independent of injection rate and stirring speed. For a molar ratio of 10:1 it could be assumed that stirring has a minor

influence, as particle size was between 144.3 ± 0.2 nm and 161.3 ± 0.7 nm for a stirring speed of 500 rpm, whereas particle size decreased for a stirring speed of 1000 rpm, being between 111.7 ± 0.2 nm and 120 ± 1.0 nm. However, these values were again independent of injection rates utilized in these experiments.

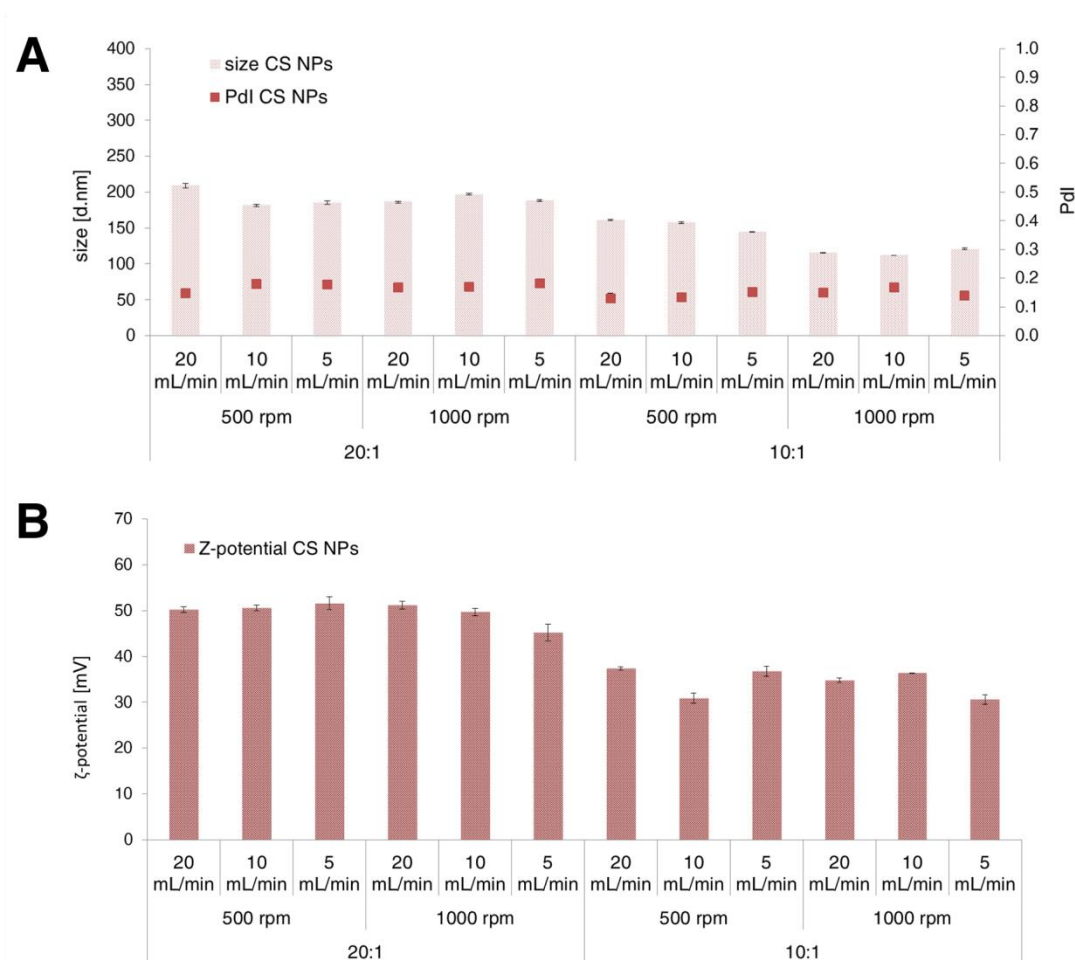


Figure 4.2: Influence of stirring speed and injection rate on the preparation of CS NPs with 0.25 mg/mL and two different molar ratios using the syringe pump. (A) size (bars) and PdI (squares); (B) ζ -potential.

ζ -potential values were again only depending on the CS:TPP molar ratio, being around +50 mV for a molar ratio of 20:1 and around +35 mV for a molar ratio of 10:1. It can be concluded that the syringe pump is a valuable tool for reproducible particle preparation. For further experiments, CS NPs were prepared with the syringe pump from 0.25 mg/mL solutions and a molar ratio of 10:1 (CS:TPP) under stirring at 500 rpm with an injection rate of 20 mL/min.

Particle preparation in buffer

To investigate the influence of preparation medium and temperature, CS NPs were prepared in a 10 mM HOAc/OAc⁻ buffer, pH 5.0 at different temperatures (4 °C, 20 °C, 45 °C). Results can be found in Table 4.1.

Table 4.1

Influence of preparation medium, temperature and NaCl concentration on physicochemical properties of CS NPs prepared from 0.25 mg/mL solutions with a molar ratio of 10:1 in a 10 mM HOAc/OAc⁻ buffer, pH 5.0.

<i>Temperature</i> [°C]	<i>NaCl</i> [mM]	<i>Size</i> [d.nm]	<i>PdI</i>	<i>ζ-potential</i> [mV]
4	-	88.1 ± 1.9	0.25	12.7 ± 0.9
20	-	84.3 ± 1.6	0.24	24.1 ± 2.9
45	-	80.9 ± 0.9	0.19	26.4 ± 0.8
20	5	74.8 ± 0.2	0.21	20.2 ± 3.2
20	10	73.7 ± 0.8	0.19	12.7 ± 0.4
20	50	55.1 ± 0.1	0.09	16.3 ± 2.2

It can be seen that the temperature had no clear effect on particle size, however for an elevated temperature, particle size distribution was somewhat improved with a PdI below 0.2 for the formulation prepared at 45 °C. The ζ-potential was by contrast clearly influenced by the temperature, with values of +12.7 ± 0.9 mV for a preparation at 4 °C and values of +24.1 ± 2.9 mV and +26.4 ± 0.8 mV for the preparation at 20 °C and 45 °C, respectively. As the ζ-potential measurement is temperature dependent, it could be assumed that for 4 °C the sample did not reach the correct measurement temperature yet, as the preparation temperature is not expected to alter the ζ-potential. To improve size distribution, NaCl was added in various concentrations to the buffer used for NP preparation (5 mM, 10 mM, 50 mM). It can be seen that, with increasing amounts of NaCl, the PdI decreased from 0.24 for the preparation in buffer without NaCl, to 0.21 for the preparation in 5 mM NaCl, to 0.09 for the preparation in 50 mM NaCl. Particle size was also affected by the NaCl amount. Particles of 84.3 ± 1.6 nm were formed from preparation in buffer without NaCl, while 74.8 ± 0.2 nm particles resulted from the preparation in 5 mM NaCl, and 55.1 ± 0.1 nm NPs were the product of preparation in 50 mM NaCl. While some variations in ζ-potential was observed, as this measure depends both on the pH and ionic strength of the dispersing medium, it could not be compared under

conditions of varying NaCl content. The preparation in buffer clearly changed the particle size of CS NPs, being around 150 nm for the preparation in water and 90 nm for the preparation in buffer and even smaller for the preparation in buffer with additional salt concentration.

To keep the formulation as simple as possible, it was decided to minimize additional material contributions from buffer components or salts. The preparation in water was used for further evaluation of the CS NPs system.

4.3.2 CHARACTERIZATION OF CHITOSAN NANOPARTICLES

Storage stability

To investigate storage stability of CS NPs, short term particle stability after preparation was studied for 7 days. Therefore, CS NPs prepared from 0.25 mg/mL and a molar ratio of 10:1 were stored at 4 °C. Samples were taken at several time points and analyzed for their size, Pdl and ζ -potential (Figure 4.3). It can be seen that particle size, Pdl and ζ -potential were stable during storage and could be prepared in advance before running further experiments.

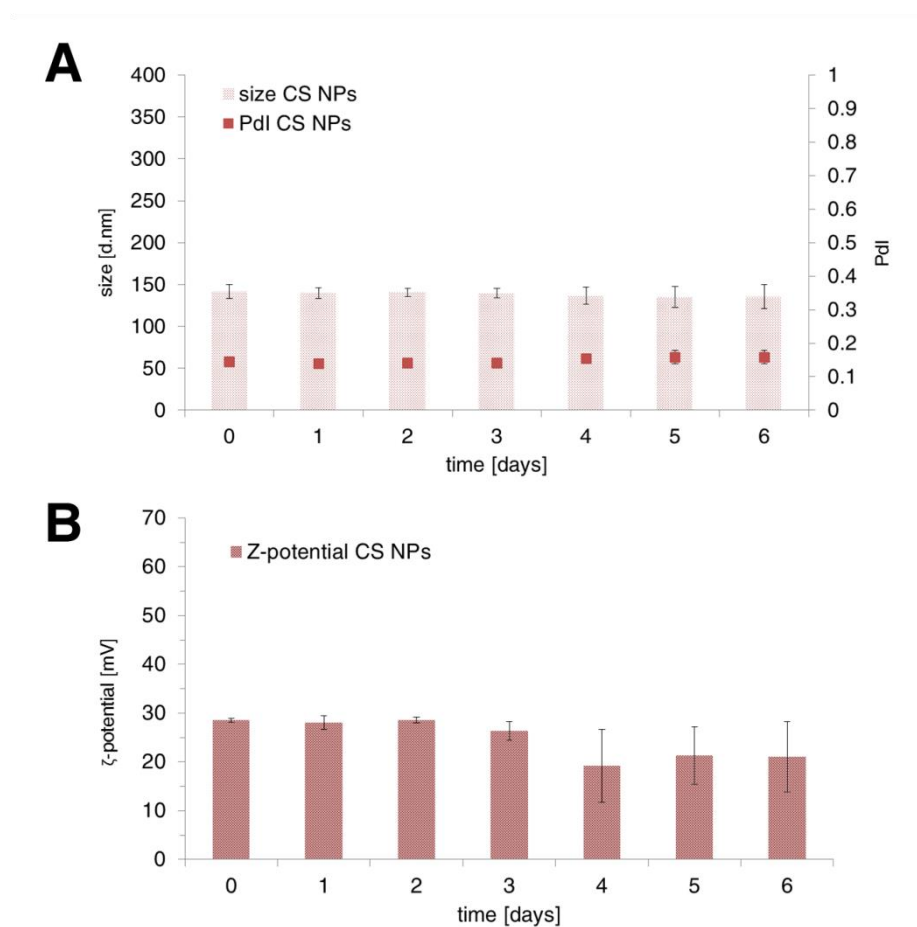


Figure 4.3: Storage stability of CS NPs prepared from 0.25 mg/mL and a molar ratio of 10:1 (CS:TPP), stored at 4 °C. (A) size (bars) and Pdl (squares); (B) ζ -potential.

Morphology

Attempts were made to evaluate the morphology of CS NPs by SEM. In contrast to PLGA NPs, where this technique has nicely been explored, the application of SEM for imaging of CS NPs was found to be of limited use. SEM images showed a polymer layer (Figure 4.4 (A)) with some particulate structures, more clearly visible at higher levels of magnification (Figure 4.4 (B)).

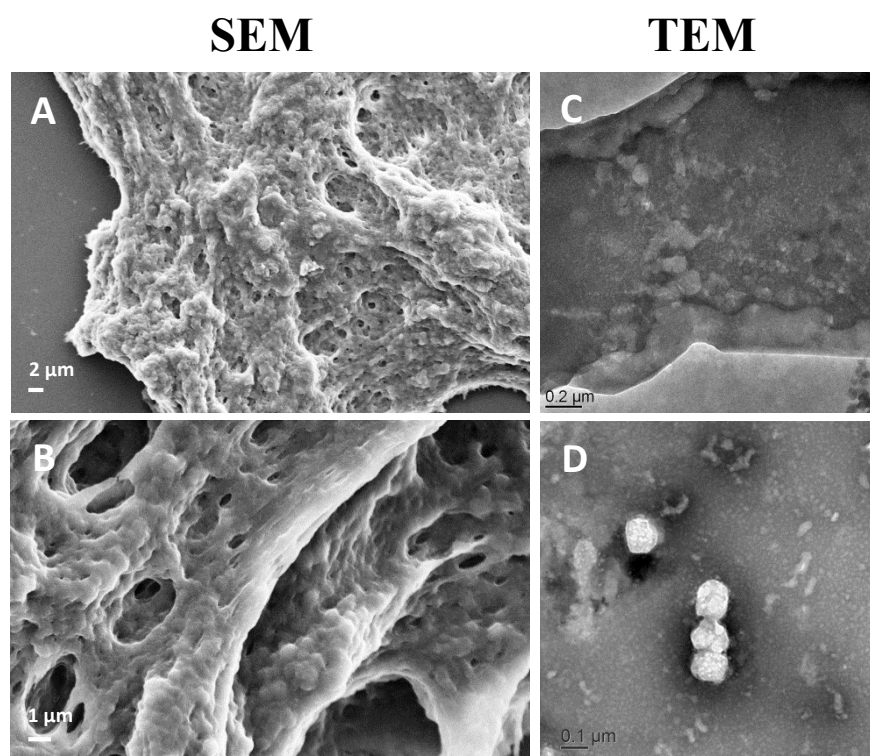


Figure 4.4: Images of CS NPs, prepared from 0.25 mg/mL solutions in a molar ratio of 10:1 (CS:TPP). SEM images (A-B). TEM images without staining (C) and with 1% PTA staining (D).

This behavior indicates an instability of the system probably occurring as a result of the drying process utilized during SEM sample preparation - as CS NPs are known to show a gel-like structure, such sample drying can be expected to result in particle aggregation. In more detail, for imaging, the sample is placed on a SEM wafer, water is evaporated and the dry image is analyzed after sputtering with gold. However, during drying, space becomes limited, with particles coming closer to each other. Once a particle comes in contact with another particle, their surfaces literally stick together. NP repulsive forces, resulting from their positive ζ -potentials, are overcome with restricted space and direct contact of the NPs. Another technique was therefore employed for imaging of CS NPs, namely TEM. Here, the sample is placed on a copper grid, allowed to dry and analyzed. The same phenomenon could be observed as for SEM imaging (Figure 4.4 (C)). However, NPs could be stabilized with 1%

PTA (Figure 4.4 (D)). After incubation of the NPs on the grid for 10 min, the residual solvent was removed by blotting with tissue paper and the grid was incubated on a 1% PTA droplet for 30 s. Although a polymer layer can still be observed, PTA working as a negative stain in this case builds a small dark layer around the particles, stabilizing them and making them “visible”.

Biodegradation

The biodegradation of a nanoparticulate system and the analysis of its degradation products is of great importance, when considering the application of such a system *in vivo*.

For this reason, the biodegradability of CS NPs by chitosanase was tested, using an adapted protocol from Sun *et al.*¹⁵⁶ Chitosanase is an enzyme, produced by many micro-organisms, including bacteria such as actinomycetes, as well as fungi.¹⁵⁴ While chitosanase is not a human enzyme, the test should act as tool to further develop a similar enzymatic method for the starch NPs.

CS NPs were incubated at 50 °C with or without chitosanase. For the samples treated with chitosanase, either 0.5 µL or 5 µL enzyme solution was added (0.0676 units and 0.676 units, respectively). At certain time points, samples were taken and particle concentration was determined with the help of nanoparticle tracking analysis. Compared to a control group (CS NPs stored at 50 °C without enzyme), the particle concentration was determined. It can be seen from Table 4.2 that the particle concentration of the control group decreased from $77.8 \pm 1.4 \times E^8$ particles/mL before the incubation to $61.9 \pm 12.5 \times E^8$ particles/mL after 24 h of incubation. This could be due to the elevated temperature of 50 °C, resulting in a higher moving speed of the particles, and leading to merging of particles as a result of this higher kinetic energy. Nevertheless, the difference in particle concentration between the control group and samples incubated with chitosanase was very clear. The 0.5 µL chitosanase samples showed a decrease in particle amount from $80.4 \pm 1.9 \times E^8$ particles/mL to $5.3 \pm 1.9 \times E^8$ particles/mL already after 24 h of incubation. This effect was even more pronounced for the samples treated with 5 µL chitosanase. Here, the particle amount of $82.99 \pm 4.1 \times E^8$ particles/mL was reduced to $0.6 \pm 0.2 \times E^8$ particles/mL after 24 h of incubation. Already after 2 h the particle concentration was reduced to $1.8 \pm 0.9 \times E^8$ particles/mL, indicating a very fast degradation mechanism of the CS NPs.

Table 4.2

Biodegradation of CS NPs by chitosanase at 50 °C, analyzed as particle concentration after 2, 4, 6, 8, or 24 h; determined by nanoparticle tracking analysis (mean \pm SD; n=3).

	<i>CS NPs</i> [$\times 10^8$ particles/mL]	<i>CS NPs + 0.5 μL chitosanase</i> [$\times 10^8$ particles/mL]	<i>CS NPs + 5 μL chitosanase</i> [$\times 10^8$ particles/mL]
before	77.8 \pm 1.4	80.4 \pm 1.9	82.99 \pm 4.1
2 h	68.8 \pm 3.9	13.3 \pm 3.6	1.8 \pm 0.9
4 h	72.2 \pm 4.2	12.1 \pm 1.2	0.9 \pm 0.3
6 h	75.2 \pm 5.9	9.1 \pm 3.7	0.8 \pm 0.4
8 h	79.4 \pm 6.2	8.7 \pm 2.8	0.7 \pm 0.2
24 h	61.9 \pm 12.5	5.3 \pm 1.9	0.6 \pm 0.2

Loading of CS nanoparticles

To investigate the use of CS NPs as DDS, five different proteins/peptides were chosen to study the loading capacity of CS NPs. The selected proteins - Nrf2 (Mw: 1.3 kDa, IEP: 3.5), Lyso (Mw: 14 kDa, IEP: 11.4), OVA (Mw: 44 kDa, IEP: 4.5), BSA (Mw: 66 kDa, IEP: 4.7), and IgG1 (Mw: 150 kDa, IEP: 8.5) – represent proteins/peptides with different net charges and molecular weights. For this experiment, CS NPs prepared from 0.25 mg/mL solutions and a molar ratio of 10:1 (CS:TPP) were chosen. For the determination of protein EE and LR of the CS NPs, they were separated from the dispersing medium, containing the free protein, after 15 min equilibration, by ultracentrifugation. EE and LR were determined indirectly, by measuring the amount of free protein in the produced supernatant with a colorimetric method (BCA assay). The BCA assay was chosen as detection method of choice due to its broad application spectrum.

Although a direct method of quantification is always favored, the dissolution of the NPs without harming the cargo (in this case the protein) has to be ensured when such a method is employed. Different dissolution strategies were in fact tried, such as dissolution with *e.g.* HCl, NaOH, and 500 mM NaCl; however, either particles could not be completely dissolved, or the pH or ionic strength of the solubilizing agent led to aggregation of the protein.

As a result, an indirect method for quantification was preferred. Ultracentrifugation was chosen as a separation method, as other methods such as Vivaspin® or Centriscart® (membrane based methods), in which the protein has shown interactions with the membrane, made a quantitative analysis impossible. Before quantifying the EE and the LR, the

ultracentrifugation method had to be validated. In this respect, three parameters had to be guaranteed: a) a NP suspension had to form a quantitative pellet during ultracentrifugation, meaning complete removal of NPs from the supernatant; b) a protein solution had to show similar concentrations in the supernatant before and after ultracentrifugation to assure no precipitation of the protein under the employed ultracentrifugation conditions; c) the applicability and linearity of the BCA assay in the measured protein concentration range had to be verified.

A quantitative pellet of CS NPs was formed with ultracentrifugation at 45 000 x g and 20 °C for 60 min. Further, the supernatant was analyzed by nanoparticle tracking analysis, and no particles could be observed. The pellet which was formed by CS NPs after ultracentrifugation can be seen in Figure 4.5 (A), with visualization by SEM. Further all tested concentrations of protein solution before (“conc theory”) and after ultracentrifugation (“conc measured”) were determined with the BCA assay. The results of such measurement for a representative employed protein concentration of 40 µg/mL are shown in Figure 4.5 (B). It can be seen that the theoretical concentration and the concentration after ultracentrifugation is almost the same, thus no aggregation and sedimentation of the protein/peptide occurred. In a third step, the applicability and linearity range of the BCA assay was determined. It could be shown that blank NP supernatant showed a slight impact on the absorbance reading as determined with the BCA assay. However, these values were constant and could be subtracted from the measurement values of samples.

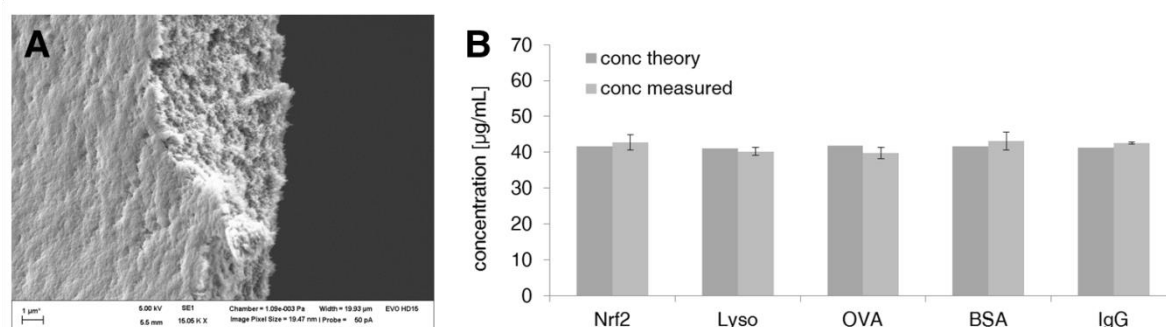


Figure 4.5: Validation of the indirect quantification method. (A) SEM image of the pellet formed by CS NPs after ultracentrifugation at 45 000 x g, 60 min, and 20 °C; (B) concentration of protein solutions before ultracentrifugation (conc theory) and after ultracentrifugation determined from the supernatant (conc measured).

NPs were washed with the Vivaflow® 50 system (100 kDa MWCO, PES membrane, Sartorius, Germany), freeze dried and weighed, for the determination of the LR. In contrast to Vivaspin® or Centrisart®, this membrane based, crossflow filtration method, also known as

tangential flow filtration, is very mild. It is stated in the Cross flow filtration method handbook that “a pressure difference across the filter drives components that are smaller than the pores through the filter. Components larger than the filter pores are retained and pass along the membrane surface, flowing back to the feed reservoir.”¹⁵⁷ With this method, NPs stay intact and do not show a blockage of the membrane as happened for the other two systems. This was verified by dynamic light scattering (DLS): before washing with the Vivaflow® 50 system, CS NPs showed a particle size of 151.1 ± 1.0 nm and a PdI of 0.14. After washing, particle size increased to 182.6 ± 3 nm with a PdI of 0.18. This slight increase in size can be explained by the concentrating effects of washing on the sample: For washing, 50 mL of nanoparticle suspension was used, but this volume was concentrated to 10 mL for freeze drying.

Physicochemical properties of loaded CS NPs from post loading experiments with different proteins/peptides can be found in Table 4.3. Further, EE and LR are shown.

Regarding size distribution, all formulations showed good PdI values, lower than 0.2, indicating a narrow particle size distribution. Blank particles showed a particle size of 155.5 ± 2.7 nm and a ζ -potential of $+31.5 \pm 0.8$ mV. In contrast to that, all formulations demonstrated a decrease in particle size varying extent when loaded with different proteins. Also a decrease in the ζ -potential could be seen following loading with proteins. The loading with OVA, however, is an exception, as both particle size and ζ -potential stayed constant.

The high EE determined for OVA and BSA of up to $82.8 \pm 1.6\%$ and $91.7 \pm 4.6\%$, as well as the high LR of $23.0 \pm 1.3\%$ and $25.6 \pm 1.3\%$, respectively, can be ascribed to the hydrophobic character of these proteins at pH 5.0. The IEP of these proteins is 4.5 (OVA) and 4.7 (BSA), meaning that both proteins are close to their IEP at the pH of the CS NP suspension. Nevertheless, compared to OVA, BSA-loaded NPs showed a decrease in particle size as well as a decrease in ζ -potential, indicating a different binding mechanism as compared to OVA. Concerning the encapsulation of the negatively charged Nrf2 (at pH 5.0), an encapsulated mass of around 50-60 μ g could not be further enhanced, meaning that such a system has a maximum LR of approximately 3%.

It can be seen that for some formulations (marked with *), the EE and LR could not been determined. This holds true for all the IgG formulations, as well as the formulation loaded with 125 μ g Lyso. For a higher mass of Lyso, however, an EE of up to $23.9 \pm 0.9\%$ and a LR of $6.6 \pm 0.3\%$ could be obtained. Surprisingly, Lyso was able to be encapsulated, although its IEP (11.4) is even higher than that of IgG (8.5), meaning a higher positively charge than the antibody at pH 5.0.

Table 4.3

Physicochemical properties of protein-loaded CS NPs as well as encapsulation efficiency (EE) and loading rate (LR), as determined indirectly with the BCA assay after separating loaded NPs from free protein *via* ultracentrifugation; *loading could not be determined; (mean \pm SD, n=3).

<i>CS NPs (loaded with)</i>	<i>mass_{initial} protein [μg]</i>	<i>Size [d.nm]</i>	<i>PdI</i>	<i>ζ-potential [mV]</i>	<i>mass_{encaps} protein [μg]</i>	<i>EE [%]</i>	<i>LR [%]</i>
blank	-	155.53 \pm 2.7	0.15	+31.5 \pm 0.8	-	-	-
IgG1 (Mw 150 kDa, IEP 8.5)							
125		133.8 \pm 8.7	0.13	+25.8 \pm 2.3	*	*	*
250		102.5 \pm 10.1	0.17	+23.3 \pm 1.6	*	*	*
500		106.3 \pm 20.3	0.18	+22.4 \pm 4.0	*	*	*
BSA (Mw 66 kDa, IEP 4.7)							
125		126.1 \pm 9.4	0.13	+21.3 \pm 1.7	144.1 \pm 8.5	113.7 \pm 6.7	7.9 \pm 0.5
250		89.6 \pm 3.5	0.17	+23.5 \pm 1.9	209.4 \pm 7.7	83.8 \pm 3.1	11.5 \pm 0.4
500		134.4 \pm 3.3	0.17	+21.4 \pm 3.7	463.8 \pm 23.1	91.7 \pm 4.6	25.6 \pm 1.3
OVA (Mw 44 kDa, IEP 4.5)							
125		154.4 \pm 24.2	0.15	+31.0 \pm 1.9	120.4 \pm 7.3	94.2 \pm 5.7	6.6 \pm 0.4
250		158.5 \pm 8.5	0.14	+31.0 \pm 1.1	228.6 \pm 13.3	90.5 \pm 5.3	12.6 \pm 0.7
500		163.7 \pm 26.0	0.18	+30.1 \pm 4.3	417.9 \pm 8.2	82.8 \pm 1.6	23.0 \pm 0.5
Lyso (Mw 14 kDa, IEP 11.4)							
125		116.9 \pm 11.8	0.13	+21.4 \pm 6.3	*	*	*
250		135.8 \pm 5.8	0.12	+24.3 \pm 2.7	48.0 \pm 10.4	19.2 \pm 4.2	2.7 \pm 0.6
500		139.1 \pm 23.6	0.11	+25.1 \pm 3.6	119.5 \pm 4.7	23.9 \pm 0.9	6.6 \pm 0.3
Nrf2 (Mw 1.3 kDa, IEP 3.5)							
125		131.6 \pm 21.6	0.13	+31.7 \pm 0.2	53.5 \pm 19.8	42.6 \pm 15.7	2.9 \pm 1.1
250		114.1 \pm 10.8	0.16	+24.6 \pm 1.3	28.0 \pm 10.4	11.1 \pm 4.1	1.5 \pm 0.6
500		105.8 \pm 5.3	0.18	+24.8 \pm 0.7	64.3 \pm 12.4	12.8 \pm 2.5	3.5 \pm 0.7

Apparently, a negative charge is not important for binding of the protein/peptide to the positively charged CS NPs. It seems that the most important factor influencing the binding is rather hydrophobicity or an approximately neutral charge at the desired pH – an observation which is entirely logical when considering the hydrophilic aqueous environment.

Stability of chitosan nanoparticles upon aerosolization

To determine their applicability for pulmonary delivery, CS NPs aerosolization properties and their stability during nebulization were studied by determining the physicochemical properties of the NPs before and after nebulization. CS NPs with a size of approximately 146.8 ± 1.4 nm and a PdI of 0.155 showed a ζ -potential of approximately $+32.7 \pm 3.7$ mV before nebulization. After nebulization, however, particle size increased to 173.3 ± 1.8 nm and a PdI of 0.195 was found, together with a ζ -potential of $+30.8 \pm 1.8$ mV. Furthermore, the nebulization process required a very long time frame, which additionally showed that the nebulization of CS NPs for pulmonary delivery is not efficient.

4.3.3 PREPARATION OF STARCH NANOPARTICLES

Starch NPs were prepared *via* charge-mediated coacervation in aqueous solution at RT. This process was adapted from Calvo *et al.*,^{113, 152} who prepared CS NPs from the interaction between CS and the small TPP. In contrast to the CS system, the starch NP formation involved the interaction of two polymeric materials of similar molecular weight. Partial charge neutralization due to the reaction of positively charged amine groups of PosSt with negatively charged carboxyl groups of NegSt led to the spontaneous formation of starch NPs, after mixing the two oppositely charged polymers under stirring. An advantage of the starch NP system is the isohydric pH of the nanoparticle suspension of 7.4 as well as the interaction of two polymers probably leading to more stable particles. The general advantage of coacervation is the mild character of this procedure as organic solvents, high temperatures, and sonication are not necessary for the NP preparation. Further, no additional stabilizers necessary for example during nanoprecipitation have to be used in this case. Therefore, it is very well suited as method to prepare NPs for loading with proteins and peptides.

The important parameters influencing particle properties, known from the CS NP preparation, were also investigated for the starch NP formation. The influence of polymer concentration (1 mg/mL, 0.5 mg/mL, 0.25 mg/mL), and different molar ratios (1:3, 1:1, 3:1 PosSt:NegSt) were studied, by adding NegSt to PosSt with the help of a syringe pump under stirring. Important physicochemical properties of the formed NPs in relation to the used material concentration and molar ratio are described in Table 4.4.

Table 4.4

Physicochemical characteristics of starch NPs related to material concentration (1, 0.5, 0.25 mg/mL) and molar ratio of components (1:3, 1:1, 3:1) used for charge-mediated coacervation.

<i>Formulation</i>	<i>PosSt conc</i> [mg/mL]	<i>NegSt conc</i> [mg/mL]	<i>PosSt:NegSt</i> [molar ratio]	<i>Size</i> [d.nm]	<i>PdI</i>	<i>ζ-potential</i> [mV]
Starch 1-1:3	1	1	1:3	181.6 ± 1.7	0.104	-31.1 ± 0.3
Starch 1-1:1	1	1	1:1	206.9 ± 0.7	0.078	-22.2 ± 0.1
Starch 1-3:1	1	1	3:1	346.9 ± 6.6	0.211	-10.3 ± 0.1
Starch 0.5-1:3	0.5	0.5	1:3	160.5 ± 0.6	0.088	-33.4 ± 1.6
Starch 0.5-1:1	0.5	0.5	1:1	179.0 ± 1.6	0.077	-23.5 ± 0.8
Starch 0.5-3:1	0.5	0.5	3:1	230.5 ± 4.2	0.084	-9.1 ± 0.1
Starch 0.25-1:3	0.25	0.25	1:3	138.9 ± 0.3	0.105	-37.0 ± 3.1
Starch 0.25-1:1	0.25	0.25	1:1	152.0 ± 0.2	0.077	-24.1 ± 0.6
Starch 0.25-3:1	0.25	0.25	3:1	209.3 ± 2.8	0.035	-8.5 ± 0.3

A narrow particle size distribution for the formulations is indicated by the consistently low PdI (always below 0.2). Particle size ranged from approximately 140-350 nm, depending on both the material concentration and molar ratio of components. The smallest particle size of 138.9 ± 0.3 nm was obtained for a molar ratio of 1:3, and 0.25 mg/mL material concentrations. Keeping the molar ratio constant, but increasing the material concentrations to 0.5 and 1 mg/mL resulted in increased particle sizes of 160.5 ± 0.6 and 181.6 ± 1.7 nm, respectively. As mentioned, varying the molar ratio also influenced particle size. NPs prepared from material concentrations of 0.25 mg/mL showed an increase in particle size from 138.9 ± 0.3 nm to 152.0 ± 0.2 nm and further to 209.2.8 nm for molar ratios of 1:3, 1:1 and 3:1, respectively, thus indicating that the particle size increased also with the content of PosSt.

The ζ-potential ranged from -35 to -10 mV in the investigated molar ratios, and in fact only depended on the molar ratio of PosSt and NegSt. For a molar ratio of 1:3 the ζ-potential was approximately -35 mV. A molar ratio of 1:1 resulted in a ζ-potential of around -25 mV, and starch NPs prepared in a molar ratio of 3:1 showed a ζ-potential of around -10 mV. Therefore, the greater the PosSt content of the formulation, the closer the ζ-potential was to 0.

4.3.4 PREPARATION OF LABELED STARCH NANOPARTICLES

For later characterization and cell interaction studies, starch NPs were prepared as described, but with different amounts of labeled PosSt_F. Results can be found in Table 4.5. It could be seen that the lower the PosSt_F content was present in the formulation, the lower the resulting ζ -potential, whereas particle size and PdI were constant. The hydrophobic character of the label probably caused the change in the ζ -potential. For later experiments, a 50:50 ratio of PosSt_F:PosSt was chosen to ensure similar physicochemical properties as the particles without label whilst at the same time a high fluorescence for analysis.

Table 4.5

Characteristics of starch NPs prepared with different amounts of labeled PosSt_F in a ratio of 1:1 (PosSt_F:NegSt) and a concentration of 0.25 mg/mL; **bold**: formulation used for uptake studies (*Chapter 6*).

<i>PosSt_F</i> [%]	<i>PosSt</i> [%]	<i>Size</i> [d.nm]	<i>PdI</i>	<i>ζ-potential</i> [mV]
100	0	132.5 ± 1.17	0.088	-26.4 ± 2.80
50	50	145.2 ± 0.7	0.1	-26.4 ± 2.8
10	90	147.1 ± 0.75	0.051	-22.7 ± 0.95
5	95	146.4 ± 0.72	0.064	-18.3 ± 0.12

4.3.5 CHARACTERIZATION OF STARCH NANOPARTICLES

Storage stability

To investigate the influence of the surface charge of the nanoparticles on storage stability, starch NPs prepared from 0.25 mg/mL formulations with a molar ratio of 1:3, 1:1 and 3:1 were chosen. Starch NP formulations showed different storage stabilities, when stored after preparation (Figure 4.6). Whilst Starch 0.25-1:3 and Starch 0.25-1:1 showed good stability with respect to size over 14 days, the formulation Starch 0.25-3:1, with a ζ -potential close to zero showed aggregation tendencies at both storage temperatures. For this formulation the weak surface charge was not able to electrostatically stabilize the NP suspension *via* repulsive forces.¹⁵⁸ Starch 0.25-1:1 showed best stability and was therefore chosen for further experiments.

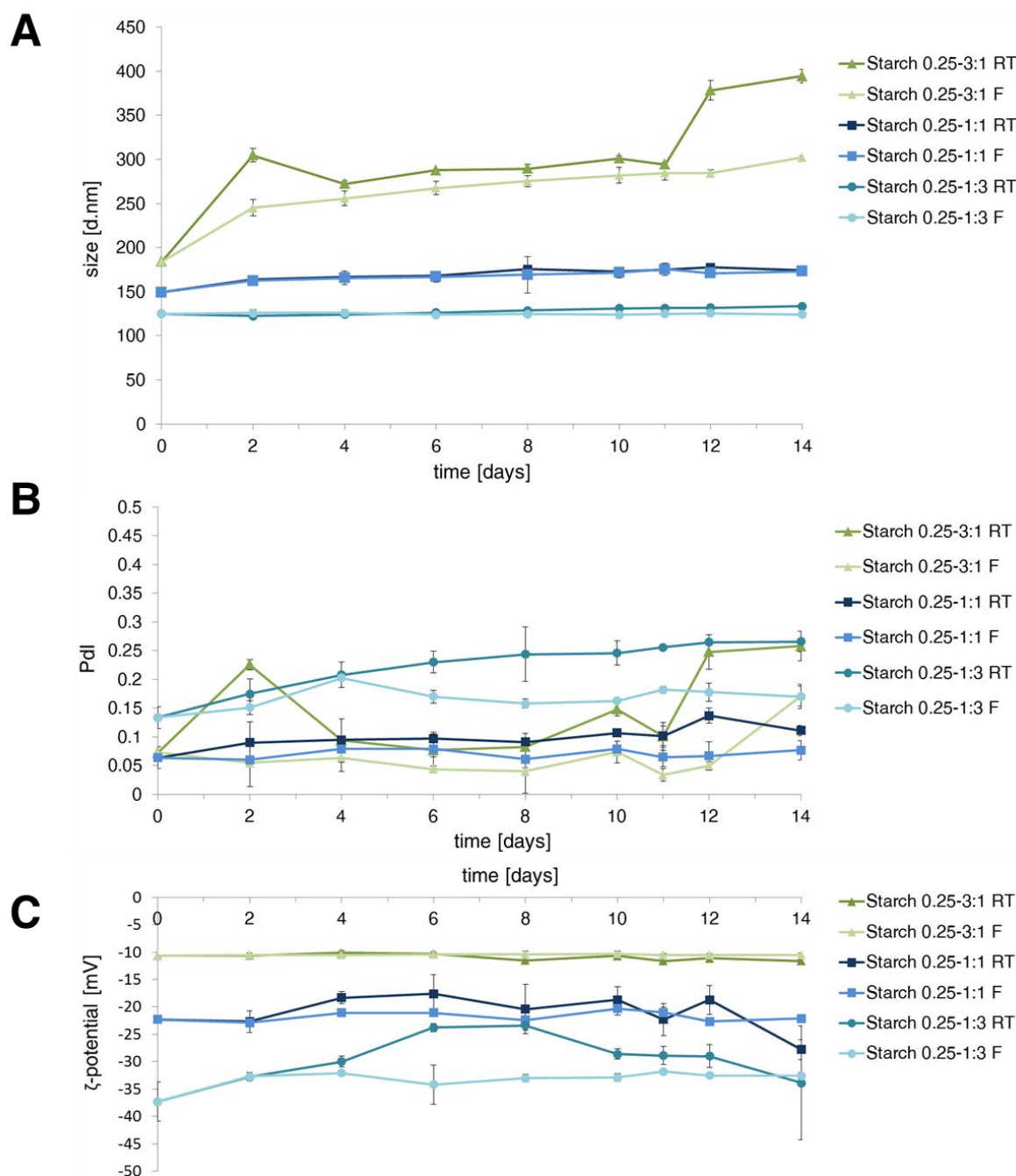


Figure 4.6: Stability study of various starch NP formulations prepared from 0.25 mg/mL solutions, stored either at RT or at 4 °C (F); (A) size; (B) Pdl; (C) ζ-potential.

Morphology

TEM images of starch NPs, prepared from 0.25 mg/mL solutions, incubated on a copper grid and stained with 1% PTA are shown in Figure 4.7. Black particles with a spherical, solid and consistent shape could be observed for all formulations. Image analysis indicated that sizes were comparable to size measurements determined by DLS. However, similar to CS NPs, starch NPs tended to aggregate during the drying process on the copper grid, forming a

polymer layer probably due to their gel-like, sticky character (data not shown). Therefore, starch NPs were stained and stabilized with 1% PTA during the drying process.

The formulation of Starch 0.25-1:3 (Figure 4.7 (C)) only showed few particles whereas a considerably greater amount of NPs could be found for formulations Starch 0.25-3:1 and Starch 0.25-1:1. The efficient interaction of the highly negatively charged starch NPs (ζ -potential of -37.0 ± 3.1 mV) with the slightly negatively charged TEM grids during the incubation time was probably hindered by repulsion.

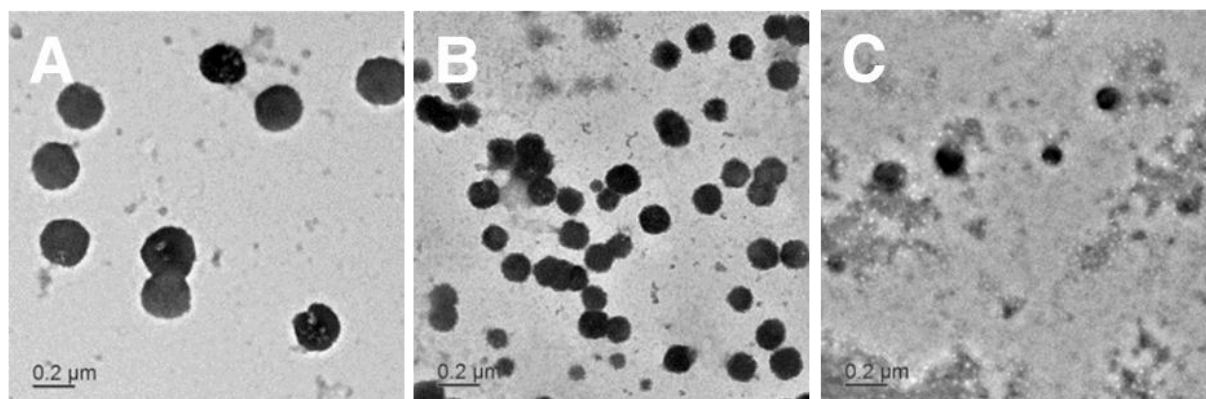


Figure 4.7: TEM images of starch NPs, positively stained with 1% PTA. (A) Starch 0.25-3:1; (B) Starch 0.25-1:1; (C) Starch 0.25-1:3.

Biodegradation

With respect to the use of NPs in the field of nanomedicine, one important point to address is the biodegradation of the system. As known, safety of NPs is not only a matter of size, but also depends on a variety of other factors such as dose frequency, toxicity of raw material, and importantly on their persistence in the body. The longer NPs stay in the human body without any biodegradation, the higher might be the risk of adverse effects, *e.g.* due to unintentional activation of the immune system.³⁴

In general, degradation products of NPs also have to be determined to be safe, otherwise these could lead to a non-specific immune response as well. However, by choosing starch and starch derivatives as material for the preparation of a DDS, this issue has already been considered. Maintenance of degradability should lead eventual breakdown to glucose and glucose units (or oligomers) with ethylenediamine side chains, which should be readily excreted due to low molecular weight. The latter is further reduced by using a NP system, consisting of both positively and negatively charged starch derivatives. To test the biodegradability of the starch NP system, not only by unspecific degradation mechanisms, but also by specific enzymatic degradation, Starch 0.25-1:1 samples were incubated in a proof of

concept study at 37 °C with or without α -amylase, an enzyme found in the human body (*e.g.* in the saliva, the pancreatic juice, the serum¹⁵⁹, or the lung¹⁶⁰). After certain time points, samples were taken and particle concentration was determined by nanoparticle tracking analysis. Compared to a control group (starch NPs stored at 37 °C without enzyme), a decrease in particle concentration could be observed already after 2 h incubation with α -amylase at 37 °C (Table 4.6). Yamada *et al.* found that modified starch-PEI derivatives were still able to be degraded by α -amylase, although the degradation was slower compared to the degradation of unmodified starch.¹²⁸ The synthesized starch derivatives in the current work showed a smaller change in molecular structure than the starch-PEI derivatives in comparison to unmodified starch. Moreover, the incubation of starch NPs with α -amylase showed that even after charge-mediated coacervation, the two starch derivatives were able to be degraded by the human enzyme α -amylase. The fluctuations in particle numbers for the control group can be ascribed to the analytical method. Only a limited amount of particles can be measured due to the high dilution necessary for this method. Thus, NTA does not allow for exact particle counting but rather gives an order of magnitude. The fluctuations seen within the control group are therefore likely the result of the intrinsic measurement error. The trend nevertheless is clear.

Table 4.6

Biodegradation of starch NPs by α -amylase incubated at 37 °C; analyzed as particle concentration after 2, 4, 6, or 8 h; determined by nanoparticle tracking analysis; (mean \pm SD, n=3).

	<i>Starch NPs</i> [x E ⁸ particles/mL]	<i>Starch NPs + α-amylase</i> [x E ⁸ particles/mL]
before	44.3 \pm 2.9	44.5 \pm 0.2
2 h	56.1 \pm 8.0	2.7 \pm 0.6
4 h	46.1 \pm 1.7	1.7 \pm 1.1
6 h	55.4 \pm 10.4	1.7 \pm 0.8
8 h	50.5 \pm 3.8	0.9 \pm 0.6

Loading of starch nanoparticles

As the starch NPs should act as DDS for the delivery of proteins, their loading capacity was evaluated, by loading of four different proteins. The selected proteins - vanco (Mw: 1.5 kDa, IEP: 7.5), insulin (Mw: 6 kDa, IEP: 5.3), RNase A (Mw: 14 kDa, IEP: 9.6), and IgG1 (Mw:

150 kDa, IEP: 8.5) – represent a range of IEP and molecular weights. Starch NPs from 0.25 mg/mL solutions and a molar ratio of 1:1 were chosen, showing best stability and a negatively surface charge of around -25 mV. Table 4.7 shows the physicochemical properties of loaded starch NPs as well as EE and LR, determined indirectly with the BCA assay after separating loaded NPs from free protein *via* ultracentrifugation. Here, the same procedure for validation was applied as for the CS NPs: the ultracentrifugation at 45 000 x g and 20 °C for 90 min showed no remaining NPs in the supernatant, as determined by nanoparticle tracking analysis. Further, tested protein solutions showed stable concentration readings before and after ultracentrifugation, indicating that no aggregation or sedimentation of the proteins occurred. The supernatant of starch NPs, similar to CS NPs, showed a low absorbance in the BCA that was stable and could therefore be subtracted from the calculations.

EE and LR differed for all four proteins, and the EE was affected by the initial amount of protein added: the lower the protein amount, the higher the EE. However, the LR was enhanced by increasing the initial amount of added protein. Calvo *et al.* observed the same phenomenon for the encapsulation of BSA into CS NPs.¹¹³ A narrow PdI could be observed for all formulations, except for the formulation loaded with 500 µg IgG1. An increase in size, combined with a decrease in ζ-potential indicated that the loading with IgG1 was successful. It seemed that the loading could be increased from approximately 4.5% (125 µg and 250 µg IgG1) up to 12.0% for the 500 µg formulation. However, when taking into account the broad size distribution of NPs (indicated by a PdI of 0.39), such data must be interpreted cautiously. As the EE was obtained *via* indirect measurement, protein aggregation could have biased the results. A saturation for IgG1-loaded starch NPs could be already found for the 125 µg formulation, as no difference was observed between the encapsulated mass and the LR of the 125 µg loaded NPs and the 250 µg loaded NPs. For these formulations, the encapsulated mass was found to be 63 and 72 µg, respectively, and the LR was determined as 4.4 and 4.9%, respectively. Starch NPs loaded with RNase A showed no saturation, as the loading could be increased from 4.9% for the 250 µg loaded formulation up to 9.6% for the 750 µg formulation; however, the EE dropped from 27.9% for the 250 µg loaded NPs to 18.1% for the 750 µg loaded NPs. The same could be observed for insulin: an EE of 24.9% was seen following loading with 250 µg of insulin, a value which dropped to 15.9% following loading with 750 µg insulin. In contrast, an increase in LR be observed from 4.3% to 8.2% for such formulations. The most promising loading however was achieved for vanco, which showed a LR of up to 22.8% for the 750 µg loaded formulation with at the same time a high EE of 43.5%.

Table 4.7

Physicochemical properties, EE and LR of starch nanoparticles loaded with different amounts of IgG1, RNase A, insulin or vancomycin. Results represent mean \pm SD, n=3.

<i>starch NP (loaded with)</i>	<i>mass_{initial} protein [μg]</i>	<i>Size [d.nm]</i>	<i>PdI</i>	<i>ζ-potential [mV]</i>	<i>mass_{encaps} protein [μg]</i>	<i>EE [%]</i>	<i>LR [%]</i>
blank	-	157.7 \pm 2.2	0.08	-23.7 \pm 0.7	-	-	-
IgG1 (Mw 150 kDa, IEP 8.5)							
	125	179.6 \pm 6.1	0.10	-18.0 \pm 0.2	63.2 \pm 14.7	50.6 \pm 11.7	4.4 \pm 1.0
	250	237.4 \pm 15.6	0.17	-13.1 \pm 0.3	71.9 \pm 1.9	28.8 \pm 0.8	4.9 \pm 0.1
	500	556.5 \pm 49.5	0.39	-11.6 \pm 0.9	174.3 \pm 2.4	35.9 \pm 0.5	12.0 \pm 0.2
RNase A (Mw 14 kDa, IEP 9.6)							
	250	171.5 \pm 0.3	0.07	-21.6 \pm 0.6	72.0 \pm 3.4	27.9 \pm 1.3	4.9 \pm 0.2
	500	172.9 \pm 1.3	0.05	-17.7 \pm 2.4	103.5 \pm 3.1	20.1 \pm 0.6	7.1 \pm 0.2
	750	195.0 \pm 31.5	0.13	-20.7 \pm 0.5	139.8 \pm 21	18.1 \pm 2.7	9.6 \pm 1.4
insulin (Mw 6 kDa, IEP 5.3)							
	250	157.6 \pm 0.7	0.09	-22.7 \pm 1.2	62.4 \pm 3.1	24.9 \pm 1.2	4.3 \pm 0.2
	500	162.3 \pm 0.4	0.06	-21.0 \pm 0.3	73.9 \pm 4.7	14.8 \pm 0.9	5.1 \pm 0.3
	750	160.3 \pm 0.9	0.07	-20.4 \pm 0.5	119.2 \pm 4.3	15.9 \pm 0.6	8.2 \pm 0.3
vanco (Mw 1.5 kDa, IEP 7.5)							
	250	163.9 \pm 0.4	0.08	-23.4 \pm 0.7	205.2 \pm 7.7	81.1 \pm 3.0	14.2 \pm 0.5
	500	164.7 \pm 0.8	0.05	-21.2 \pm 0.3	258.6 \pm 0.2	51.1 \pm 0.1	17.8 \pm 0.1
	750	164.5 \pm 0.6	0.06	-21.2 \pm 0.4	330.1 \pm 4.1	43.5 \pm 0.5	22.8 \pm 0.3

The differences in EE and LR can be ascribed to the differences in IEP and molecular weight of the various proteins and peptides. Calvo *et al.*, amongst others, described the phenomenon of particle protein loading as a function of electrostatic interactions between protein and polysaccharide.¹¹³ As the loading of the proteins into the starch NPs is a result of the electrostatic interactions between negatively charged NPs and protein, the IEP of each protein at the pH of the starch NP suspension (pH 7.4) has to be taken into account. Both IgG1 and RNase A are positively charged at pH 7.4, whereas insulin is negatively charged and vancomycin is neutral. A high EE and loading for IgG1 and RNase A would therefore be expected. However, IgG1 and RNase A loaded starch NPs showed rather low LR of 4.9% and 9.6%, respectively. This low loading, which was slightly higher in the case of RNase A, could be a result of the fact that the system loaded with IgG1 was already saturated in the case of the 250 μg formulation, due to steric hindrance. IgG1 is an antibody with a molecular weight of around 150 kDa that needs more space, when binding to the NP surface than *e.g.*

RNAse A with a molecular weight of around 14 kDa. Insulin showed a similar behavior to RNAse A: a loading of 8.2% could be achieved for the 750 μ g formulation, although insulin is negatively charged at pH 7.4. Vancomycin, which is neutral at pH 7.4, showed the highest loading of 22.8% probably due to a combined effect of low water solubility at this pH, and the small molecular weight of 1.5 kDa.

In order to evaluate protein integrity during the loading, sodium dodecyl sulfate polyacrylamide gel electrophoresis (SDS-PAGE) was performed. For such investigations, IgG1 was chosen as model protein and SDS-PAGE was run on a precast 10% polyacrylamide gel at 10 mA. Results can be found in Figure 4.8. It can be seen that the band of IgG1 loaded into starch NPs (lane 1) is at the same level as IgG1, stored at 4 °C (lane 3), indicating that no protein aggregation or loss of molecular weight occurred during the loading of the starch NPs with IgG1. The smearing in lane 1 can be ascribed to some interaction between blank starch NPs and the stain Coomassie Blue, as this was also visible for blank starch NPs (lane 2). Further studies showed, that the smearing was due to some unspecific interaction between PosSt and the staining.

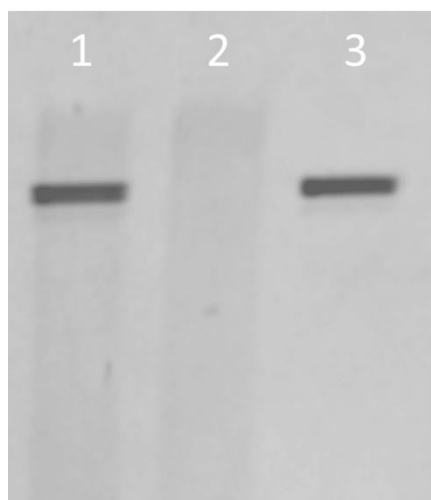


Figure 4.8: SDS-PAGE of IgG1 loaded starch NPs (lane 1), blank starch NPs (lane 2) and IgG1 standard (lane 3); samples were stained with Coomassie Blue.

Aerosolization properties of starch nanoparticles

To determine their applicability for pulmonary delivery, the aerosolization properties and stability of starch NPs during nebulization was studied. Physicochemical properties of the starch NPs were measured before and after nebulization. Further, the nebulization of labeled starch NPs and of starch NPs loaded with IgG1 was studied; results can be found in Table 4.8.

Table 4.8

Physicochemical properties of various starch NP formulations before and after nebulization.

<i>Starch NPs</i>	<i>Size [d.nm]</i>	<i>PdI</i>	<i>ζ-potential [mV]</i>
before	147.9 ± 2.4	0.074	-21.8 ± 1.1
after	152.4 ± 1.6	0.058	-23.5 ± 1.3
labeled before	145.2 ± 0.7	0.1	-26.4 ± 2.8
labeled after	145.2 ± 2.2	0.089	-14.9 ± 6.62
IgG1 loaded before	184.0 ± 2.9	0.21	-18.5 ± 1.3
IgG1 loaded after	212.3 ± 1.8	0.25	-19.3 ± 2.4

Starch NPs showed similar physicochemical properties before and after nebulization, which was observed to run smoothly. Labeled starch NPs showed similar size and PdI values before and after nebulization, however, ζ-potential decreased from about -26 mV to about -15 mV. This could be ascribed to the hydrophobic label of the polymer, which might change the hydrophobicity of the NPs and thus the tightness of the surface binding of the ion layers, contributing to the ζ-potential. The physiochemical properties of starch NPs loaded with IgG1 were seen to change upon nebulization, observed as an increase in size from 184 nm up to 212 nm and an increase in PdI from 0.21 to 0.25. Although the ζ-potential did not change before and after nebulization, the stability of IgG1 NPs during nebulization was not deemed to be satisfactory, indicating a destabilization of the loaded nanoparticles during nebulization.

For uptake studies (*Chapter 6*), the deposited amount of starch NPs on a Transwell® membrane was studied by applying different volumes of starch NP suspension with the Aeroneb®Lab nebulizer, followed by weighing and calculation of the amount of deposited starch NPs. The results can be found in Figure 4.9. It can be seen that increasing the applied volume resulted in an increase in the deposited mass. The volume that was chosen for uptake studies was 250 µL, meaning a deposited mass of starch NPs of approximately 41.1 ± 0.7 µg.

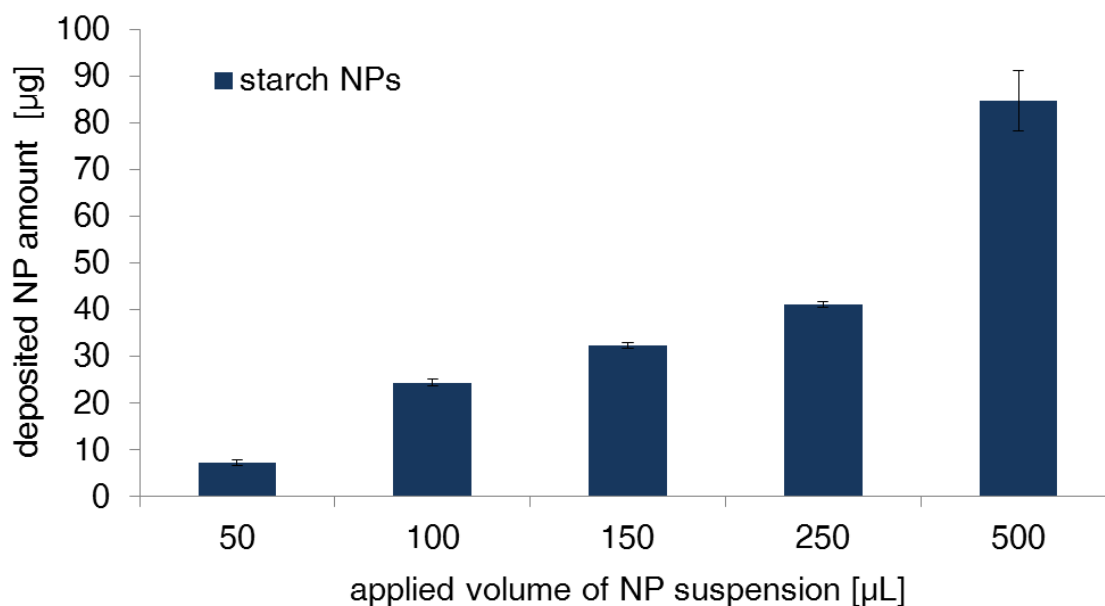


Figure: 4.9: Deposited starch NP amount on a Transwell® membrane, after nebulization of different volumes of starch NP suspension with the Aeroneb®Lab nebulizer.

4.4 COMPARISON OF CHITOSAN AND STARCH NANOPARTICLES

Regarding the preparation process, both nanoparticle types were able to be prepared in aqueous medium. Compared to CS NPs, starch NPs were prepared from two polymers instead of a polymer interacting with a highly charged small compound. The parameters influencing physicochemical properties of NPs were similar for both NP types. The material concentration was the most important factor with respect to influence on particle size, whereas the molar ratio of components was important for the surface charge. Both particle types showed particle sizes of around 150 nm, but differed in their ζ -potential. CS NPs showed a positive surface charge, whereas starch NPs showed a negative surface charge. Due to the fact that the systems are based on electrostatic interactions, the preparation medium was, not surprisingly, found to influence particle properties. As the labeling of CS was not successful, labeled CS NPs could not be prepared. The preparation of labeled starch NPs, however, was successful, with particle properties being similar to the unlabeled starch NPs.

Regarding their morphology, both particle types showed a spherical appearance with a gel-like character. It has to be mentioned that the addition of PTA facilitated a negative staining of the CS NPs, whereas the starch NPs were positively stained with PTA (being taken up into the particles).

The chosen starch NP formulation (Starch 0.25-1:1) showed better storage stability, although CS NPs storage stability was only evaluated for a short period of time and therefore is hard to compare. Also, both NP types were able to be degraded by their specific enzyme.

The loading behavior was also similar for both types of NPs. Molecules with an IEP close to the pH of the NP suspension showed the best LR.

Aerosolization properties differed a lot between the two particle types. Whilst CS NPs were not stable during nebulization, starch NPs and also labeled starch NPs were stable during nebulization. Loaded starch NPs, however, showed destabilization tendencies.

4.5 CONCLUSION

CS NPs were used as a well-known and well-described model DDS to evaluate a mild preparation process to be further employed for the production of starch NPs, and to develop analytical methods suitable for characterization of the newly developed starch NPs. For the preparation process, key parameters were found to be the polymer concentration, influencing the size of the NPs, as well as molar ratio of employed components, which influence the surface charge of the NPs. Due to their gel-like structure, CS NPs were not stable during drying, which was a challenge for imaging the CS NPs. One possible solution for studying the morphology of CS NPs was found in TEM imaging after 1% PTA staining of the CS NPs. Storage stability of CS NPs in the fridge was evaluated for 6 days. Particles were stable during that time. The biodegradation of CS NPs with the help of an enzyme (chitosanase) was successfully demonstrated.

The derivatization of potato starch into water soluble, positively (PosSt) and negatively charged (NegSt) starches enabled the formation of starch NPs in aqueous medium *via* charge-mediated coacervation. As determined by TEM images after 1% staining with PTA, starch NPs showed a spherical shape. Physicochemical properties of NPs (namely size and surface charge) could be tuned by varying the molar ratio and concentration of the two components. Starch NPs were demonstrated to be biodegradable by α -amylase. Further, starch NPs were loaded with proteins and peptides of different net charges and molecular weights. Vanco was found to be the best suitable candidate, with a LR of 23% and an EE of 44%, probably favored by the combination of the low molecular weight and the hydrophobicity of the peptide at the pH of the NP suspension. It can therefore be concluded that starch NPs, prepared by the utilized mild and easy technique, have the potential to be further explored as platform for pulmonary delivery of proteins and peptides.

5. AEROSOL DELIVERY OF NANOPARTICLES TO THE DEEP LUNG – NANOPARTICLES EMBEDDED IN MICROPARTICLES

The author of the thesis made the following contribution to the chapter:

Planned and designed all experiments, performed experiments related to particle preparation and characterization, analyzed all data from the above mentioned studies, interpreted all experimental data and wrote the chapter, if not stated otherwise.

Dr. Robert Haberkorn performed the XRPD studies at the Department of Inorganic Solid State Chemistry, Saarland University.

Charlotte Steinmetz, who did an internship at the institute and who was instructed by the author of the thesis, contributed to the chapter by performing some NGI experiments.

5.1 INTRODUCTION

The pulmonary application of proteins and peptides is a promising non-invasive route of administration. Systemic delivery *via* the lungs is an interesting approach as a large absorptive surface area, a high vascularization and a thin air-blood-barrier support the uptake of APIs from this site. Additionally, the avoidance of the first-pass effect, known to be present in the case of oral delivery, shows further advantages for pulmonary administration.⁸⁹ Local delivery to the lungs may also present a number of benefits, and as such, COMPACT has chosen local lung delivery as one of their preferred routes of administration. This is of importance for diseases such as asthma, chronic obstructive pulmonary disease (COPD), lung cancer, cystic fibrosis (CF), idiopathic pulmonary fibrosis (IPF) and pulmonary infections. The direct application to the site of action is favored, due to reduced systemic side effects and a rapid onset of action. The actual target of course depends on the disease, and was chosen in the context of COMPACT to be the alveolar epithelium. This site is heavily affected in IPF, in which repeated cycles of epithelial cell injury may lead to an activation of alveolar epithelial cells, resulting in an abnormal wound repair with exaggerated accumulation of fibroblasts and extracellular matrix.¹⁶¹⁻¹⁶⁴ A first model drug, that could actually function as API in the context of IPF is the intracellularly-active peptide Nrf-2.¹⁵³ Achieving uptake of such a peptide into non-phagocytic, epithelial cells is however considerably more challenging compared to *e.g.* macrophages, which are known to engulf nearly everything (in accordance with their physiological function). The previously developed nanoparticle formulation (*Chapter 4*) shows a good size range suitable for the uptake into epithelial cells of the deep lung, which requires nanoparticle carriers below 200 nm in size.^{165, 166}

Amongst other factors, the deposition of particles in the lung is influenced by the physical and chemical properties of the particles, which can be easily addressed, by controlling the preparation parameters of the particles. It is known, that particle deposition occurs due to three major mechanisms: impaction, sedimentation and diffusion.⁸³ Very large particles ($> 8 \mu\text{m } d_{\text{aero}}$) deposit already in the mouth and throat. Medium sized particles ($d_{\text{aero}} \sim 4 - 10 \mu\text{m}$) tend to deposit in the bronchioles, whilst smaller particles ($20-50 \text{ nm} < d_{\text{aero}} < 2-5 \mu\text{m}$) deposit in the alveolar region.^{101, 167-169} As can be seen, the size of developed nanoparticles ($\sim 150 \text{ nm}$) is not ideally suited for respiration¹⁷⁰ and delivery to the deep lung.

Thus, the previously developed formulation needs further optimization in order to allow for efficient deposition in the deep lung. Besides applying APIs by nebulizers, and metered dose inhalers (MDI), dry powder inhalers (DPI) are favored. These systems show numerous

advantages, being propellant-free, portable and easy to operate, and showing an improved stability of the formulation as a result of existence in a dry state.¹⁷¹⁻¹⁷³

Spray drying is a mild, commonly used method for preparation of dry powders.^{168, 174} It has been applied to a variety of substances, such as antibiotics,¹⁷⁵ vaccines,¹⁷⁶ and peptides.¹⁷⁷ The Nano Spray Dryer (Büchi B-90) is furthermore a good choice, as it is known to facilitate the preparation of particles in a size range of a few μm , interesting for deep lung delivery. Different particle types can be produced by spray drying. Hollow Trojan microparticles, as prepared by Tsapis *et al.*, consist of a NP layer building the microparticle.¹⁰³ Various porous particle types were introduced by Yang *et al.*¹⁷⁸ and Ungaro *et al.*¹⁷⁹ Also matrix particles are known, where the nanoparticles are embedded in a microparticle matrix.^{180, 181}

An advanced carrier system was designed for deep lung deposition of nanoparticles developed as nano- in microparticle dry powder formulation. This system was proposed to a) escape macrophage clearance and b) mediate alveolar epithelial cell uptake of the NPs. Selection of excipients used for microparticle formation was made based on their possession of high water solubility. Consequently, in this chapter, the advanced carrier system for pulmonary application was prepared from CS and Starch NPs, spray dried with different excipients, *i.e.* lact, treha, and manni. Various characterization methods were used to assess the properties of the microparticles: the most important investigation being the redispersion behavior of NPs after disintegration of the microparticles, followed by assessment of morphology, powder crystallinity, and localization of NPs in the microparticles, as well as particle size, and aerodynamic properties.

5.2 MATERIALS AND METHODS

5.2.1 MATERIALS

Partially hydrolyzed potato starch (M_w 1 300 000 g/mol, approx. 33% amylose content) was a gift from AVEBE (Netherlands). Negatively (NegSt) and positively (PosSt) charged starches were synthesized in house. Chitosan UP CL 113 (CS) was bought from NovaMatrix (Norway). Sodium tripolyphosphate (TPP) was purchased from Merck (Germany). IgG1 was kindly donated by Boehringer Ingelheim (Germany). Mannitol (manni), trehalose dihydrate (treha) and α -lactose monohydrate (lact) were bought from Sigma Aldrich (USA). G-Blocks (guluronic acid oligomers, consisting of more than 90% guluronic acid residues and some mannuronic acid residues, dp10 and d22) were a kind gift from the Department of Biotechnology, Norwegian University of Science and Technology (NTNU). Alexa Fluor 647 carboxylic acid (succinimidyl ester) and Bodipy FL-C5 NHS Ester (succinimidyl ester) were

obtained from Life Technologies (USA). Purified water was produced by a milliQ water purification system (Merck Millipore, USA). All other reagents were of analytical grade.

5.2.2 PREPARATION OF MICROPARTICLES

Scale-up of nanoparticle preparation

For upscaling of CS NPs, the preparation was performed as described earlier (*Chapter 4*), but with an increased volume: NP formation therefore occurred spontaneously after adding 10 mL of TPP solution to 50 mL of CS solution under stirring at 300 rpm (molar ratio 10:1, CS:TPP). The final pH value was 5.5.

Upscaling of starch NPs was also facilitated by an increase of volume: 20 mL of NegSt were added to 20 mL of PosSt under stirring at 700 rpm (molar ratio 1:1). The final pH value was 7.4. For loaded starch NP samples, 150 μ L of IgG1 solution (5 mg/mL) was added to 40 mL of starch NP suspension. Stirring speed and injection rate were adjusted for both CS and starch NP formulations to obtain NPs of similar physicochemical properties compared to NP prepared in *Chapter 4*.

Microparticle preparation

Either blank NP suspension or NP suspension with excipient was spray dried with a nano spray dryer (Büchi B-90, Büchi, Switzerland). Lact, treha or manni was added to the NP suspension prior to spray drying, in mass ratios of NP:excipient 1:5, 1:10 and 1:20. Additionally, the influence of microparticle matrix forming G-Blocks (dp10, dp22) on the physicochemical properties of NP suspensions was tested. Different spray caps (4 μ m, 5.5 μ m and 7 μ m) and inlet temperatures (90 °C, 70 °C, and 50 °C) were investigated for spray drying. The spray dryer was equilibrated with water prior to every spray drying run. The spray drying process for further particle analysis was performed at 70 °C inlet temperature, an outlet temperature of maximum 40 °C and a gas flow of 130 L/min, using the 5.5 μ m spray cap. The spray rate was always 100% and samples - typical batch size was 40 or 50 mL feed volume - were kept on ice during the spray drying process. For NGI experiments, 10 μ L sodium fluorescein solution (FluNa, 5 mg/mL) was added to each sample and spray drying was performed under light protection. Samples were stored in a desiccator until usage.

5.2.3 NANOPARTICLE RELEASE FROM MICROPARTICLES

Release of NPs from the microparticle matrix was tested in a proof of concept study by dissolving approximately 1 mg of microparticles in 1 mL of purified water. After 10 s

vortexing, the particle size and PDI of released NPs was determined by DLS using the Zetasizer Nano ZSP (Malvern Instruments, UK) with a scattering angle of 173 °.

5.2.4 MORPHOLOGY

Morphology of microparticles was examined by SEM (JSM 7001F Field Emission SEM (Jeol, Japan)). Samples were immobilized on a carbon disc and sputtered with gold (layer thickness approx. 10 nm) prior to scanning. The accelerating voltage was 5 kV. In case of the Pharmaceutical Aerosol Deposition Device on Cell Cultures (PADD OCC) deposition study, samples were directly deposited on SEM carbon discs and analyzed as mentioned above.

5.2.5 PARTICLE SIZE DISTRIBUTION

Particle size distribution was determined by image analysis of SEM images, using the Fiji Software (Fiji is a distribution of ImageJ available at <http://fiji.sc>). Particle sizes were measured, grouped into different intervals and plotted as number of particles [%]. More than 100 particles were analyzed per image. Additionally, particle size distribution was analyzed by static laser light diffraction using the HORIBA LA-950 (HORIBA, Japan) powder feeder attachment. Vibration and air suction allowed the powder to pass through a laser light beam and to be analyzed directly as dry powder without the need of applying a non-solvent.

5.2.6 POWDER CRYSTALLINITY

For X-ray powder diffraction (XRPD) experiments, samples were analyzed by a diffractometer of the type Bruker D8 Advance, equipped with an 1D-detector 'Lynxeye' using variable divergence slit and Cu-K α radiation. X-ray diffraction is based on radiation scattering and interference. Diffraction occurs when light is scattered by a periodic array with long-range order, producing constructive interference at specific angles. The scattering of X-rays from atoms produces a diffraction pattern, which contains information about the atomic arrangement within the crystal. The conditions for constructive interference are described by Braggs Law, where n is the order of the diffracted beam, λ is the wavelength of the x-ray radiation, d is the distance between the parallel lattice planes from which the waves are scattered and θ is the angle between the x-rays and the lattice plane:¹⁸²

$$n * \lambda = 2 * d * \sin\theta$$

According to Bragg's law, constructive interference for a set of atomic planes with d -spacing only occurs when the incident angle is θ . When the scattered waves interfere constructively,

they remain in phase, as the path length of each wave is equal to an integer multiple of the wavelength. Such an occurrence yields a peak in the diffractogram.

The position and intensity of peaks in a diffraction pattern are determined by the crystal structure. The absence of peaks in the diffractogram or the presence of so-called halos indicates a completely amorphous material, which does not have a periodic array with long-range order, and so does not produce a diffraction pattern.¹⁸²

5.2.7 LOCALIZATION OF NANOPARTICLES IN MICROPARTICLES

The internal composition of the carrier system was observed by a confocal laser scanning microscope (Zeiss LSM710, Zeiss, Germany). Lasers at 405 nm (4',6-Diamidino-2-phenylindole, DAPI), 488 nm (starch NPs) and 633 nm (IgG1) were used for detection. Labeled starch NPs were spray dried with treha (mass ratio 1:20) and DAPI (12.5 ng/mL). For loaded particles, 150 μ L labeled IgG1 (5 mg/mL) was added to the labeled starch NP suspension beforehand. Aliquots of the spray dried powders were fixed on a glass slide. Confocal images were analyzed using the Zen 2012 software (Carl Zeiss Microscopy GmbH). IgG1 was labeled with Alexa Fluor 647 carboxylic acid (succinimidyl ester) according to the manufacturers' protocol (Life Technologies, USA). Purification was performed with PD-10 Desalting Columns (GE Healthcare, UK).

5.2.8 AERODYNAMIC PROPERTIES

The mass median aerodynamic diameter (MMAD), the geometric standard deviation (GSD), and the fine particle fraction (FPF) of microparticles prepared by spray drying of NPs with excipient in a mass ratio 1:20 and 10 μ L FluNa (5 mg/mL) for analysis were determined with the Next Generation Impactor (NGI). For NGI experiments, the flow rate was adjusted to 60 L/min and the time of aspiration was set to 4 s. The powder inhaler (Handihaler[®], Boehringer Ingelheim, Germany) was loaded with a hard gelatin no.3 capsule, filled with 10 mg of powder ($n = 3$). After inhaler actuation, particle deposition on the NGI was determined by correlating fluorescence intensity to deposited mass. Therefore, a standard curve was prepared from each sample and fluorescence intensity was measured at $\lambda_{\text{ex}} = 485$ nm and $\lambda_{\text{em}} = 530$ nm. The fluorescent dye FluNa was equally distributed throughout the formulation. FPF is defined as the part of the inhaled dose with an aerodynamic diameter < 5 μ m in %. Further important parameters are the MMAD and the GSD. The MMAD is correlated to the detected mass within the NGI and is the mass median aerodynamic diameter, meaning that 50% of the

particles are smaller than this value and 50% are larger. The GSD gives an idea of the particle distribution.

5.2.9 PADD OCC DEPOSITION

The deposition of microparticles was studied with the help of the PADD OCC (Pharmaceutical Aerosol Deposition Device on Cell Cultures), which is a deposition device for dry powder, developed in-house.^{183, 184} Particles were analyzed qualitatively and quantitatively for following cell interaction studies (*Chapter 6*). Deposition behavior and morphology was analyzed after direct deposition on carbon disc wafers, by SEM. Particle deposition was determined quantitatively by correlating fluorescence intensity to deposited mass. For quantification, microparticles, co-spray dried with FluNa were used; a standard curve was prepared from each sample and fluorescence intensity was measured at $\lambda_{\text{ex}}=485$ nm and $\lambda_{\text{em}}=530$ nm.

5.3 RESULTS AND DISCUSSION

5.3.1 PREPARATION OF MICROPARTICLES

Scale-up of nanoparticle preparation

For preparing the microparticles from the NP suspension *via* spray drying, the preparation method of NPs was up-scaled. As an increase in concentration of the solutions led to an increased size of the NPs (*Chapter 4*), the process was up-scaled by increasing the volume but keeping the concentration constant at 0.25 mg/mL. Different beaker types and injection rates were tested and the impact on physicochemical properties of NPs is shown in Table 5.1.

Both NP types showed a size around 150 nm, with a narrow particle size distribution. They differed, however, in their ζ -potential, with CS NPs showing a positive ζ -potential of approximately +35 mV and starch NPs showing a negative ζ -potential of approximately -20 mV.

It could be concluded that the NP preparation process was suitable for up-scaling by increasing the volume. However, a good solvent mixture has to be assured, by selection of a suitable beaker type, magnetic stirrer and injection rate, depending on the kind of syringe to be employed in the preparation process. Following investigation and control of these process parameters, the physicochemical properties of NPs stayed constant as compared to the original preparation process.

Table 5.1

Characteristics of NPs in process upscaling studies prepared from 0.25 mg/mL solutions and a molar ratio of 1:1 (PosSt:NegSt) and 10:1 (CS:TPP) with varying process parameters; **bold**: formulations used for microparticle preparation. Beaker type 1123: 150 mL; beaker type 1122: 100 mL; beaker type 1169: 50 mL; all from VWR, USA).

<i>Beaker type</i>	<i>Syringe volume [mL]</i>	<i>Injection rate [mL/min]</i>	<i>Size [d.nm]</i>	<i>PdI</i>	<i>ζ-potential [mV]</i>
CS NPs					
1122	10	30	175.9 ± 1.5	0.159	+35.1 ± 0.9
1122	20	60	199.0 ± 1.5	0.163	+35.2 ± 0.5
1123	10	20	136.1 ± 0.4	0.151	+35.5 ± 2.8
Starch NPs					
1169	20	20	180.8 ± 1.5	0.055	-19.5 ± 1.3
1169	20	40	157.9 ± 1.6	0.071	-17.9 ± 2.3
1169	20	60	145.1 ± 0.7	0.066	-18.1 ± 3.5

Microparticle preparation

Microparticles were prepared from aqueous CS NP or starch NP suspensions (Table 5.1, **bold**) spray dried with a nano spray dryer with or without different excipients. An influence of the spray cap on the size of microparticles was disproved and the 5.5 µm spray cap was chosen for all following experiments. To ensure a dry product while at the same time ensuring mild preparation conditions feasible for protein encapsulation, an inlet temperature of 70 °C was selected. Although this temperature seems to be quite high, the most important temperature influencing product stability is in fact the outlet temperature, which was always below 40 °C in this case. To further ensure a mild preparation process, samples were kept on ice during spray drying. To determine NP stability during the pumping process, physicochemical properties of NPs were determined before spray drying and almost at the end of the spray drying process by taking samples from the remaining NP suspension. Size and ζ-potential of NPs remained the same prior to and at the end of spray drying, meaning that the pumping process as well as temperature differences did not influence particle properties over the duration of the spray drying process, which usually took approximately 2 – 2.5 h for the applied volumes.

NP suspensions were spray dried with excipient; therefore, the influence of the excipient on physicochemical properties of NPs was investigated. Here, a focus was placed on excipients

that were highly water soluble, in order to easily release the NPs after deposition in the deep lung. Further, excipients with GRAS status were favored, resulting in a choice of excipients being lact, treha, and manni. Solid excipient was either added after NP preparation and stirred for 10 min for equilibration, or NPs were directly prepared in excipient solution. For the latter, each material for NP preparation (*i.e.* CS, TPP, NegSt, PosSt) was dissolved in an excipient solution instead of purified water. As no differences between the two preparation methods was observed, it was decided to add the solid excipient after NP preparation. The influence of excipients on physicochemical properties of NPs can be found in Table 5.2. As can be seen, the addition of excipients, *i.e.* manni, lact, and treha did not change the physicochemical properties of NPs. Particles were in general around 150 nm with a PDI of around 0.16 for CS NPs and 0.07 for starch NPs. The ζ -potential was approximately +35 mV and -25 mV for CS NPs and starch NPs, respectively.

Table 5.2

Influence of excipient on physicochemical properties of NPs, after applying to the NP suspension as dry powder; measured after stirring for 10 min for equilibration. Dp10 and dp22 are G-Blocks, with the number indicating their oligomer length. Manni: mannitol, lact: lactose, treha: trehalose.

	<i>Size</i> [d.nm]	<i>PdI</i>	ζ -potential [mV]
CS NPs + manni 1:20	149.4 \pm 1.9	0.171	+37.1 \pm 1.4
CS NPs + lact 1:20	150.3 \pm 1.5	0.175	+36.6 \pm 0.9
CS NPs + treha 1:20	135.9 \pm 1.5	0.152	+36.4 \pm 1.2
Starch + manni 1:20	153.3 \pm 0.4	0.085	-23.0 \pm 0.2
Starch + lact 1:20	152.7 \pm 1.9	0.065	-23.4 \pm 0.3
Starch + treha 1:20	154.1 \pm 1.5	0.083	-23.6 \pm 0.8
CS + dp22 1:0.4	588.5 \pm 120.7	0.733	+11.0 \pm 0.2
CS + dp10 1:0.4	6471 \pm 545	0.630	+1.7 \pm 0.1
CS + dp10 1:1	2710 \pm 1224	0.897	-14.6 \pm 0.2
CS + dp10 1:1.8	337.6 \pm 3.5	0.369	-21.6 \pm 0.3
CS + dp10 1:3.6	6584 \pm 2282	0.675	+0.5 \pm 0.1
Starch + dp10 1:0.4	150.0 \pm 1.4	0.077	-32.2 \pm 1.7
Starch + dp10 1:3.6	128.9 \pm 0.7	0.097	-34.7 \pm 2.2
Starch + dp22 1:3.6	127.7 \pm 0.4	0.106	-36.4 \pm 2.4

Additionally, the approach of using smart excipients was followed by testing G-Blocks (guluronic acid oligomers, dp10 and dp22) for building the microparticle matrix. This material was evaluated for mucosal delivery of NPs and it could be shown that applying the G-Blocks together with NPs improved particle mobility in mucus due to a reduced mucus barrier function.^{97, 185} The idea of additionally selecting G-Blocks as part of the microparticle preparation was that this could potentially improve bronchiolar uptake of particles that impact in the upper lung, where mucus is present as a non-cellular barrier. CS NPs showed signs of aggregating upon G-Block addition, with large particles between a few hundred nanometers up to the μm range being formed. From the ζ -potential values, which are often around 0 ± 10 mV, it can be concluded that (partial) charge neutralization led to aggregation of the particles. An interaction between the positively charged surface of CS NPs and the negatively charged G-Blocks acids can be assumed. In contrast, starch NPs with added G-Blocks showed particles around or smaller than 150 nm with a PDI below 0.1 and a ζ -potential around -35 mV. Here, the NP suspension was not negatively influenced by aggregation, probably due to the fact, that both starch NPs and G-Blocks acids were negatively charged. Nevertheless, there was an influence of G-Blocks, as can be seen by the increase in ζ -potential magnitude from approximately -25 to -35 mV, indicating that G-Blocks might have been associated with the particle surface. As a conclusion, non-charged excipients for spray drying were favored, as they did not influence physicochemical properties of NPs.

A first result regarding powder properties after spray drying was powder flowability, which differed for the various formulations. Although manni samples were more difficult to collect from the collecting electrode of the spray dryer, the powder flow appeared to be more regular compared to lact or treha samples – in these cases material was easy to remove from the electrode, however particles showed signs of aggregation during the collection process. Here, adhesion interaction between the particles was more pronounced than for manni samples. This is in accordance with literature data, in which manni has been reported to show good powder flowability.¹⁸⁶

5.3.2 RELEASE OF NANOPARTICLES FROM MICROPARTICLES

The successful release of NPs from the microparticle matrix was one of the main requirements for the formulation. *In vivo*, this is an important point to be addressed, so it was the first parameter to be explored. The uptake of particles into cells is amongst other factors size dependent. For example, Desai et al. have shown that the uptake of NPs into Caco-2 cells is significantly greater compared to their microparticle counterparts.^{141, 187} In general, it is

known that NPs in a size range between 100 - 200 nm are taken up by cells *via* endocytosis. Thus, NPs released from the microparticle matrix should have a size around or below 200 nm, and a narrow size distribution.

In a proof of concept study, approximately 1 mg each of the microparticle formulations was dissolved in 1 mL aqueous solution and vortexed for 10 s (to speed up the dissolution process). Released NPs were measured for their size and size distribution. Results for different formulations can be found in Figure 5.1, where CS NP formulations are shown in (A) and starch NP formulations are shown in (B). It could be seen that blank NPs, spray dried without excipient, were not able to be redispersed. This was the case for CS NPs, which showed aggregates in the μm size range and a PDI close to 1. Compared to that, starch NPs showed an improved behavior, nevertheless, the size distribution was not satisfactory. During the drying process, the gel-like NPs probably came into contact with each other, forming larger particles.

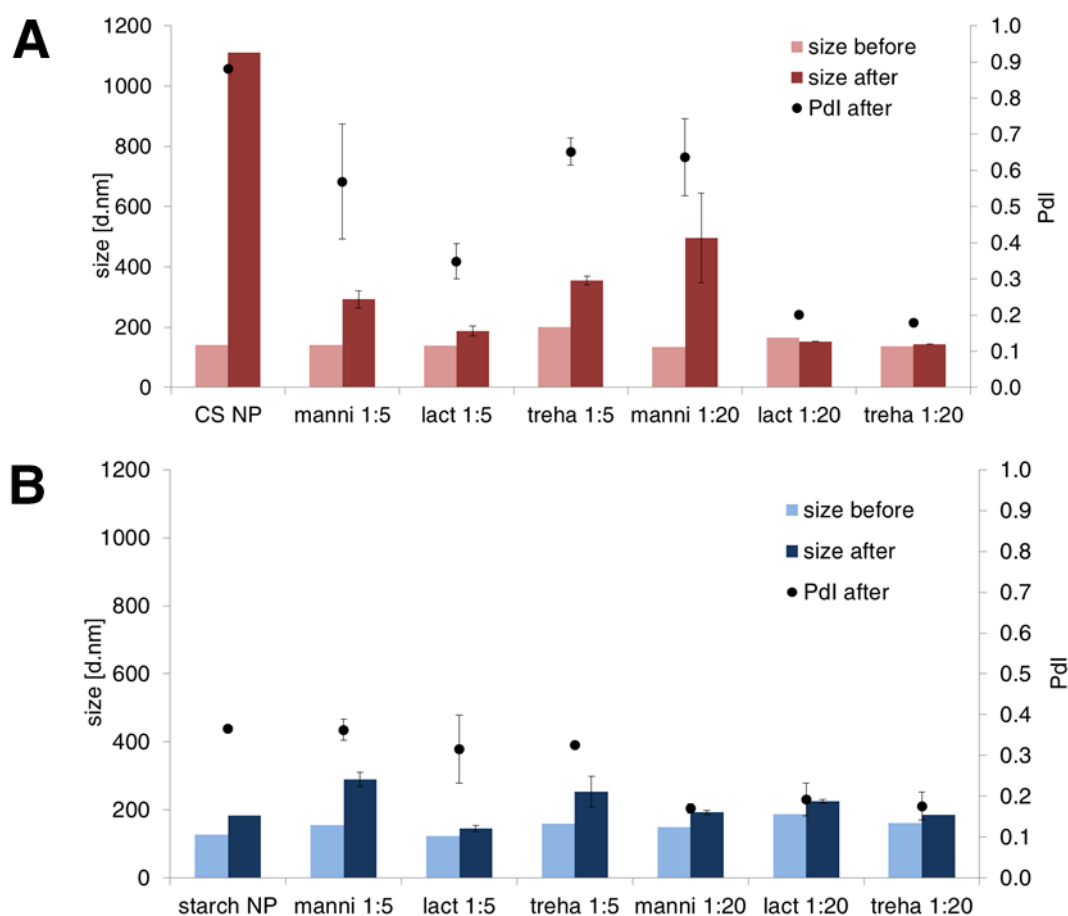


Figure 5.1: Dissolution behavior of microparticles, and comparison of physicochemical properties of NPs before spray drying and after being released from the microparticles. (A) CS NPs spray dried with different amounts of excipient. (B) Starch NPs spray dried with different amounts of excipient.

Adding different excipients in a mass ratio 1:5 (NP:excipient) could not improve the redispersion behavior of both NP types. However, a mass ratio of 1:20 led to a good redispersion of NPs with physicochemical properties being similar to the NP suspension before spray drying. The excipient served as drying protectant, probably due to steric hindrance, so that the NPs were not able to merge into larger particles. One exception is manni, which could still not improve the dissolution behavior of CS NPs in a mass ratio of 1:20. Loaded starch NPs with 150 μ L IgG1 solution (5 mg/mL) also showed a good redispersion when spray dried with treha in a mass ratio NP:excipient of 1:20. The size of these loaded NPs after redispersion was 243.0 ± 9.2 nm with a PdI of 0.2.

As a result, a mass ratio of 1:20 NP:excipient was chosen for further experiments. The material of choice was determined to be manni or treha, showing good protection of the NP suspension during spray drying.

5.3.3 MORPHOLOGY

The morphology of all spray dried samples was examined using SEM. Representative images of spray dried NPs without excipient and with excipient in a mass ratio of 1:20 (NP:excipient) are shown in Figure 5.2. It could be seen that both types of NPs, when spray dried without excipient, were very small and had an undefined shape. In contrast, NPs spray dried with excipient were larger and of defined shape. Depending on the kind of NP, the morphology differed: microparticles prepared from CS NPs spray dried with different excipients had a spherical and smooth surface, whereas starch NPs spray dried with excipient additionally had wrinkled shapes.

Iskandar *et al.* have shown that morphology of spray dried particles depends on parameters such as droplet size of the material to be spray dried, viscosity of the droplet, size of the sol in the droplet, drying temperature, gas flow rate and addition of surfactant. From a theoretical perspective they concluded that the structural stability of the droplet and the hydrodynamic effects during the drying process might play important roles in controlling the morphology of the resulting particles.¹⁸⁸ As spray drying parameters, such as droplet size (determined by the spray cap), gas flow rate and drying temperature was kept constant, the differences in morphology are likely chiefly influenced by formulation parameters in this case.

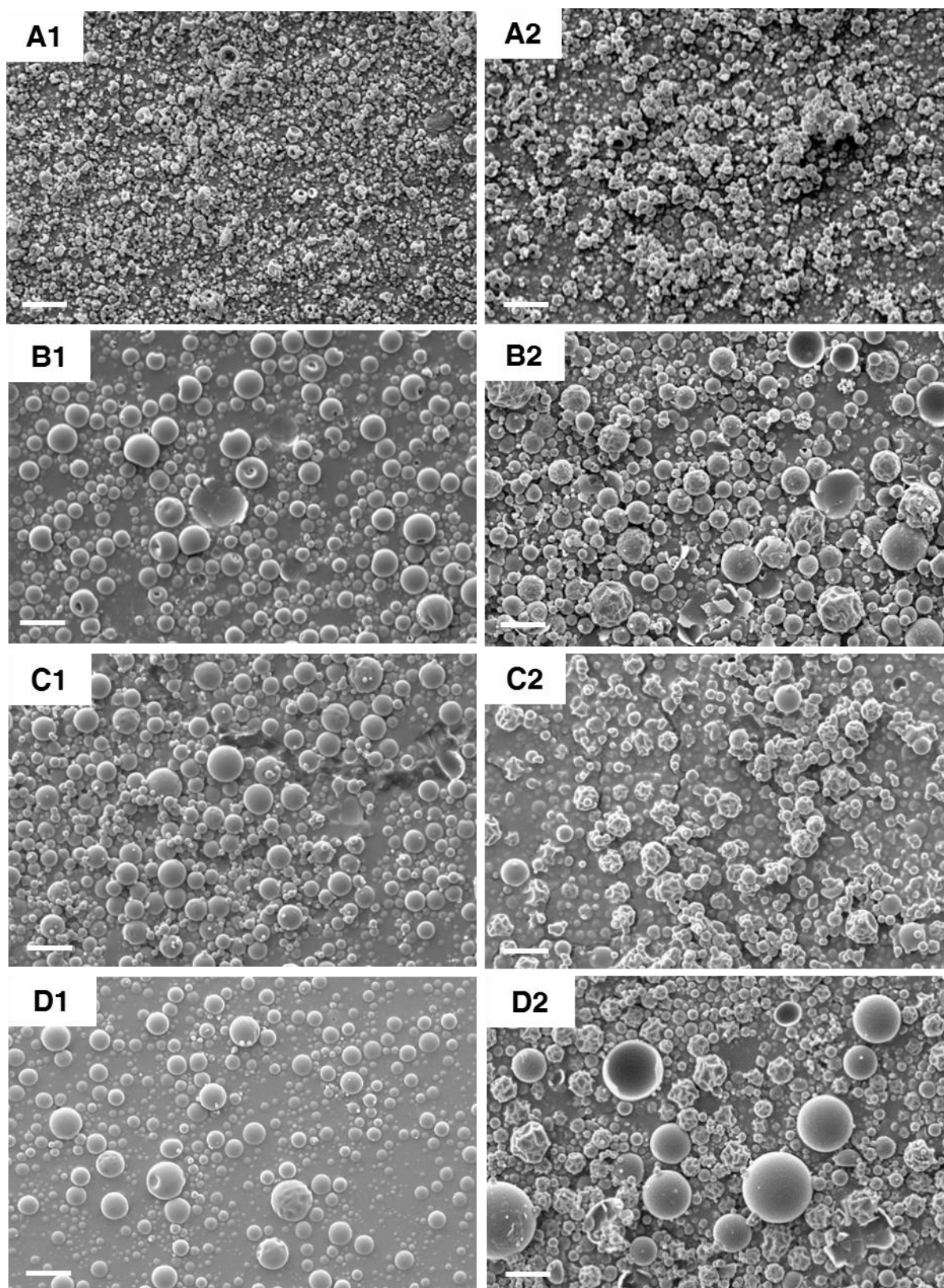


Figure 5.2: SEM images of spray dried NPs without (A) or with 1:20 excipient: manni (B) lact (C) treha (D); column on the left: CS NPs (1); column on the right: starch NPs (2); scale bar: 1 μm.

Spray drying of blank NPs led to a collapse of the droplet during the drying process, resulting in particles of undefined shape. Adding an excipient, however, increased the mass fraction in the droplet, stabilizing the droplet due to its internal stiffness, meaning that prepared particles showed a more defined shape and were almost spherical. A review from Vehring presented a classification based on dimensionless numbers (*e.g.* Peclet number) that can be used to estimate how excipient properties in combination with process parameters influence the morphology of engineered particles.¹⁸⁹ The differences in shape of microparticles have to do with the NP type, as process parameters and excipients were kept constant. It could be assumed that starch NPs have a different Peclet number compared to CS NPs, resulting in a different diffusion behavior in the droplet, leading to a different particle shape.

5.3.4 PARTICLE SIZE AND PARTICLE SIZE DISTRIBUTION

Particle sizes were measured with the Fiji Software, grouped into different intervals and plotted as number of particles [%] (Figure 5.3). More than 100 particles were analyzed per image. Therefore, images were divided into sections and only particles completely visible were chosen for measurement. It can be seen that CS NPs, spray dried without excipient are mostly in the nanometer size range (87%), and mostly around 400 – 800 nm, with 13% of particles being between 1-2 μm . This is in accordance with the redispersion behavior observed after spray drying: during the drying process, the gel-like NPs come into contact with each other, forming larger particles. This differed for the starch NPs. Here, only 59% of NPs were found to be below 1 μm , 33% were between 1-2 μm in size, and 8% were between 2-4 μm . As the redispersion of starch NPs spray dried without excipient was easier to achieve than the CS NPs, it could be assumed that the starch NPs do not show this gel-like character to such an extent as the CS NPs do.

For the samples spray dried with excipient, this looked different. The particle fraction below 1 μm was decreased, whereas the fractions of a few μm in size increased. Adding more mass for the spray drying process with at the same time a constant volume, led to increased particle size and improved the redispersion behavior. It could be assumed that the excipient is building a matrix into which the NPs are embedded.

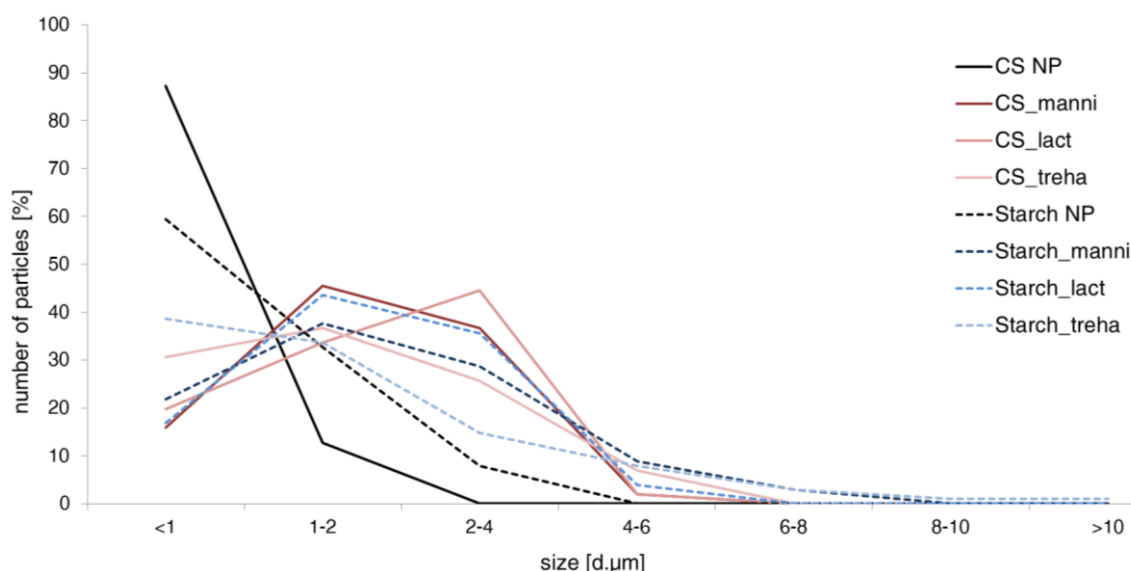


Figure 5.3: Particle size distribution of optimized microparticles spray dried with various excipients, compared to NPs, spray dried without excipient.

Additionally, particle size was measured with the HORIBA LA-950 using static laser light diffraction and the dry powder feeder apparatus. As can be seen in Figure 5.4 (A), the sample is applied as dry powder and dispersed either *via* pressurized air or sucked up *via* low pressure. With the help of a laser light beam, particle size is determined while the powder is in the air stream passing the measurement window. Applying pressurized air is a rather harsh and fast method, and as such a certain amount of sample mass is necessary to be able to detect particles in the air stream. Using low pressure instead is a mild method, where particles are passing through the measurement window with less speed, thus less amount of sample is needed. However, the ability to de-agglomerate particles is less effective in this case.

The dry feeder apparatus is a useful tool to analyze the particle size of a powder, as there is no need to apply a non-solvent, which could influence the physicochemical properties of the microparticles. In general, a mass of a few grams is needed to give a good signal when the sample is dispersed *via* pressurized air. The yield of the spray drying process, however, was usually between 150 - 200 mg. Deciding for a manual measurement and applying a low pressure instead of pressurized air made possible a detection of the particles within the air stream. Nevertheless, the mild dispersion method was not able to de-agglomerate particles of all samples, as can be seen in Figure 5.4 (B), where the cumulative volume of particles [%] is shown. The two manni formulations showed a good particle size distribution between 2 and 10 µm, with the CS NPs spray dried with manni 1:20 being slightly smaller than the starch NPs spray dried with manni 1:20. The other formulations showed large aggregates up to the mm size range. This behavior is in accordance with the differences in powder flowability

observed during sample collection after the spray drying process. As known from the SEM images, particle size was below 10 μm , indicating that the mild low pressure during measurement was not able to de-agglomerate the particles. This further approved manni as excipient, showing good powder flowability.

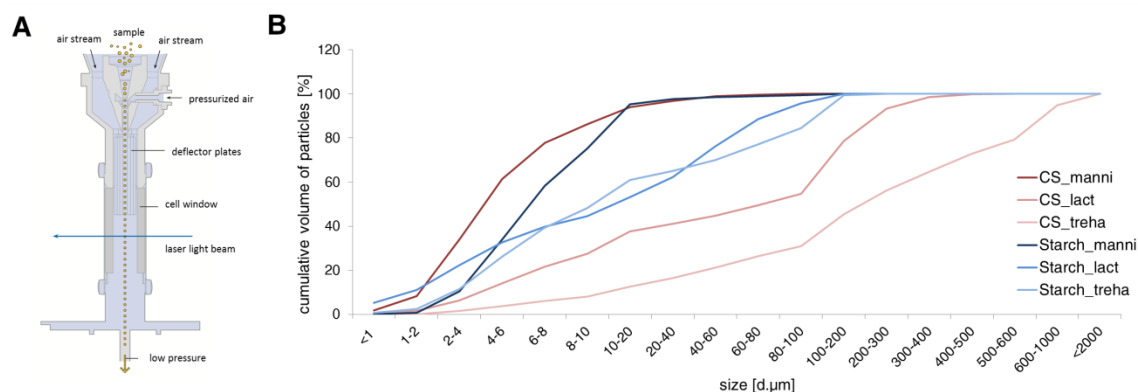


Figure 5.4: Particle size distribution of microparticles (mass ratio 1:20), determined with the HORIBA LA-950.

5.3.5 POWDER CRYSTALLINITY

To fully characterize a powder formulation, its solid state form should be analyzed. This was done by XRPD. Microparticles were prepared in a mass ratio 1:20 (NP:excipient) and results can be found in Figure 5.5. For lact and treha samples, there was only a halo visible, indicating that the samples were amorphous. Manni samples instead showed distinct patterns, typical for crystalline material, and indicating the existence of long-range molecular order. Analyzing the spectrum resulted in approximately 17% α -form, 25% β -form, and 59% δ -form for Starch_manni and 13% α -form, 84% β -form, and 3% δ -form for CS_manni. Bulk material of manni before spray drying showed 100% β -form. Hulse *et al.* found structural variations of spray dried manni depending on the supplier. There were basically two different polymorphic forms, being either α -form or β -form or a mixture of both.¹⁹⁰ Comparing the samples of CS_manni and Starch_manni showed that the NP type had an effect on the recrystallization behavior of manni. In Starch_manni, the original β -form transformed mainly into the δ -form and also into the α -form, although to a lower extent, so that only 25% of the β -form was left. In CS_manni, the β -form was better preserved, so that only a low amount transferred into the α -form and even less into the δ -form. As Hulse *et al.* did not find the δ -form, this polymorph could be a result of the included NPs, which is also underlined by the different amount of δ -form being present for the two different formulations. A similar influencing effect was seen

by Hulse *et al.*, who co-spray dried proteins (trypsin and lysozyme) with manni and analyzed the influence of protein on manni polymorphism.¹⁹¹

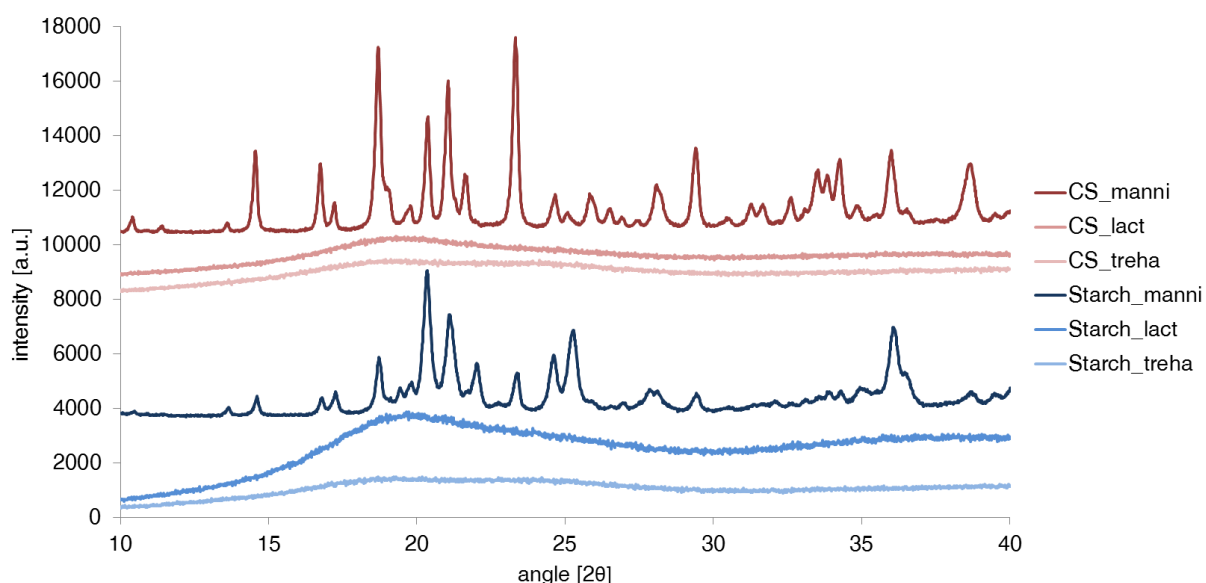


Figure 5.5: XRPD diffractograms of microparticles.

5.3.6 LOCALIZATION OF NANOPARTICLES IN MICROPARTICLES

From SEM images, it was not possible to visualize the localization of NPs within the microparticles. Confocal microscopy however is able to distinguish between different fluorescent labels, each representing an independent structure. Therefore, labeled starch NPs were spray dried as usual after adding treha (mass ratio 1:20, NP:excipient) and the fluorescent dye DAPI (12.5 ng/mL). Particles were analyzed by confocal microscopy, with Figure 5.6 representing a cross-section of microparticle. It can be seen that the NPs are distributed throughout the whole microparticle, rather than building a ring at the surface. Sham *et al.*¹⁸⁰ obtained similar results for dry powder comprised of polycyanoacrylate NPs and lact. In this study, NPs were also embedded in a microparticle matrix, however, the NPs appeared in clusters, rather than being distributed equally throughout the microparticle. Another study into embedding NPs in microspheres was performed by Grenha *et al.* They showed that CS NPs were equally distributed throughout the whole microparticle matrix. However, they have seen that manni also completely coated the microparticle, giving a wall-like structure.¹⁸¹

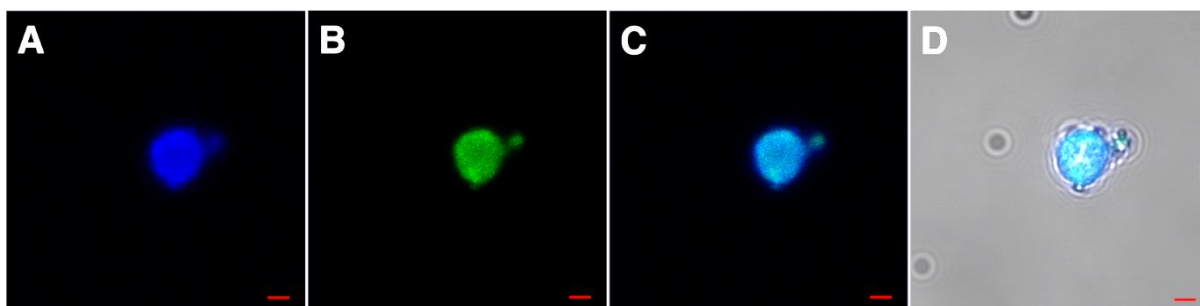


Figure 5.6: Confocal images of labeled starch NPs (green), co-spray dried with treha (mass ratio 1:20) and DAPI (blue). (A) DAPI, representing the microparticle matrix, (B) Bodipy (green label), representing the NPs; (C) fluorescence overlay; (D) additional overlay with light microscopic image; scale bar: 2 μm .

Furthermore, the composition of starch NPs loaded with 150 μL labeled IgG1 and spray dried with treha and DAPI was investigated (cross-section shown in Figure 5.7). IgG1 was labeled for such investigations with Alexa Fluor 647 carboxylic acid (succinimidyl ester) according to the manufacturer's protocol. From the confocal images it could be concluded, that also here, the loaded starch NPs are distributed throughout the microparticle. In addition, the visualization of several microparticles provides proof of a rather equal distribution of NPs throughout the sample.

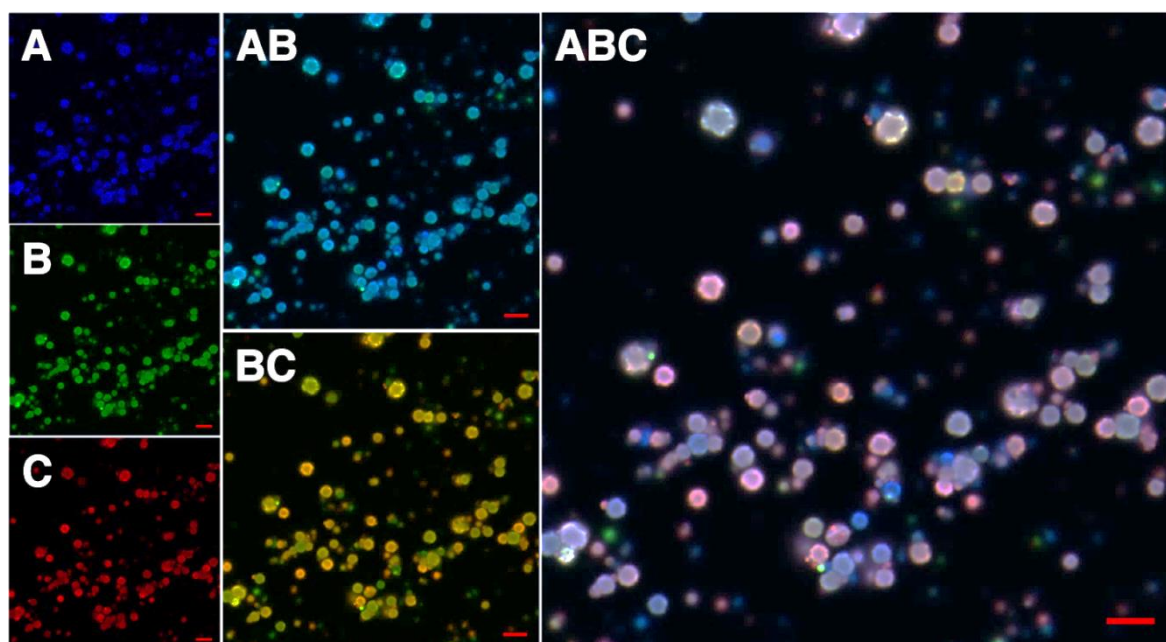


Figure 5.7: Fluorescence images of labeled starch NPs, loaded with labeled IgG1 and co-spray dried with treha (mass ratio 1:20) and DAPI. (A) DAPI, representing the microparticle; (B) Bodipy, representing the nanoparticles; (C) Alexa Fluor 647, representing IgG1; (AB) overlay of (A) and (B); (BC) overlay of (B) and (C); (ABC) overlay of (A), (B) and (C); scale bar: 10 μm .

5.3.7 AERODYNAMIC PROPERTIES

The aerodynamic properties of a formulation intended for pulmonary application are essential to both characterize and optimize, as a high deposition in the deep lung depends on the physical and chemical properties of the particles amongst other factors (*e.g.* breathing of the patient, lung physiology). Parameters to be determined are the MMAD, the GSD and the FPF. The FPF, being defined as the part of the inhaled dose being $< 5 \mu\text{m}$ in aerodynamic diameter, gives an indication of the amount of the applied dose reaching the deep lung. The MMAD indicates the median aerodynamic diameter within the measured particle population and is correlated to the detected mass within the NGI. Additionally, the GSD gives an idea of particle distribution and homogeneity of the sample.

In general, when speaking about the size of particles, it is the geometric diameter that is being referred to. However, the inhalation process is characterized by the flight behavior of a particle, which depends not only on its size, but also on its density (and shape). Therefore, the aerodynamic diameter was introduced as a more meaningful measure. Assuming an appropriate MMAD between 1-5 μm , a high deposition in the deep lung is expected.^{192, 193}

Aerodynamic properties of different formulations can be found in Table 5.3.

Table 5.3

Mass Median Aerodynamic Diameter (MMAD), Geometric Standard Deviation (GSD), and Fine Particle Fraction (FPF) of microparticles prepared by spray drying of NPs with excipient in a mass ratio 1:20. Parameters were determined with the Next Generation Impactor (NGI); for analysis, sodium fluorescein (FluNa) was added before the spray drying process; (mean \pm SD, $n = 3$).

	<i>MMAD</i> [μm]	<i>GSD</i> [μm]	<i>FPF</i> [%]
CS_manni	3.8 ± 0.3	3.2 ± 0.1	52.5 ± 7.9
CS_lact	4.0 ± 0.5	1.8 ± 0.6	27.4 ± 7.0
CS_treha	3.4 ± 0.6	2.6 ± 0.3	42.7 ± 5.4
Starch_manni	2.1 ± 0.3	4.9 ± 0.5	41.3 ± 2.9
Starch_lact	2.5 ± 0.3	4.2 ± 0.4	36.7 ± 3.9
Starch_treha	2.1 ± 0.2	7.0 ± 0.5	40.5 ± 3.5

Formulations based on CS NPs showed an MMAD around 3.5 μm with a narrow GSD. In comparison, the starch NP formulations were smaller, with an MMAD around 2 μm . Nevertheless, the GSD was higher compared to the CS NP formulations. This is in accordance with the SEM images, showing a broader size distribution for the starch NP formulations than the CS NP formulations. The FPF was dependent on the excipient used for microparticle preparation. Here, manni samples showed the best results with around 40% FPF for Starch_manni and around 50% for CS_manni. These findings are in agreement with those reported in literature, where an FPF between 5 and 50% is common, varying as a result of the type of carrier^{194, 195} and drug morphology¹⁹⁶ rather than as a function of the utilized inhalation device.¹⁹⁷

5.3.8 PADD OCC DEPOSITION

Qualitative and quantitative deposition of microparticles was studied with the PADD OCC (Photo 5.1), which is a set-up, consisting of (A) an air-flow control unit (Akita®, Activaero, Germany), (B) an aerosolization unit (fitting a HandiHaler®, Boehringer Ingelheim, Germany), and (C) a custom-made sedimentation chamber, holding three Snapwell® inserts containing monolayers of pulmonary epithelial cells.^{183, 184} The device should mimic the process of aerosol drug delivery by sedimentation as a deposition mechanism, and should allow for evaluating the interaction of a specific formulation with the pulmonary epithelial cells.



Photo 5.1: Setup of the PADD OCC. (A) Air-flow control unit; (B) aerosolization unit; (C) sedimentation chamber, holding three Snapwell® inserts. The latter two components are placed in a heating chamber, for performance of the cell experiments at 37 °C.

Before studying the interaction of the microparticle formulations with the pulmonary epithelia, the deposition of the formulations with the PADD OCC onto SEM wafers, in the absence of a cell monolayer, was examined qualitatively and quantitatively. More than 90%

of the total formulation mass was released from the capsule for all experiments. In a first step the deposition was analyzed qualitatively: Figure 5.8 shows SEM images of deposited microparticle formulations.

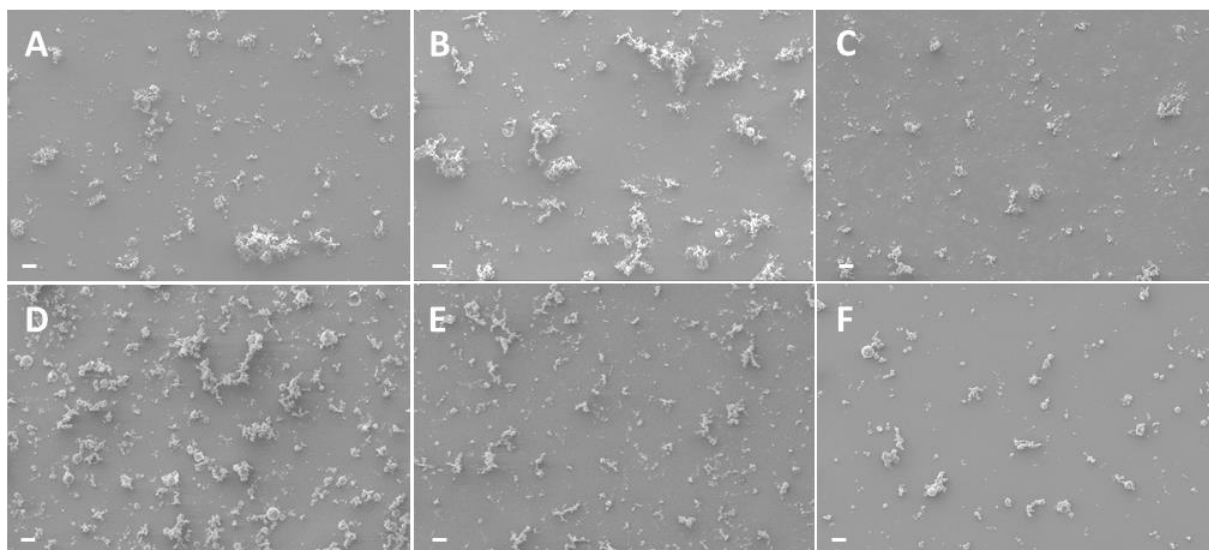


Figure 5.8: SEM images of microparticles, deposited with the PADD OCC onto SEM wafers. CS NPs spray dried with excipient: (A) manni; (B) lact; (C) treha. Starch NPs spray dried with excipient: (D) manni; (E) lact; (F) treha. All samples were spray dried in a mass ratio 1:20 (NP:excipient); scale bar: 10 μm .

It could be seen that only small particles were deposited and that, although some agglomeration occurred, particles were spread over the entire surface of the SEM wafers. It seemed that a greater degree of deposition occurred on the case of the sample starch_manni (D), compared to other formulations. This was in accordance with the particle size measurements and the powder flowability observations made during formulation collection from the spray dryer.

In a second step, the quantitative deposition of the formulations was studied; results can be found in Figure 5.9.

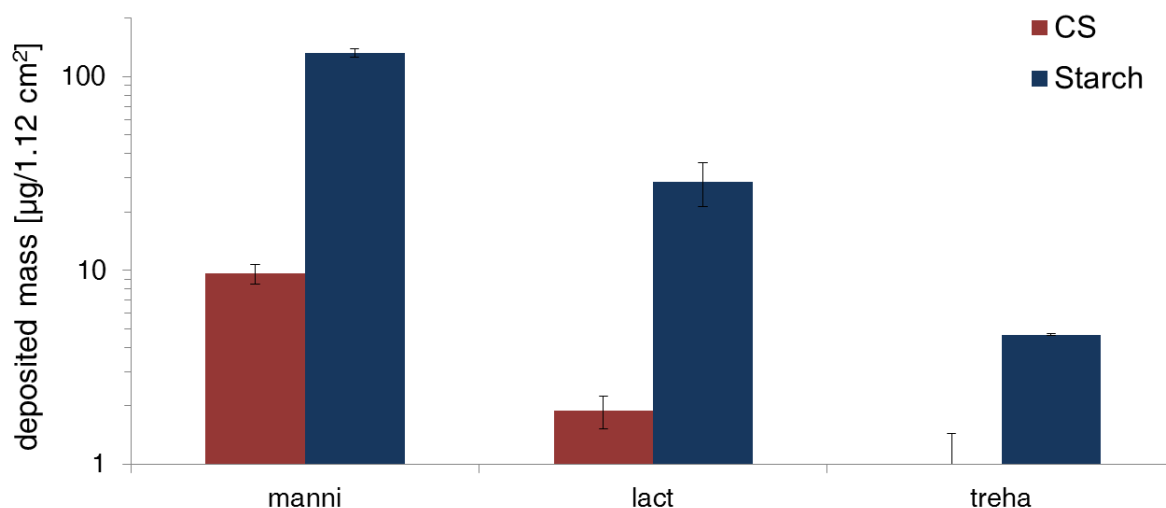


Figure 5.9: Quantitative deposition of microparticles prepared by spray drying of NPs with excipient in a mass ratio 1:20. For analysis, FluNa was added before the spray drying process. Deposited mass is calculated per Transwell® area (1.12 cm²). A mass of 10 mg of particles per capsule was used for deposition studies.

Two trends could be observed from these experiments: the deposited mass depended on the excipient, with manni showing the highest deposited mass and treha showing the lowest deposited mass. Further, the NP type was of importance, as formulations consisting of starch NPs showed a higher deposition than formulations of CS NPs. These results are underlined by the qualitative analysis, shown by the SEM images. Comparison of these results to those obtained for particle size measurements with the dry feeder apparatus of the HORIBA LA-950 is further possible. With respect to size measurements facilitated by the dry feeder apparatus, lact and treha aggregates were not able to be redispersed within the air stream for measurement purposes. This observation can be correlated to the findings of the PADD OCC experiments, where lact- and treha-containing particles probably impacted as larger aggregates in the PADD OCC device, mimicking the *in vivo* aerosol deposition situation, before reaching the Snapwell® region. Manni samples, however, showed good dispersion behavior within the air stream and reached the Snapwell® region in high doses. Starch_manni showed better deposition behavior than CS_manni. As mentioned before, the different formulations showed different flow properties as well as different cohesive natures, probably leading to the different deposition. In summary, manni showed potential as an excipient for bringing high particle amounts to the deep lung, which is in accordance with literature,¹⁹⁵ whereas spray dried particles resulting in amorphous lact and treha, showed poor dispersibility leading to low predicted particle deposition in the alveolar region.

5.4 CONCLUSION

The successful spray drying process was mainly influenced by the working of the spray cap, together with the piezo driven mesh used for droplet formation. A dysfunction of the spray cap resulted in a poor yield or bad product quality. An inlet temperature of 70 °C ensured a dry product and resulted in an outlet temperature below 40 °C indicating a low thermal burden for the encapsulated protein. Adding different non-charged excipients (manni, lact, and treha) did not change the physicochemical properties of the NP suspension. Also so-called smart excipients, *i.e.* G-Blocks, were tested. However, these molecules are negatively charged; as such they were seen to be appropriate as excipients for starch NPs, but showed aggregation after addition to CS NP suspensions. It can therefore be concluded that non-charged excipients are favored for the microparticle preparation.

Spray drying the NP suspension without excipient resulted in particles with an indistinct shape. Adding an excipient led to particles distinctly spherical in shape, with specific morphology depending mostly on the NP composition - spray dried CS samples with different excipients showed rather smooth and round surfaces, while spray dried starch samples with different excipients showed rather wrinkled shapes. NPs spray dried without excipient were not able to be redispersed. Depending on the amount of excipient, NPs were able to be redispersed in aqueous solution (mass ratio 1:20, NP:excipient).

The particle size distribution clearly depended on the specific excipient employed. Samples spray dried with manni showed the narrowest particle size distribution, whereas samples spray dried with lact or treha showed a broad size distribution.

Also crystallinity of the samples depended on the kind of excipient used. Manni samples showed a crystalline appearance after spray drying, whereas lact and treha samples were completely amorphous.

The internal structure of the microparticles was evaluated by confocal fluorescence microscopy, using the formulation of Starch_treha (loaded with IgG1) as model formulation to get an idea of whether the NPs are located at the surface, or rather spread throughout the excipient matrix. It was seen that the latter phenomenon occurred with starch NPs being present throughout the entire microparticle and not only at the surface. The same was true for the formulation loaded with IgG1.

The aerodynamic properties of the formulations differed with respect to measure of MMAD, GSD and FPF. The MMAD was slightly larger for the CS NP formulations, whereas the GSD was higher for the starch NP formulations, independent of the used excipient. The FPF, however, depended rather on the excipient than on the NP type, with the highest FPF between

40% and 50% noted for Starch_manni and CS_manni formulations, respectively. The deposition with the PADD OCC worked for all formulations, however differences between the formulations were found. Quantitatively speaking, the manni samples looked best, from which Starch_manni showed the highest deposited amounts.

In summary, taking into consideration all tested excipients, there is no clear advantage of one special excipient. Lact and treha showed a good redispersion behavior of NPs, however their amorphous and highly cohesive character was detrimental for their delivery to the deep lung. Manni showed a high degree of deposition and good redispersion in the case of starch NPs, however, its influence on protein stability has to be further evaluated. A mixture of treha and manni as matrix builder for the microparticle preparation could be proposed. Assessing the NP type, starch NPs clearly show an advantage for both important parameters - redispersion of the NPs after microparticle dissolution and high deposition in the deep lung - compared to CS NPs. Due to that fact, starch NPs were further evaluated for their cell uptake ability (*Chapter 6*).

6. *IN VITRO* BIOPHARMACEUTICAL EVALUATION OF THE NOVEL CARRIERS

The author of the thesis made the following contribution to this chapter:

Planned, designed and performed experiments related to particle preparation and characterization, cytotoxicity and endoLISA assays as well as uptake studies, analyzed data from the mentioned studies, interpreted the experimental data and wrote the manuscript, if not stated otherwise.

The cell culture was performed by Stephanie Kletting.

The immunogenicity studies were performed by Anne Marit de Groot at Utrecht University. She analyzed data from the mentioned studies and interpreted the experimental data.

6.1 INTRODUCTION

After successful DDS preparation, *in vitro* biopharmaceutical evaluation of the prepared system, including cytotoxicity and immunogenicity assessment as well as the conduction of first uptake studies is crucial, before testing the uptake and efficacy of the developed DDS *in vivo*.

As the carrier system introduced in this thesis was developed for pulmonary delivery, the various cellular and non-cellular barriers of the lung must be considered during *in vitro* DDS assessment. These include the epithelial barriers of the upper and the deep lung, mucus as a non-cellular barrier and clearance mechanism of the upper lung, as well as macrophages patrolling in the deep lung. One of the main barriers to be overcome by the DDS is the epithelial barrier of the alveolar region, as these are the specific cells to be targeted by the DDS. Nevertheless, interactions could still occur between DDS + macrophages (clearance mechanism in the deep lung), but also between DDS + barriers of the upper lung. As a result, cytotoxicity testing of the DDS was performed not only with alveolar epithelial cells, but also with macrophages and bronchiolar epithelial cells.

For pulmonary delivery, various cell culture models of the respiratory system are available. Regarding epithelia, A549 cells are a well-established cell line of the alveolar region. Additionally, Calu-3 cells and 16HBE14o- cells are commonly used to mimic the epithelia of the upper airways.¹⁹⁸ Further, THP-1 cells have been utilized as a model for macrophages, present as a clearance system in the deep lung. While advanced systems, such as co-cultures,^{199, 200} or triple-cultures²⁰¹⁻²⁰³ are available, in the context of the current work, monocultures composed of the above mentioned cells were of interest for a first evaluation.

In this chapter cytotoxicity studies of the source materials used for NP preparation were performed on A549 cells, as there is a lack of data related to the pulmonary toxicity of such materials. Formulation into nano-sized carriers could alter material toxicity, as well as the form of deposition. Thus, both CS and starch NPs were evaluated regarding their cytotoxicity in different cell lines. Such testing is of additional importance as recently the OECD guideline for the testing of chemicals for subchronic inhalation toxicity was updated, and now includes also NPs.²⁰⁴ Additionally, microparticles were evaluated regarding their cytotoxicity in different cell lines under liquid covered conditions (LCC) as well as air-liquid-interface (ALI), as the deposition under ALI will lead to a different local concentration of the applied particles. Immunogenicity experiments with microparticles were conducted by the University of Utrecht, a collaboration partner in COMPACT. Due to some surprising results, an

endoLISA was performed to investigate any potential source of contamination with endotoxins.

As intracellular delivery was of specific importance in this thesis, investigation of the uptake of the particles is necessary in order to assess and ensure efficacy of the DDS-associated protein/peptide; therefore, ALI uptake studies of starch NPs on alveolar and bronchial epithelia cell lines, *i.e.* A549 and 16HBE14o-, were conducted. Microparticles were also deposited on A549 cells, and NP uptake was studied to see whether microparticles could be dissolved on epithelial cells cultivated under ALI.

Unless stated otherwise, α -starch derivatives, named NegSt and PosSt, were used for experiments.

6.2 MATERIALS AND METHODS

6.2.1 MATERIALS

Protasan UPCL 113 (chitosan, CS) was bought from Novamatrix, Norway. Sodium tripolyphosphate (TPP) was purchased from Merck KGaA, Germany. Negatively (NegSt) and positively (PosSt) charged starches were synthesized in house. IgG1 was kindly donated by Boehringer Ingelheim (Germany). Mannitol (manni), trehalose dihydrate (treha) and α -lactosemonohydrate (lact) were bought from Sigma Aldrich (USA).

A549 cells (No. CCL-185) and Calu-3 cells (No. HTB-55) were purchased from American Type Culture Collection (ATCC). 16HBE14o- cells were a kind gift from Dr. Dieter C. Gruenert (Department of Otolaryngology, University of California, San Francisco, CA, USA). THP-1 cells (No. ACC-16) were bought from DSMZ. Cell culture medium (RPMI 1640), minimum essential medium eagle (MEM), fetal bovine serum (FBS), phosphate buffered saline (PBS), Hank's balanced salt solution (HBSS) and sodium pyruvate were obtained from Life Technologies (USA), and non-essential amino acids (NEAA) from GE Healthcare Life Sciences. Thiazolyl blue tetrazolium bromide (MTT reagent) was bought from Sigma Aldrich (USA). TritonTM X-100 was purchased from Sigma Aldrich (U.S.A.). The endoLISA[®] assay endotoxin test kit was purchased from Hyglos GmbH (Germany). Purified water was produced by a milliQ water purification system (Merck Millipore, USA). All other reagents were of analytical grade.

6.2.2 CELL CULTURE

A549 and THP-1 cells were cultivated in RPMI 1640 medium. Calu-3 and 16HBE14o- cells were cultivated in MEM medium containing 1% NEAA, and 1% sodium pyruvate (Calu-3) or 300 mg glucose (16HBE14o-), respectively. All media contained 10% FBS (v/v). For cell viability assays and uptake studies, 1% (v/v) penicillin/streptomycin (P/S, 10 000 U/mL, Gibco life technologies, USA) was added to media.

6.2.3 CELL VIABILITY

Cell viability was evaluated by using the 3-(4,5-dimethylthiazol-2-yl)-2,5-diphenyltetrazolium bromide (MTT) assay. This colorimetric assay is based on the reduction of the tetrazolium dye MTT to its insoluble formazan, by mitochondrial enzymes. The formazan crystals can be dissolved in DMSO and show a purple color, the intensity of which depends on the metabolic activity of cells. Thus, quantification of the absorbance of solubilized formazan crystals gives an indication of how many viable cells are present, in relation to a positive and negative control.

For assessing the cytotoxicity of materials used for NP preparation, 2×10^4 A549 cells were seeded into 96 well plates under LCC. After reaching approximately 90% confluence, the cell medium was removed and the cells were washed once with 200 μ L HBSS (composed of 1.12 mM CaCl_2 , 0.49 mM $\text{MgCl}_2 \cdot 6\text{H}_2\text{O}$, 0.41 mM $\text{MgSO}_4 \cdot 7\text{H}_2\text{O}$, 5.33 mM KCl, 0.44 mM KH_2PO_4 , 4.17 mM NaHCO_3 , 137.93 mM NaCl, 0.34 mM Na_2HPO_4 , 5.55 mM D-glucose, pH 7.4). Afterwards, the cells were incubated with material solutions of CS, TPP, NegSt, or PosSt dissolved in HBSS (4 h incubation) or RPMI (24 h incubation).

NP toxicity was studied using A549 (2×10^4) and THP-1 (1×10^5) cells, seeded into 96 well plates (LCC). Cells were incubated with NP suspensions, diluted with RPMI medium (concentrations of 133, 67, 33, 17, and 8 $\mu\text{g/mL}$) for 4 h and 24 h, respectively.

To evaluate the microparticles, A549 and Calu-3 cells were seeded into 96 well plates to enable LCC investigations, as well as cultivated on Transwell® plates (3460, 1.12 cm^2 , Corning, USA) to enable ALI investigation. The particles were applied after dissolution/redispersion of NPs in RPMI (A549) or MEM (Calu-3) in the case of LCC or after PADD OCC deposition (10 mg per capsule, in the case of ALI cultures) and incubated for 4 h or 24 h.

In all cases, following incubation of cells with NP materials, NPs or microparticles, cells were washed once with 200 μ L HBSS buffer. A 100 μ L volume fresh HBSS buffer, containing 10% (v/v) MTT reagent (5 mg/mL) was then added and incubated for a further 4 h. HBSS

buffer was aspirated and 100 μ L DMSO was added and incubated for 20 min. Absorbance was then measured at 550 nm with the Tecan Infinite[®] 200 microplate reader (Tecan Deutschland GmbH, Germany). All incubation steps were done at 37 °C, under gentle shaking and light protection. Cell viabilities were calculated in comparison to negative controls (untreated cells as 100% value of cell viability) and positive controls (1% Triton[™] X-100 solution as 0% value of cell viability).

6.2.4 IMMUNOGENICITY

Immunogenicity experiments were carried out by our project partner from Utrecht University. Assays were performed according to Zeng *et al.*²⁰⁵ as follows:

Toll-like receptor activation assay

Toll-like receptor (TLR) reporter cell lines (HEK-Blue[™]-hTLR2, -hTLR3, -hTLR4, -hTLR7, and -hTLR9 reporter cells) were cultured as instructed by the manufacturer (InvivoGen, France). The TLR reporter cell lines were stimulated with the unloaded or loaded (IgG1) microparticles at concentrations of 1, 0.5, 0.1 and 0.05 mg/mL or with the solvent alone, in a total volume of 100 μ L for 16 h at 37 °C. As positive controls, the following agonists were used: PAM3SCK (100 ng/mL) for TLR2, polyinosinic-polycytidylic acid [poly(I:C)] (5 μ g/mL) for TLR3, lipopolysaccharide (LPS)-EK (10 ng/mL) for TLR4, CL264 (5 μ g/mL) for TLR7 and ODN2006 (10 μ g/mL) for TLR9 (all from InvivoGen). To detect the reporter protein, secreted alkaline phosphatase (SEAP), 20 μ L of the supernatant was added to 180 μ L of QUANTI-Blue[™] substrate (InvivoGen) and incubated for 1 h at 37 °C. Levels of SEAP were determined by measuring the absorbance using a microplate reader at 650 nm. Relative SEAP levels were defined as the sample level divided by the solvent control level.

Dendritic cell maturation assay

Femurs and tibia of adult CB6F1/CrL mice (6-12 weeks old) were flushed with culture medium (Iscove's Modified Dulbecco's Medium) supplemented with 5% (v/v) FBS (Lonza, Verviers, Belgium), 50 μ M 2-mercaptoethanol (Sigma-Aldrich), penicillin and streptomycin, and the cells were seeded in 12-well plates at a concentration of 4.5×10^5 cells in 1 mL culture medium (adapted from Lutz *et al.*²⁰⁶). Dendritic cells were expanded with 20 ng/mL murine recombinant granulocyte macrophage colony stimulating factor (rGM-CSF) (Cytogen, The Netherlands). On day 2, the volume of complete growth medium was doubled and on day 5, an additional 20 ng/mL rGM-CSF was added. On day 7, bone marrow dendritic cells were

stimulated with PBS (1:250), LPS (10 ng/mL) or the unloaded or loaded (IgG1) microparticles at concentrations of 1, 0.5, 0.1 and 0.05 mg/mL for 16 h at 37 °C in a humidified CO₂ incubator. Staining of surface markers with the indicated antibodies was performed in the presence of Fc block (2.4 G2) for 30 min on ice. Anti-CD11c (N418) and I-Ad/I-Ed (M5/114) were purchased from eBioscience (San Diego, CA, USA), and anti-CD40 (3/23) and -CD86 (GL1) were obtained from BD Biosciences (Breda, the Netherlands). Samples were measured on a FACS CantoII (BD Biosciences, San Jose, CA, USA) and analyzed using the FlowJo software. Ethical approval for the mouse experiments was obtained from the Animal Experiment Committee of Utrecht University, The Netherlands.

6.2.5 *ENDOLISA*

Endotoxin amounts were determined with an endoLISA[®] endotoxin test kit from Hyglos GmbH (Germany). Materials were dissolved or particles were dispersed in endotoxin-free water at 1 mg/mL. LPS standard was freshly prepared as follows: the lyophilized LPS standard was dissolved completely in 2.06 mL endotoxin-free water (500 EU/mL). It was vortexed at 1 400 rpm for 10 min and a dilution row was prepared with concentrations of 500, 50, 5, 0.5, 0.05, and 0 EU/mL. Each sample was vortexed thoroughly before pipetting. A 100 µL volume of sample was added to a coated 96 well plate, followed by 20 µL of 6x binding buffer. The wells were sealed with cover foil and incubated at 37 °C for 90 min with continuous mixing at 450 rpm. Afterwards, the plate was washed carefully 3 times with 150 µL wash buffer per well. Then, 100 µL assay reagent was added to each well. Fluorescence was measured at $\lambda_{\text{ex}} = 380$ nm and $\lambda_{\text{em}} = 440$ nm and set as time point zero. The plate was incubated at 37 °C for another 90 min, following which the fluorescence was again determined and designated as time point 1. Endotoxin amount was calculated afterwards according to the standard curve.

6.2.6 *UPTAKE STUDIES*

For the evaluation of starch NP uptake into A549 and 16HBE14o- cells, 1×10^5 and 0.6×10^5 cells/well, of the respective cell lines were seeded on Transwell[®] membranes (3460, 1.12 cm²). After 24 h, A549 cells were set on ALI, *i.e.* medium was aspirated and 500 µL of fresh medium was added to the basolateral compartment only. Two days later, 250 µL of labeled starch NPs were deposited onto A549 cells with the Aeroneb[®]Lab nebulizer (Aerogen Ltd., Ireland) and incubated at 37 °C or 4 °C, respectively. Regarding the 16HBE14o- cells, an ALI

was established after 48 h in culture. After reaching 90% confluence, 250 μ L starch NPs were nebulized in the same procedure as for deposition on A549 cells.

For studying the uptake of the microparticles, A549 were seeded in Snapwell[®] plates (3801, 1.12 cm²; Corning, USA) and 10 mg of labeled starch NPs in mannitol (mass ratio 1:20) were deposited with the PADD OCC at 37 °C.

In all cases, after 1 h, 4 h, and 24 h of incubation, cells were washed with PBS and fixed with 3% paraformaldehyde (PFA) for 30 min at RT. After fixation, cells were permeabilized with a BSA/saponin/PBS solution, followed by an anti-phalloidin staining (1:143 and 1:100 in 16HBE14o- in BSA/saponin/PBS; actin) for 30 min. After washing, the samples were counterstained with DAPI (1:50 000 in PBS; nuclei) and subsequently mounted with DAKO mounting medium (DAKO, USA). The samples were analyzed by a confocal laser scanning microscope (Zeiss LSM710, Zeiss, Germany). Lasers at 405 nm (DAPI), 488 nm (starch NPs) and 633 nm (actin) were used for detection. Microscopic images of fixed samples were acquired at 1024 \times 1024 resolution, using a 63X water immersion objective. Confocal images were analyzed using Zen 2012 software (Carl Zeiss Microscopy GmbH) and Fiji Software (Fiji is a distribution of ImageJ available at <http://fiji.sc>).

6.3 RESULTS AND DISCUSSION

6.3.1 CYTOTOXICITY SCREENING

Material used for nanoparticle preparation

The use of cell lines in general is advantageous in comparison to primary cells, as the latter are donor dependent and often lack reproducibility. That is particularly true for lung tissue extracted from patients in a diseased state (lung cancer, CF, etc.) for which variations between each patient are known. A549 cells were chosen as an epithelium model of the deep lung. This was deemed to be a necessary model for investigation, as intracellular delivery to the alveolar region requires uptake into such cells; assessment of the toxicity of applied materials to such cells is therefore of great importance. A549 cells constitute a human pulmonary adenocarcinoma-derived cell line,²⁰⁷ which is both an easily accessible and well-established model of the alveolar region for first tests. For evaluating cell viability on exposure to NP materials, A549 cells were incubated with CS, TPP, NegSt and PosSt (α -starch derivatives) for 4 h and 24 h at 37 °C. Materials were dissolved in HBSS (4 h) or RPMI (24 h) and added in various concentrations to the A549 cells. Results can be found in Figure 6.1 with (A) representing 4 h of incubation and (B) representing 24 h of incubation.

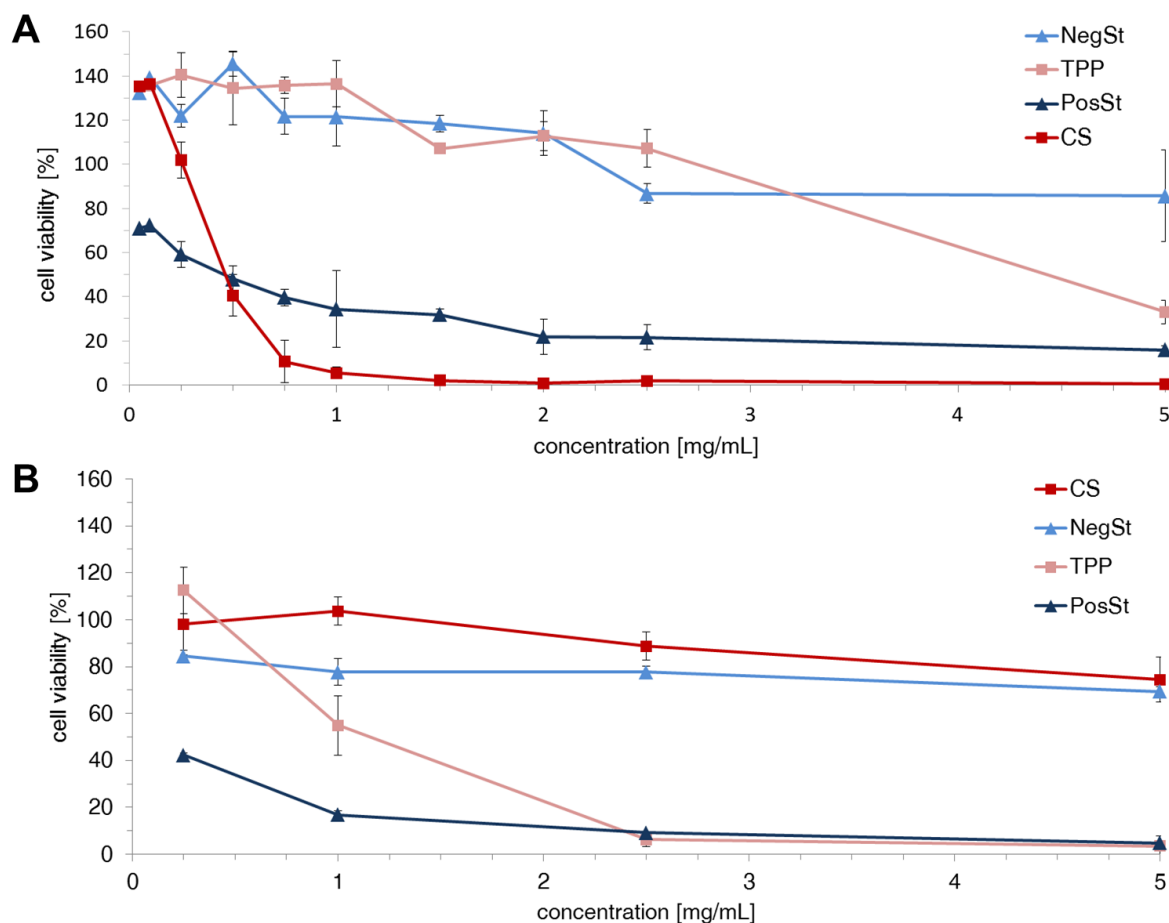


Figure 6.1: Viability of A549 cells after incubation with material used for NP preparation (CS, TPP, NegSt, and PosSt); after 4h incubation, samples dissolved in HBSS (A) and after 24 h incubation, samples dissolved in RPMI (B). Data represent two independent experiments (n=3, each).

After 4 h of incubation it could be seen that positively charged polymers were more toxic than negatively charged materials, which is in accordance with literature, showing that positively charged materials are more toxic compared to negatively charged ones.^{128, 208} A cell viability of 71 ± 6 % was found for the lowest concentration (0.05 mg/mL) of PosSt, which slowly decreased with increasing concentration up to 5 mg/mL. In contrast to PosSt, a cell viability of 135 ± 8 % was observed for the lowest tested concentration of CS, indicating that the cells were under stress. Here, a drastic decrease in cell viability was observed for concentrations of around 0.4 mg/mL and greater. In comparison, Huang *et al.*, found that the cytotoxicity of CS only significantly increased at concentrations higher than 0.7 mg/mL, and that the cytotoxicity was independent of CS molecular weight; toxic effects could also be reduced by reducing the degree of CS deacetylation. Additionally, no difference was observed in the cytotoxicity of

CS applied as a raw material or as NP suspension.²⁰⁹ The cytotoxic effects in the current work could be at least partially ascribed to the low pH of the CS solution. This highlights an advantage of the starch material, in that it does not alter the pH of the applied medium. Negatively charged materials showed similar cell viabilities for concentrations up to 2.5 mg/mL, however, whilst NegSt showed a good cell viability of 85 ± 6 % for the highest tested concentration, a high concentration of TPP led to a decrease in cell viability to 33 ± 12 %. This could be attributed to an increase in osmolality with increasing concentration of TPP. A 1 mg/mL concentration of TPP was still isotonic (osmolality of around 286 mOsm/kg), whereas 2.5 mg/mL already showed an increase up to approximately 310 mOsm/kg and 5 mg/mL showed an osmolality of approximately 330 mOsm/kg. Polymeric materials showed no effect on osmolality so that samples were always isotonic.

A general drop in cell viability could be found for the 24 h incubation (Figure 6.1 B), as the assay also detected a drop in cell proliferation rather than purely toxicity. In contrast to this, CS showed more or less constant cell viabilities of around 70-80%. This could be explained by the fact that CS was not soluble in RPMI medium and was applied as suspension, meaning that significant interaction with the A549 cells was possibly not taking place.

Cytotoxicity of nanoparticles

NPs were evaluated for their cytotoxicity using A549 cells, as an uptake of NPs by alveolar epithelial cells was the objective. Knowing from the previously conducted formulation studies that the molar ratio of NP components strongly influences the ζ -potential, it was aimed here to understand the effect of surface charge on cytotoxicity. Thus, three different starch NP formulations were studied, employing molar ratios of 3:1, 1:1, and 1:3 PosSt:NegSt, prepared from 0.25 mg/mL solutions. For comparison, CS NPs (0.25 mg/mL, molar ratio 10:1 CS:TPP) as well as NegSt, PosSt, and a water soluble potato starch (PSs) as control were tested in a concentration range from 8 to 133 μ g/mL. Viability data of A549 cells after treatment with aforementioned samples for 4 h (A) and 24 h (B) are shown in Figure 6.2.

At the routinely-employed 4 h measurement time point, as suggested by the manufacturers, A549 cells incubated with PSs, or NegSt both showed cell viabilities of around 100%. Treatment with PosSt resulted in a decrease in cell viability to 65.4 ± 5.5 % for the highest tested concentration. Such results were comparable to the experiments performed on source material (Figure 6.1). Similar results were also obtained for Starch 0.25-3:1 NPs with cell viabilities of around 71.3 ± 1.9 %. Decreasing the PosSt amount in the NP formulation led to an increase in cell viability, which is not surprising bearing in mind that positively charged

polymers usually show higher toxicities.^{128, 208} CS NPs showed a similar behavior to Starch 0.25-1:1 NPs for the 4 h incubation, while after the 24 h incubation period, a decrease in cell viability to 60.9 ± 2.2 % was noted for the highest tested concentration. This is in contrast to the cell viability studies performed by Grenha *et al.*, who found a minimum cell viability of 80% for their tested CS NP suspension.¹¹⁴ However, the CS they were using was of higher molecular weight (150 000 - 400 000 g/mol) compared to the CS used in this thesis, with a molecular weight of approximately 50 000 - 150 000 g/mol. Although the aforementioned Huang *et al.* found that the molecular weight does not influence toxicity of CS,²⁰⁹ it may change the pH of the applied NP suspension so resulting in cell damage.

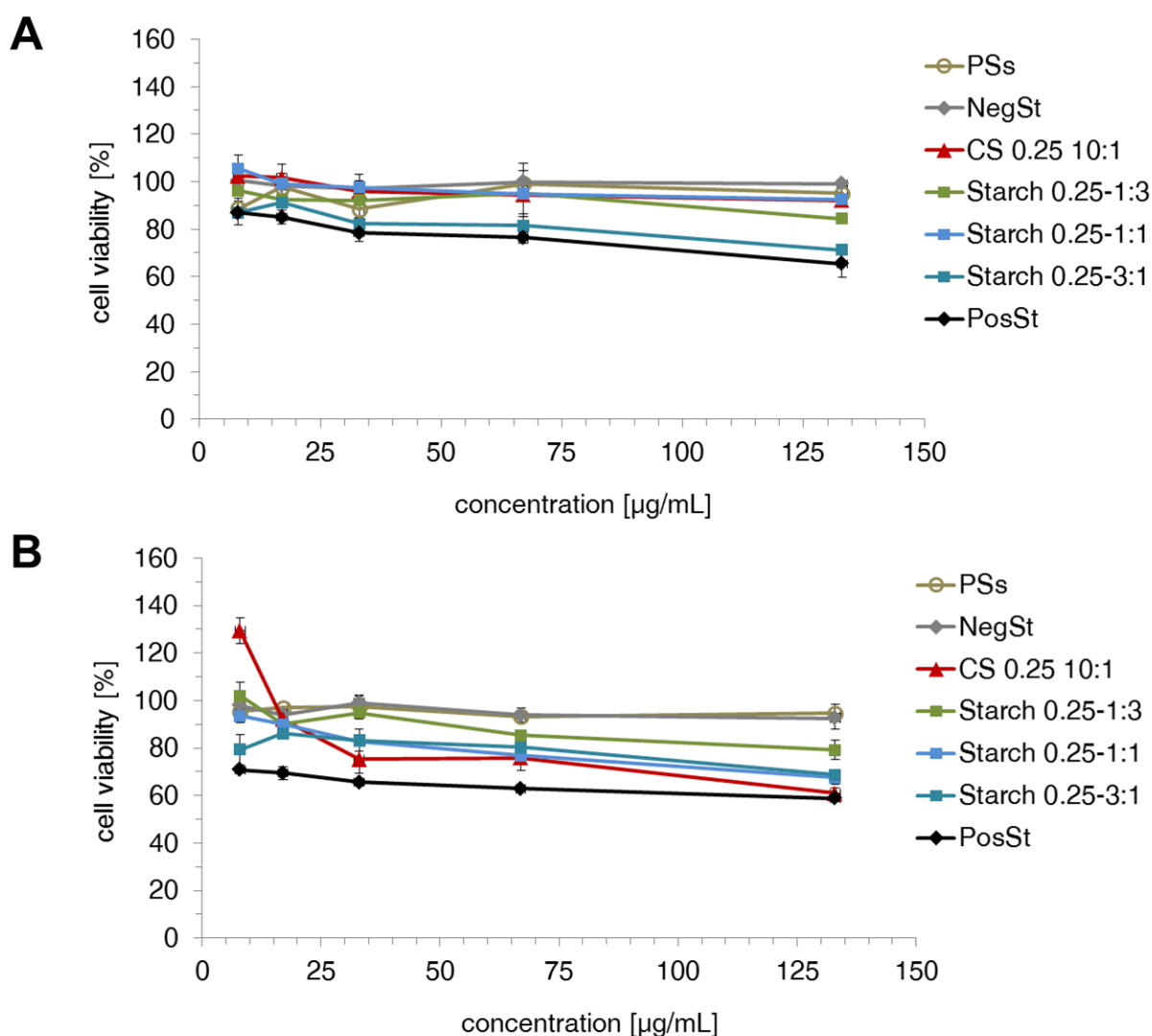


Figure 6.2: Viability of A549 cells after exposure to starch NPs, starch derivatives (PosSt, NegSt), or a soluble potato starch (PSs) for 4 h (A) or 24 h (B). Data represent two independent experiments ($n = 3$, each).

It can be concluded that, the greater the amount of positively charged material present in the starch NP formulation, the lower the observed cell viability. In addition, the chosen starch NP formulation Starch 0.25-1:1 showed similar or even better cell viabilities after 4 h and 24 h compared to the tested CS NP formulation. In the applied dose of 40 μg for uptake experiments, starch NPs showed cell viabilities of 80% or higher.

Additionally to the A549 epithelial cell line, THP-1 cells, representing alveolar macrophages, were used to study the cytotoxicity of NP formulations. In this respect, the formulations CS 0.25 10:1 (CS NP) and Starch 0.25-1:1 (Starch NP) were chosen. Figure 6.3 shows the cell viabilities of THP-1 cells after 4 h, 8 h, and 24 h treatment with CS NPs or starch NPs.

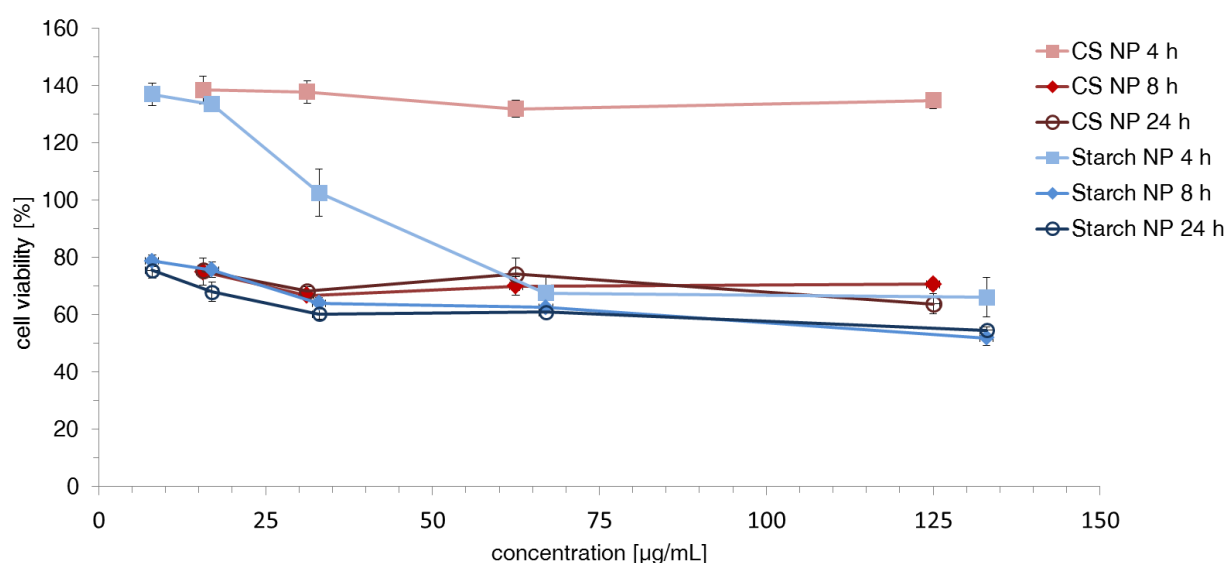


Figure 6.3: Viability of THP-1 cells after exposure to CS NPs, or starch NPs (Starch 0.25-1:1) for 4 h (■), 8 h (♦) or 24 h (○). Data represent two independent experiments (n = 3, each).

For the THP-1 cells, it could be seen that CS NPs showed better cell viabilities compared to starch NPs after 4 h of incubation. CS NPs showed constant cell viabilities around 135%, indicating that the THP-1 cells were under stress. High viabilities can be a sign of positive stimulation; however, they are often also seen before cell viability decreases, demonstrating a type of rescue mechanism of the cell. Starch NPs showed a decrease in cell viability to 66.1 ± 6.9 % for the highest tested concentration. The differences in cell viability of the two formulations after 4 h could perhaps be ascribed to differences in uptake kinetics, as the results obtained after 8 h and after 24 h of incubation were similar, with CS NPs showing slightly higher cell viabilities.

Cytotoxicity of microparticles

Microparticles, consisting either of starch NPs or CS NPs embedded in a microparticle matrix of manni, lact, or treha, were tested for their cytotoxicity using A549 and Calu-3 cells. These two cell types were chosen for investigation as microparticles would be required to pass through the whole respiratory system before deposition in the deep lung (represented by A549 cells), meaning that they could also interact with epithelial cell lines of the upper lung (modeled by Calu-3 cells).

Therefore, microparticles were dissolved in medium and applied under LCC to A549 or Calu-3 cells and incubated for 4 h and 24 h, respectively. The results can be found in Figure 6.4.

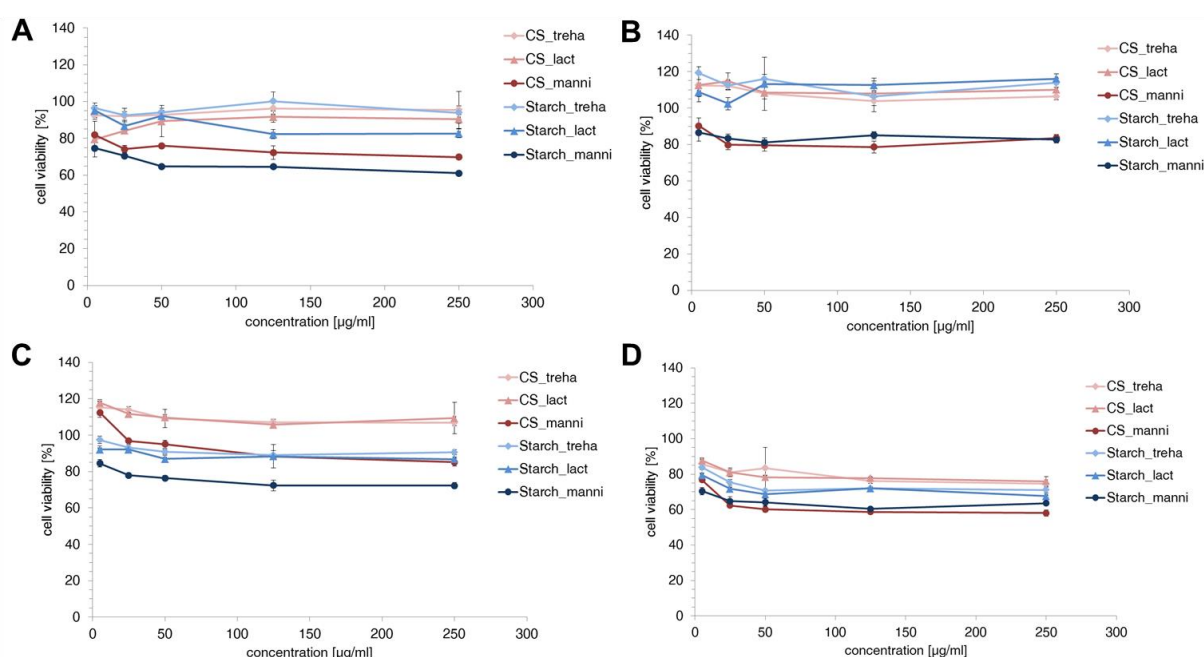


Figure 6.4: Cell viability after incubation with microparticles. Calu-3 cells after (A) 4 h incubation; (B) 24 h incubation; A549 cells after (C) 4 h incubation; (D) 24 h incubation; concentration [µg/mL] - representative of NP amount in microparticles.

The x-axis represents the concentration of NP in microparticles, to make a comparison to Figure 6.2 possible. It was observed that cell viability was independent from the NP material, and depended rather on the kind of excipient used for microparticle preparation. Manni samples led to a more pronounced decrease in cell viability compared to lact or treha samples. No big difference between the two cell lines was found, with the exception of the 24 h time point, at which Calu-3 cells seemed to show better cell viabilities compared to A549 cells. This is most likely caused by the longer doubling time of Calu-3 cells, leading to a lower uptake of particles in comparison to A549 cells within the same time interval, and less pronounced effects resulting from particle-induced downregulation of cell proliferation. The

differences in excipient tolerability could be attributed to their chemistry, as no differences in osmolality were found between the samples. Trehalose and lactose are disaccharides of glucose or glucose and galactose monomers, respectively and as such are probably positively influencing the cells' metabolism.

The cytotoxicity of microparticles was further tested by the University of Copenhagen, a COMPACT project partner, using the MTS assay with an incubation time of 1 h. Particles showed slightly increased viability, but in general no toxicity was observed (data not shown). Further, cytotoxicity was tested under ALI conditions by applying microparticles (10 mg per capsule) with the PADD OCC. The results of these investigations are shown in Figure 6.5. It could be seen that within cell lines, the differences in cell viabilities between the formulations are negligible, although differences in deposited amounts of sample expected to reach cells were found in *Chapter 5* (Figure 5.9). Calu-3 cells seemed to show higher cell viabilities, compared to A549 cells, which is in accordance with results found for LCC (Figure 6.4). As mentioned before, this could be due to the fact that Calu-3 cells have a longer doubling time compared to A549 cells.

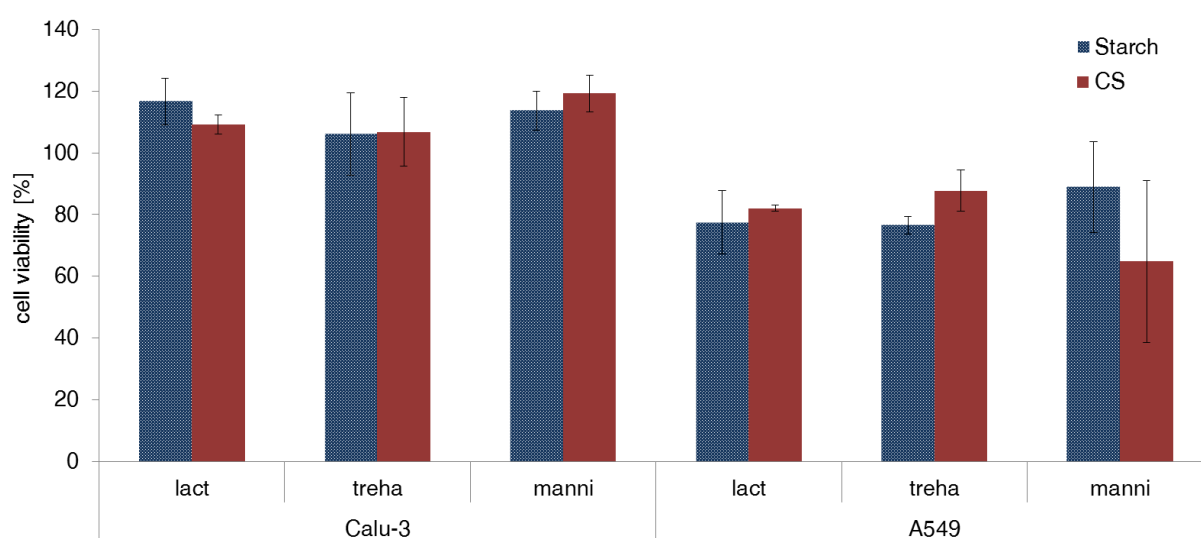


Figure 6.5: Cell viability of A549 and Calu-3 cells after deposition of microparticles (10 mg per capsule) with the PADD OCC and incubation at 37 °C for 4 h; cell viability determined with the MTT assay.

6.3.2 IMMUNOGENICITY SCREENING

To prevent an undesirable inflammatory and immunological response (in which CD4⁺ T cells may be activated and B cell-derived antigens may be formed) and to prevent the premature elimination of the DDS from the body, the immunogenicity of microparticles was tested based

on induction of dendritic cell maturation and TLR activation (extracellular: hTLR2, 4; intracellular: hTLR 3, 9) *via* NF κ B.

Antigen-presenting cells, such as dendritic cells, recognize pathogens *via* pattern-recognition receptors. These receptors can recognize peptidoglycan-, RNA- or DNA-associated patterns, which are characteristic for pathogens but absent in eukaryotic cells. TLRs are widely studied pattern-recognition receptors, and as such in the present experiment the potential activation of four different human TLRs (TLR2, TLR3, TLR4, and TLR9) was measured. Additionally, dendritic cell maturation was studied. These two assays were used in combination. The human TLR reporter assay was used as it is a straightforward and relatively quick human based assay, and allows for prediction of which TLR pathway may be activated *in vivo*. Moreover, the dendritic cell maturation assay links the innate and adaptive immune system, and gives a prediction regarding whether T cells could become activated in response to administration of a specific material.

Cells were stimulated with microparticles or IgG1 for 16 h in triplicates; results for extracellular hTLR2 (A), and hTLR4 (B) can be found in Figure 6.6, whereas results for intracellular hTLR3 (B), and hTLR9 (D) can be found in Figure 6.7. In general, no inhibition (small diagrams) should be observed, as this could lead to a false negative result. If inhibition of the agonist by the sample occurs, the activation (large diagrams) of hTLR cannot be interpreted.

Regarding the hTLR2, no inhibition *i.e.* SEAP activity was measured and no activation from IgG1 and CS particles was observed. Starch particles also showed no inhibition of hTLR2, but demonstrated a concentration dependent activation, *i.e.* DDS particles consisting of starch activated TLR more than IgG, thus being more immunogenic than the drug itself.

Regarding the hTLR4, inhibition in combination with CS particles was lower than the agonist, meaning that TLR4 activation data is also inconclusive. The negatively charged agonist (LPS)-EK could have been bound by the positively charged CS NPs, hTLR4 is in fact activated by CS particles. Starch particles, however, showed no inhibition of hTLR4 - a concentration dependent activation of hTLR4 starch particles to a greater extent than IgG was observed, meaning that the starch particles were more immunogenic than the drug itself.

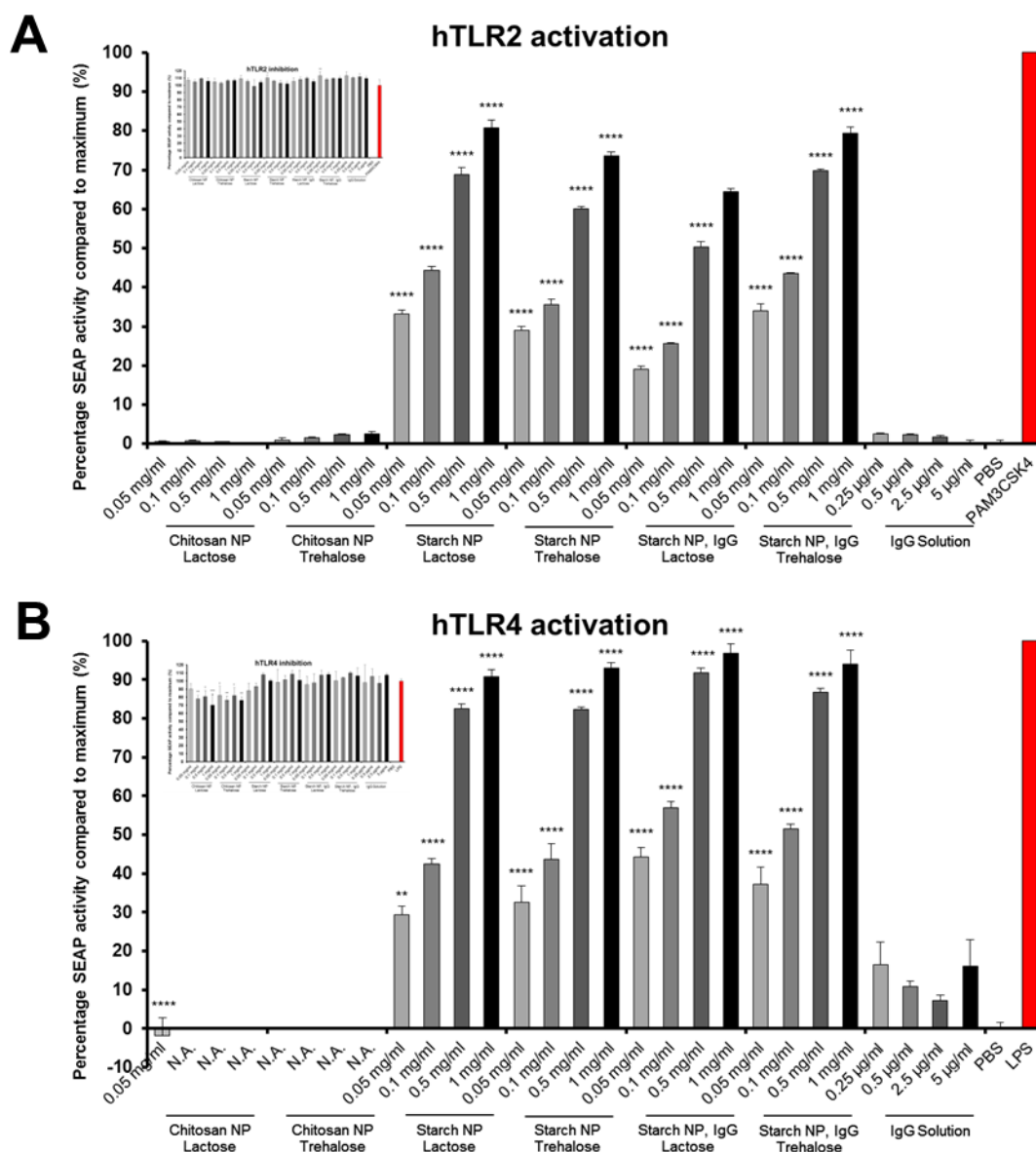


Figure 6.6: Immunogenicity. Inhibition (small images) and activation (large images) of TLR. Percentage of SEAP activity compared to maximum (TLR agonist) is displayed on the y-axis. Statistical significance was measured using two-way ANOVA. Statistical analysis was performed between drug/DDS and positive control (inhibition) or between drug (IgG) and DDS with corresponding concentration, e.g. DDS with concentration of 0.05 mg/mL was compared to IgG with a concentration of 0.25 µg/mL (activation). Samples that are statistically lower compared to positive control, have inhibited the TLR signaling pathway/TLR receptor. Therefore, the data in the activation graph is n.a. It could not be concluded if there was an activation/inhibition present. (A) hTLR2; (B) hTLR4.

For the hTLR3, a concentration dependent inhibition of hTLR3 (*i.e.* SEAP activity) measured in combination with CS particles was determined, meaning that the data of hTLR3 activation is inconclusive. It is likely, that the agonist for this hTLR, poly(I:C), a nucleotide which is negatively charged, was bound by the CS NPs. Thus, it could not be concluded if hTLR3 is

showed significantly lower SEAP activity compared to corresponding IgG concentrations. Also starch particles showed no inhibition and no activation of hTLR9; also here, the starch DDS showed significantly lower SEAP activity compared to corresponding IgG concentrations in some cases.

It could be concluded, that starch microparticles were more likely to activate TLR than CS microparticles. However, only an activation of extracellular hTLR, *i.e.* 2 and 4, was observed, whereas intracellular hTLR3 and hTLR 9 were not activated. As an activation of the TLR is a hindrance for pulmonary applications, these results were followed up by an endotoxin assay (Chapter 6.3.3) to identify the source of TLR activation.

For the murine bone marrow-derived dendritic cells (BMDC) maturation assay, cells were stimulated with microparticles or IgG1 for 20 h in duplicates. Results can be found in Figure 6.8.

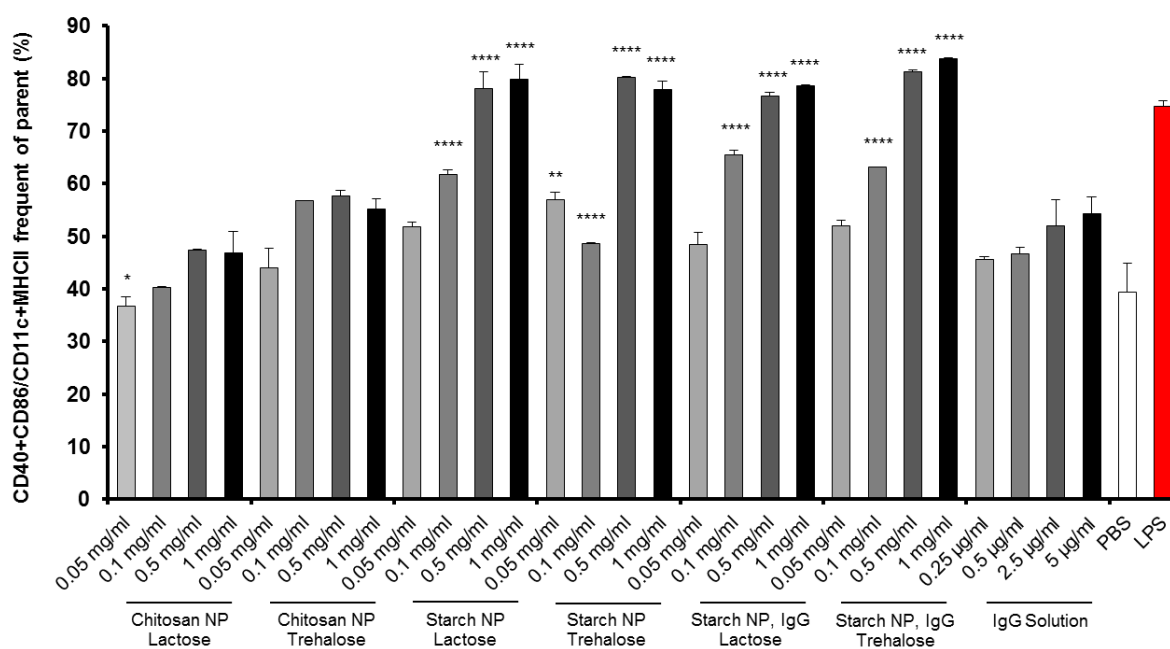


Figure 6.8: BMDC maturation assay. CD40+CD86/MHCII+CD11c frequency as a percentage of the parent population is displayed on the y-axis. Statistical significance was measured using two-way ANOVA. Statistical analysis was performed between drug (IgG) and DDS with corresponding concentration, *e.g.* DDS with concentration of 0.05 mg/mL was compared to IgG with a concentration of 0.25 µg/mL.

Chitosan particles showed no increased maturation of dendritic cells. In some cases however, the percentage of CD40⁺CD86⁺ cells was lower compared to the corresponding IgG1 concentration. In the case of starch particles, there was an increased maturation of dendritic

cells especially at the two highest concentrations (0.1, 0.5 and 1 mg/ml). The effect was also concentration dependent: the percentage CD40⁺CD86⁺ cells increased with increasing concentration.

6.3.3 ENDOLISA

Due to the results from the immunogenicity data, an endoLISA was performed to see whether the material itself was immunogenic or whether any endotoxin impurities may have been present, leading to false positive results. Therefore, all synthesized starch derivatives were tested as well as CS and TPP. To identify the source of any potential contamination within the preparation steps, also NPs, as well as microparticle formulations were also applied. The results can be found in Figure 6.9.

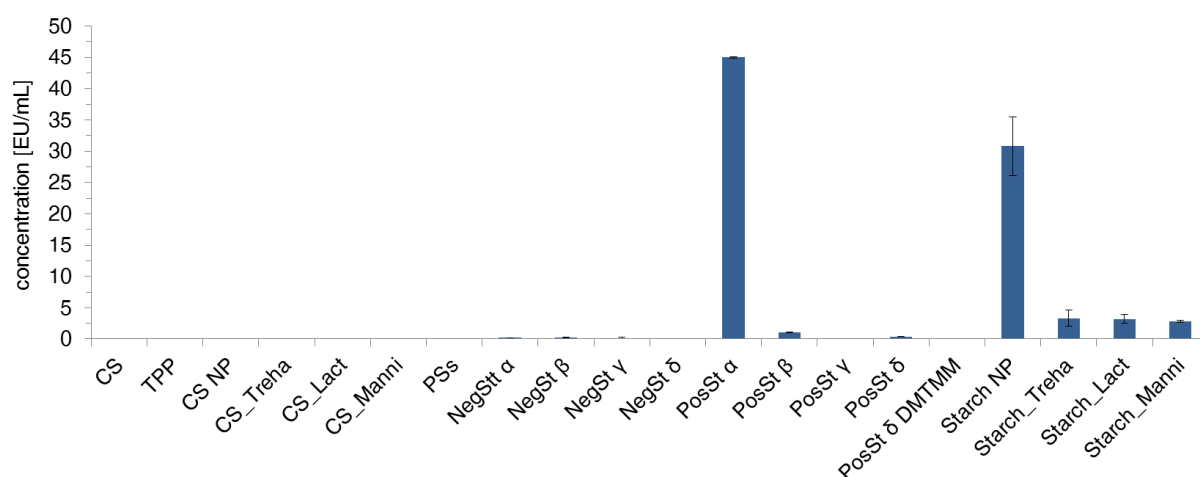


Figure 6.9: Endotoxin concentration in material samples (dissolved in endotoxin-free water) as well as NP or microparticle formulations (dispersed in endotoxin-free water). For particle preparation α -starch derivatives were used.

It could be seen that no endotoxins were found for CS material or for CS formulations. This is in accordance with the statement of the manufacturer, who guarantees an ultra-low level of endotoxins in this material. Negatively charged starches showed only very little amounts of endotoxin, independent of the degree of starch oxidation. In contrast, PosSt α , with a degree of substitution of 33%, showed a very high endotoxin concentration of approximately 45 EU/mL. All other PosSt derivatives, however, showed only a low concentration of endotoxins. This was independent of the degree of substitution, as PosSt β with a degree of substitution of around 47% showed only around 1 EU/mL. This further decreased for PosSt γ and PosSt δ . Starch NPs, consisting of 50% PosSt α , showed a concentration of 31 EU/mL.

starch microparticles consisting of starch NPs and excipient (mass ratio 1:20) showed again a decreased concentration of approximately 3 EU/mL.

As the found endotoxin concentration was independent of the degree of substitution (comparison of PosSt α and PosSt β), a direct activation from the starch material itself could be excluded. It was however interesting that a lower endotoxin concentration was observed when comparing the PosSt δ derivative to the PosSt α derivative. This result could indicate that the synthesis time point and storage time could have had an influence, as PosSt α was synthesized at least one or two years before PosSt β . The other PosSt derivatives were all synthesized over a short period of time. The strong immune activation observed in the TLR assays and the DC maturation assay was thus most likely due to the contamination of the cationic starch derivative during storage and not by one of the preparation steps. It could be concluded, that the conditions for storage of PosSt are very important to control. This gives some perspective to eliminate this problem in further studies. During the experiments, PosSt was kept light protected at RT. Storage at 4 °C or even -20 °C could show an improvement. Also storage in a desiccator under low relative humidity could show an advantage. Keeping this in mind, the cytotoxicity data as well as immunogenicity data should be interpreted with care and ideally be performed for carriers prepared from newly synthesized starch derivatives.

6.3.4 UPTAKE STUDIES

Nanoparticles

In order to evaluate uptake of starch NPs into A549 cells, PosSt was labeled with a green fluorescent dye (Bodipy[®] FL C5 NHS Ester, for synthesis see *Chapter 3*), following which starch NPs were prepared from 0.25 mg/mL solutions in a ratio of 1:1. The size of these labeled starch NPs was 145.2 ± 0.1 nm, with a PdI of 0.1, indicating a narrow size distribution. The ζ -potential was -26.4 ± 2.8 mV. As a control, A549 cells were grown under ALI conditions without treatment. Starch NPs were stable during nebulization (with a slight decrease in the ζ -potential, *Chapter 4*), and were deposited onto A549 cells and further incubated for 1 h, 4 h and 24 h at 4 °C or 37 °C. Endocytosis, as an energy-driven uptake mechanism, is highly reduced in cells when incubated at 4 °C. If NPs are taken up by the cells at 4 °C, it can be concluded that the uptake is not mediated by an energy-dependent mechanism. The binding and uptake of starch NPs by A549 cells can be seen in Figure 6.10 as z-stacks. Usually, the thickness of the samples is greater than that of a single focal plane. Z-stacks are created by incrementally stepping through the sample and taking images at different focal planes. The advantage of this technique is that the complete sample can be visualized.

For this study, the ability to create z-stacks means that NP localization with respect to surface binding vs. uptake into cell can be visualized, as indicated in Figure 6.10 as either an arrow (extracellular NPs) or arrow head (intracellular NPs).

Particles (green) showed an uptake already after 1 h of incubation at 37 °C. There was also some uptake after 1 h of incubation at 4 °C, although to a lower extent under these conditions, suggesting that at least a part of the uptake mechanism is energy dependent, *i.e.* normally occurs by endocytosis. The cell-associated fluorescence as observed at 4 °C could be either due to mere binding to the cell membrane or indicate some nonspecific, energy independent uptake. Such nonspecific uptake is known for A549 cells, suggesting that this could be a cell-dependent phenomenon.⁹¹

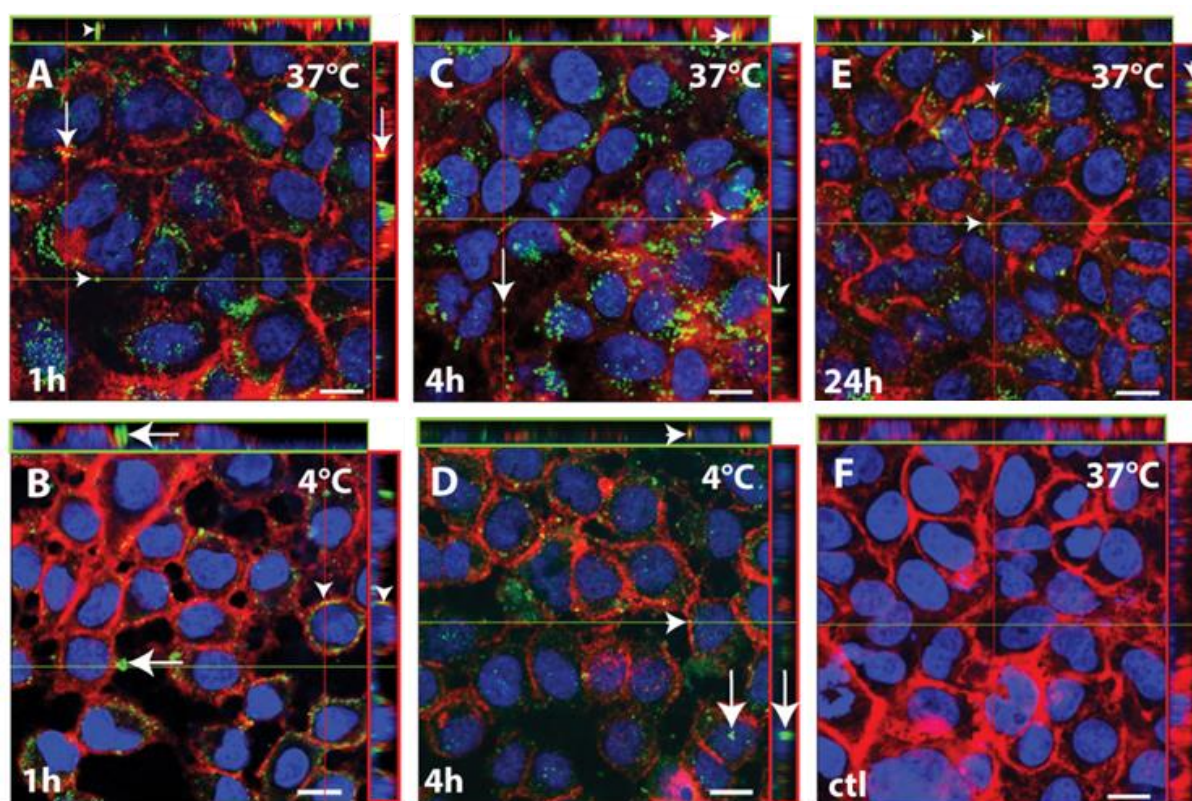


Figure 6.10: Confocal laser scanning microscopy (CLSM) images of 250 µl nebulized starch NP onto A549 cells, cultivated at the ALI. (A) after 1 h incubation at 37°C; (B) after 1 h incubation at 4°C; (C) after 4 h incubation at 37°C; (D) after 4 h incubation at 4°C; (E) after 24 h incubation at 37°C; (F) A549 without treatment, incubated at 37°C. Cells were washed with PBS, fixed with 3% PFA and stained. Blue: DAPI; red: actin; green: starch NP; scale bar: 10 µm; arrow: extracellular NPs; arrow head: intracellular NPs; (n=2).

To investigate this possibility further, the interaction of starch NPs with 16HBE14o- cells, a cell line generated by transformation of normal human bronchial epithelial cells that does not show carcinoma-like properties,^{210, 211} was also tested at 37 °C. The size of starch NPs in this

case was 114.6 ± 2 nm, with a Pdl of 0.12 and a ζ -potential of -28.1 ± 0.6 mV. The results of this study can be found in Figure 6.11. No particle uptake was seen after 1 h of incubation. However, after 4 h and 24 h of incubation, particles could be internalized. In this case, the confocal microscopy analysis provides qualitative data only - uptake amount should not be compared between the two cell types since the particle batch and the instrument settings (*e.g.* laser power) were not identical. From the images it seemed that the uptake into A549 was more pronounced; however, the experiment on the 16HBE14o- cells was only performed once, and it is suspected that the result may be influenced by a problem with the level of particle fluorescence, as an A549 cells experiment was run in parallel and showed the same effect. Nevertheless, an interaction of starch NPs with non-cancer pulmonary cell lines could be suggested.

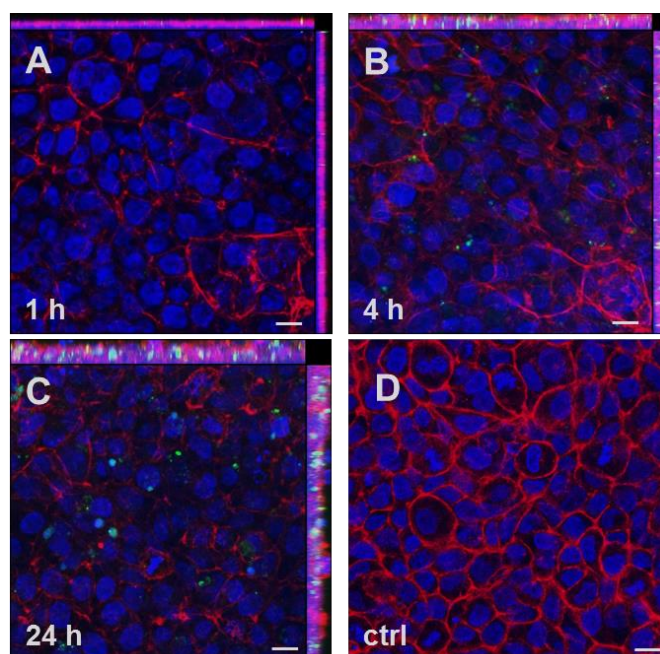


Figure 6.11: CLSM images of 250 μ l nebulized starch NP onto 16HBE14o- cells, cultivated at the ALI at 37 $^{\circ}$ C. (A) after 1 h incubation; (B) after 4 h incubation; (C) after 24 h incubation; (D) control; cells were washed with PBS, fixed with 3% PFA and stained. Blue: DAPI; red: actin; green: starch NP; scale bar: 10 μ m.

In summary, starch NPs were able to be internalized by A549 cells, and, from a preliminary study also potentially taken up by cells of a non-cancer cell line, 16HBE14o-. Thus, NPs should be able to be internalized once released from the microparticles following lung deposition.

Microparticles

To investigate the uptake of starch NPs when applied as dry powder formulation, microparticles (Starch_manni 1:20) were deposited on A549 cells with the PADD OCC (10 mg per capsule). The uptake was studied after 1 h, 4 h and 24 h of incubation at 37 °C and can be found in Figure 6.12. Compared to the starch NP uptake on A549 cells, fewer particles can be found for the application of the microparticles. This is reasonable, due to the fact that only 1:20 of the microparticles consisted of starch NPs and that only a limited amount of the applied fraction reached the cells after deposition with the PADD OCC. Nevertheless, particles can be found already after 1 h of incubation, suggesting that the microparticles were rapidly dissolved, releasing the starch NPs. Also after 4 h and 24 h of incubation, particles were internalized. In contrast to the direct application of starch NPs, where NPs could be found throughout the sample, microparticles were not homogenously distributed, but rather showed some high deposition and low deposition spots.

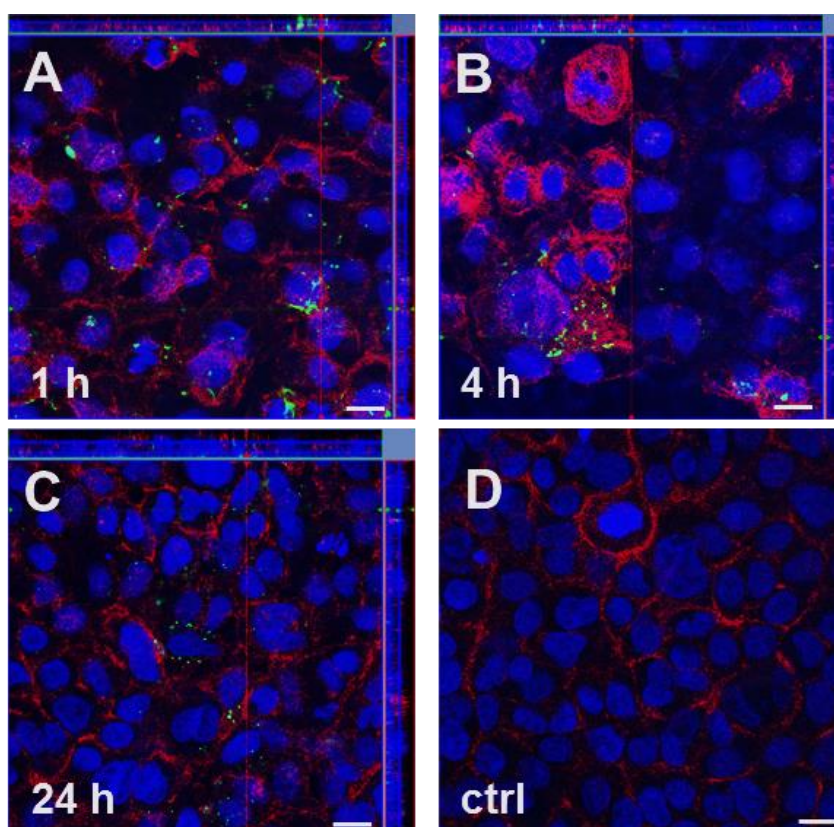


Figure 6.12: CLSM images of Starch_manni 1:20 deposited with the PADD OCC (10 mg per capsule) onto A549 cells, cultivated at the ALI at 37 °C. (A) after 1 h incubation; (B) after 4 h incubation; (C) after 24 h incubation; (D) control; cells were washed with PBS, fixed with 3% PFA and stained. Blue: DAPI; red: actin; green: starch NP; scale bar: 10 µm.

6.4 CONCLUSION

The cytotoxicity screening on A549 cells revealed that positively charged materials were more toxic, compared to negatively charged materials. NegSt, however, showed a higher tolerance compared to TPP, probably due to the effect of TPP on osmolality. On A549 cells, starch NP formulations showed a decrease in cell viability with increasing PosSt amount, thus a final formulation consisting of a molar ratio of 1:1 (PosSt: NegSt) was chosen. Additionally, starch NPs were comparable or better than the standard CS formulation. This behavior was different for the cytotoxicity on THP-1 cells, where CS NPs showed an advantageous behavior after an incubation of 4 h. Following 24 h of incubation, however, it was revealed that both particle types showed more or less comparable effects. Cytotoxicity testing of microparticles under LCC revealed a detrimental effect of manni samples, independent of the NP formulation. However, this effect was not pronounced under ALI conditions. It could be suggested that Calu-3 cells were less sensitive than A549 cells, due to their longer doubling time, thus leading to a lower endocytic uptake of particles per unit time.

Immunogenicity data indicated that the starch delivery system was more immunogenic compared to the CS NPs, thus not suitable for application *in vivo*. However, CS NPs often interfered with the assay, due to presumed binding of the agonist to CS NP surfaces, meaning that an accurate analysis of the results was not possible. Additionally, results obtained from the endotoxin assay suggested that the observed apparent immunogenicity of the starch system could be due to suboptimal storage conditions of PosSt α , leading to incorporation of immunogenic endotoxin impurities. It could be shown that the endotoxin concentration was independent of the degree of substitution of PosSt and also that the closer the starch derivative synthesis was to the performed endoLISA experiment, the lower the found endotoxin concentration. An alternative could therefore be the use of newly synthesized PosSt derivatives for DDS and additional cytotoxicity and immunogenicity screenings, or the removal of endotoxin impurities. The latter is challenging, as endotoxins are heat resistant, meaning that samples must be stored at 200 °C for at least 4 h or treated with 1 M NaOH in order to facilitate endotoxin removal. An alternative approach could be the application of EndoTrap[®] from Hyglos, which is a chromatography based method for endotoxin removal. In comparison to starch derivatives, CS and its formulation did not show any endotoxin impurities, due to the fact that the material was bought in high quality from Novamatrix, who also guaranteed a very low content of endotoxins. These findings show, how important a detailed material characterization is, with regards to material purity and presence of

impurities, especially with respect to new materials that cannot be bought from a manufacturer.

The uptake of starch NPs after aerosolization onto A549 cells and 16HBE14o- cells indicate that starch NPs could be suitable for intracellular protein/peptide delivery. Also the application of the dry powder formulation led to an uptake of starch NPs in A549 cells that was already visible after 1 h of incubation, demonstrating that the microparticles were able to quickly dissolve and release the NPs.

In a next step, intracellular protein/peptide delivery by loaded starch NPs should be evaluated, as well as a competitive particle uptake between macrophages and epithelial cells. Results of those experiments are included in the thesis *A new cell line-based coculture model of the human air-blood barrier to evaluate the interaction with aerosolized drug carriers* by Stephanie Kletting.

7. SUMMARY AND OUTLOOK

Protein and peptide delivery is a demanding task. The pulmonary route of administration in particular, requires special attention regarding formulation strategy and a good knowledge of the used materials, in order to facilitate effective delivery of proteins and peptides.

The aim of this thesis was focused on the development of a novel nanotechnology enabled DDS suitable for pulmonary protein and peptide delivery, using novel excipients.

In this context, the synthesis and characterization of starch derivatives was performed, including an optimization of product purification performed by precipitation of the material, as well as introducing an alternative coupling agent, DMTMM.

NP preparation from synthesized starch derivatives *via* charge mediated coacervation in aqueous medium was successfully performed, offering a mild preparation method for loading with proteins and peptides. This procedure was seen to be most successful for NP loading with vanco, with an EE of ~43% and a LR of ~23% obtained in this case. No organic solvents, no harsh preparation conditions, and no additional excipients, *e.g.* for stabilization purposes, had to be used for such NP preparation.

A carrier system for the delivery of NPs to the deep lung was further developed. The market situation shows that APIs for inhalation are usually applied as physical mixture with larger carrier particles acting as a vehicle for deep lung deposition. This often results in a high fraction of particles that do not reach the lung, as de-agglomeration in the air-stream is required. The developed carrier system instead consists of a fast dissolving carrier matrix with aerodynamic properties, suitable for deep lung deposition, which incorporates the NPs and facilitates a fast NP release in the deep lung.

In vitro experiments revealed opportunities but also drawbacks of the developed DDS. It could be shown that starch NPs applied without but also with the microparticle carrier system were able to be taken up by alveolar epithelial cells (A549), ensuring an intracellular delivery of the cargo. However, immunogenicity data revealed a contamination with endotoxins, which could to a certain extent also explain the obtained cytotoxicity data.

In summary, these findings underline the close interplay between knowledge of the material used for drug delivery preparation, and *in vitro* testing approaches, in addition to the development of a suitable DDS for APIs from a technological viewpoint. Additionally, in the case of proteins and peptides as API, a sound knowledge of their characteristics is also necessary.

Although a few questions could be answered in the current work, several open questions still remain and could form the basis of future work. In the course of material synthesis an alternative coupling reagent was found in DMTMM, and an improvement in the purification method could be shown; however, scalability from milligram to gram, and further to kilogram, is of interest from an industrial point of view. Furthermore, although a possible explanation for the apparent immunogenicity of the system was found – namely, contamination with endotoxins – the application of different elimination techniques (*e.g.* with EndoTrap®) followed by further evaluation with the endoLISA are of importance to substantiate this hypothesis. Cytotoxicity and immunogenicity data should also be repeated in conjunction with such investigations.

NP preparation and loading was successful with model proteins. The loading with an actual disease-relevant cargo with subsequent efficacy testing is however of interest. The release kinetics of such a cargo from NPs could be investigated.

The microparticles (and especially Starch_manni) showed a high degree of deposition in the deep lung, and a considerable uptake of starch NPs, when deposited as dry powder formulation. However, release studies of the NPs in lung relevant medium (*e.g.* simulated lung fluid) as well as real-time imaging of the dissolution of the microparticles on pulmonary epithelial cells are of interest. Further, particle uptake by epithelial cells *vs.* macrophages should be evaluated (*e.g.* with a co-culture model).

8. LIST OF ABBREVIATIONS

ALI	air-liquid-interface
ANOVA	analysis of variance
API	active pharmaceutical ingredient
AT-I	alveolar type I cell
AT-II	alveolar type II cell
BCA	bicinchoninic acid
BMDC	murine bone marrow-derived dendritic cells
BSA	bovine serum albumin
CLSM	confocal laser scanning microscopy
COMPACT	collaboration on the optimization of macromolecular pharmaceutical access to cellular targets
CS	chitosan
DAPI	4',6-diamidin-2-phenylindol
DCC	N,N'-dicyclohexylcarbodiimide
DDS	drug delivery system
DLS	dynamic light scattering
DMSO	dimethyl sulfoxide
DMTMM	4-(4,6-dimethoxy-1,3,5-triazin-2-yl)-4-methylmorpholinium chloride
DPI	dry powder inhaler
DSMZ	Deutsche Sammlung von Mikroorganismen und Zellkulturen
EE	encapsulation efficiency
efpia	European Federation of Pharmaceutical Industries and Association
EMA	European Medicines Agency
FACS	fluorescence-activated cell sorting
FBS	fetal bovine serum
FDA	(US) Food and Drug Administration
FPF	fine particle fraction
FT-IR	fourier transform infrared spectroscopy
GPC	gel permeation chromatography
GRAS	generally recognized as safe
GSD	geometric standard deviation

HBSS	Hank's balanced salt solution
HOBt	1-hydroxybenzotriazole
hTLR	human toll-like receptor
IEP	isoelectric point
IMI	Innovative Medicines Initiative
IPF	idiopathic pulmonary fibrosis
lact	lactose
LCC	liquid covered condition
LPS	lipopolysaccharide
LR	loading rate
Lyso	lysozyme
manni	mannitol
MDI	metered dose inhaler
MEM	minimum essential medium eagle
MMAD	mass median aerodynamic diameter
MTT	3-(4,5-dimethylthiazol-2-yl)-2,5-diphenyltetrazolium bromide
FluNa	sodium fluorescein
NaOCl	sodium hypochlorite
NCS	nanotoxicology classification system
NEAA	non-essential amino acids
NegSt	negatively charged starch derivative
NGI	next generation impactor
NMR	nuclear magnetic resonance
NP	nanoparticle
OVA	ovalbumin
PADDOCC	pharmaceutical aerosol deposition device on cell culture
PBS	phosphate buffered saline
PdI	polydispersity index
PFA	paraformaldehyde
PosSt	positively charged starch derivative
PTA	phosphotungstic acid
RNase A	ribonuclease A
RPMI	Roswell Park Memorial Institute (cell culture medium)
SDS-PAGE	Sodium dodecyl sulfate polyacrylamide gel electrophoresis

SEAP	secreted embryonic alkaline phosphatase
SEM	scanning electron microscopy
TEM	transmission electron microscopy
TEMPO	(2,2,6,6-tetramethylpiperidin-1-yl)oxidanyl
TPP	sodium tripolyphosphate
treha	trehalose
vanco	vancomycin
XRPD	x-ray powder diffraction

9. BIBLIOGRAPHY

- (1) Lipinski, C. A. (2000), Drug-like properties and the causes of poor solubility and poor permeability. *Journal of Pharmacological and Toxicological Methods* 44, 235-249.
- (2) Lipinski, C. A., Lombardo, F., *et al.* (2001), Experimental and computational approaches to estimate solubility and permeability in drug discovery and development settings. *Advanced Drug Delivery Reviews* 46, 3-26.
- (3) Ötvös, L. (2014), Relative success rates by drug class: The case for peptides. *Pharmaceutical Outsourcing* 15, 6.
- (4) Reichert, J. M. (2003), A guide to drug discovery: Trends in development and approval times for new therapeutics in the United States. *Nature Reviews Drug Discovery* 2, 695-702.
- (5) Singh, A., Talekar, M., *et al.* (2014), Macrophage-targeted delivery systems for nucleic acid therapy of inflammatory diseases. *Journal of Controlled Release* 190, 515-530.
- (6) Patil, S. D., Rhodes, D. G., *et al.* (2005), DNA-based Therapeutics and DNA Delivery Systems: A Comprehensive Review. *The AAPS Journal* 7, E61-E77.
- (7) Cox, D. B. T., Platt, R. J., *et al.* (2015), Therapeutic genome editing: prospects and challenges. *Nature Medicine* 21, 121-131.
- (8) Hope, M. J., Mui, B., *et al.* (1998), Cationic lipids, phosphatidylethanolamine and the intracellular delivery of polymeric, nucleic acid-based drugs (Review). *Molecular Membrane Biology* 15, 1-14.
- (9) Voet, D., Voet, J. G., *et al.* (2002), Lehrbuch der Biochemie (Fundamentals of Biochemistry), Wiley-VCH Verlag.
- (10) Alberti, K. G. M. M., and Zimmet, P. Z. (1998), Definition, Diagnosis and Classification of Diabetes Mellitus and its Complications Part 1: Diagnosis and Classification of Diabetes Mellitus Provisional Report of a WHO Consultation. *Diabetic Medicine* 15, 539-553.
- (11) Fujino, M., Fukuda, T., *et al.* (1974), Synthetic analogs of luteinizing hormone releasing hormone (LH-RH) substituted in position 6 and 10. *Biochemical and Biophysical Research Community* 60, 406-413.
- (12) Monahan, M. W., Amoss, M. S., *et al.* (1973), Synthetic Analogs of the Hypothalamic Luteinizing Hormone Releasing Factor with Increased Agonist or Antagonist Properties. *Biochemistry* 12, 4616-4620.
- (13) Sharifi, R., Ratanawong, C., *et al.* (1997), Therapeutic effects of leuporelin microspheres in prostate cancer. *Advanced Drug Delivery Reviews* 28, 121-138.
- (14) Voulgari, P. V., and Drosos, A. A. (2006), Adalimumab for rheumatoid arthritis. *Expert Opin. Biol. Ther.* 6, 1349-1360.
- (15) Frokjaer, S., and Otzen, D. E. (2005), Protein drug stability: a formulation challenge. *Nature Reviews Drug Discovery* 4, 298-306.
- (16) Knudsen, L. B., Nielsen, P. F., *et al.* (2000), Potent Derivatives of Glucagon-like Peptide-1 with Pharmacokinetic Properties Suitable for Once Daily Administration. *J. Med. Chem.* 43, 1664-1669.
- (17) Kurtzhals, P., Havelund, S., *et al.* (1995), Albumin binding of insulins acylated with fatty acids: characterization of the ligand-protein interaction and correlation between binding affinity and timing of the insulin effect in vivo. *Biochem J.* 312, 725-731
- (18) Foldvari, M., Attah-Poku, S., *et al.* (1998), Palmitoyl Derivatives of Interferon α : Potential for Cutaneous Delivery. *Journal of Pharmaceutical Sciences* 87, 1203-1208.
- (19) Matthews, S. J., and McCoy, C. (2004), Peginterferon Alfa-2a: A Review of Approved and Investigational Uses. *Clinical Therapeutics* 26, 991-1025.
- (20) Lee, H., and Park, T. G. (2002), Preparation and Characterization of Mono-PEGylated Epidermal Growth Factor: Evaluation of in Vitro Biological Activity. *Pharmaceutical Research* 19, 845-851.
- (21) Sozer, N., and Kokini, J. L. (2009), Nanotechnology and its applications in the food sector. *Trends in Biotechnology* 27, 82-89.

- (22) Vettiger. (2002), The "Millipede" - Nanotechnology Entering Data Storage. *IEEE Transactions on Nanotechnology* 1, 39-55.
- (23) De Franceschi, S., and Kouwenhoven, L. (2002), Electronics and the single atom. *Nature* 417, 701-702.
- (24) Law, M., Greene, L. E., *et al.* (2005), Nanowire dye-sensitized solar cells. *Nature Materials* 4, 455-459.
- (25) Chan, C. K., Peng, H., *et al.* (2007), High-performance lithium battery anodes using silicon nanowires. *Nature Nanotechnology* 3, 31-35.
- (26) Sumer, B., and Gao, J. (2008), Theranostic nanomedicine for cancer. *Nanomedicine : nanotechnology, biology, and medicine* 3, 137-140.
- (27) Sahoo, S. K., and Labhasetwar, V. (2003), Nanotech approaches to drug delivery and imaging. *Drug Discovery Today* 8, 1112-1120.
- (28) Jain, K. K. (2005), Nanotechnology in clinical laboratory diagnostics. *Clinica Chimica Acta* 358, 37-54.
- (29) Liu, H., and Webster, T. J. (2007), Nanomedicine for implants: A review of studies and necessary experimental tools. *Biomaterials* 28, 354-369.
- (30) Donaldson, K. (2004), Nanotoxicology. *Occupational and Environmental Medicine* 61, 727-728.
- (31) NanoMedicine. (2005), Vision paper and basis for a strategic research agenda for nanomedicine. *European Technology Platform on NanoMedicine*, 1-40.
- (32) Barthold, S., Kunschke, N., *et al.* (2015), (Rothen-Rutishauser, B., and Dhand, R., Eds.).
- (33) Lehr. (2014), Wirksame und sicherere Medikamente mit Hilfe der Nanotechnologie. *nanotechnologie aktuell*.
- (34) Keck, C. M., and Müller, R. H. (2013), Nanotoxicological classification system (NCS) – A guide for the risk-benefit assessment of nanoparticulate drug delivery systems. *European Journal of Pharmaceutics and Biopharmaceutics* 84, 445-448.
- (35) Birrenbach, G., and Speiser, P. (1976), Polymerized Micelles and Their Use as Adjuvants in Immunology. *Journal of Pharmaceutical Sciences* 65, 1763-1766.
- (36) Allen, T. M. (2004), Drug Delivery Systems: Entering the Mainstream. *Science* 303, 1818-1822.
- (37) Bawa, R. (2009), Nanopharmaceuticals for Drug Delivery – A Review. *Touch Briefings* 6, 135-155.
- (38) Bawa, R. (2008), Nanoparticle-based Therapeutics in Humans A Survey. *Nanotechnology Law & Business*, 135-155.
- (39) Merisko-Liversidge, E., Liversidge, G. G., *et al.* (2003), Nanosizing: a formulation approach for poorly-water-soluble compounds. *European Journal of Pharmaceutical Sciences* 18, 113-120.
- (40) Liversidge, G. G., and Cundy, K. C. (1995), Particle size reduction for improvement of oral bioavailability of hydrophobic drugs. *International Journal of Pharmaceutics* 125, 91-97.
- (41) Liversidge, G. G., and Conzentino, P. (1995), Drug particle size reduction for decreasing gastric irritancy and enhancing absorption of naproxen in rats. *International Journal of Pharmaceutics* 125, 309-313.
- (42) Mathew, T. H., Van Buren, C., *et al.* (2006), A Comparative Study of Sirolimus Tablet Versus Oral Solution for Prophylaxis of Acute Renal Allograft Rejection. *The Journal of Clinical Pharmacology* 46, 76-87.
- (43) Adler-Moore, J. P., and Proffitt, R. T. (1993), Development, Characterization, Efficacy and Mode of Action of AmBisome, a unilamellar liposomal formulation of Amphotericin B. *Journal of Liposome Research* 3, 429-450.
- (44) Bekersky, I., Fielding, R. M., *et al.* (2002), Pharmacokinetics, Excretion, and Mass Balance of Liposomal Amphotericin B (AmBisome) and Amphotericin B Deoxycholate in Humans. *Antimicrobial Agents and Chemotherapy* 46, 828-833.
- (45) Boswell, G. W., Bekersky, I., *et al.* (1998), Toxicological Profile and Pharmacokinetics of a Unilamellar Liposomal Vesicle Formulation of Amphotericin B in Rats. *Antimicrobial Agents and Chemotherapy* 42, 263-268.

- (46) Pardridge, W. M. (2003), Blood-brain barrier drug targeting the future of brain drug development. *Molecular Interventions* 3, 90-105.
- (47) Tosi, G., Constantino, L., *et al.* (2008), Polymeric nanoparticles for the drug delivery to the central nervous system. *Expert opinion on drug delivery* 5, 155-174.
- (48) Matsumara. (1986), A New Concept for Macromolecular Therapeutics in Cancer Chemotherapy: Mechanism of Tumor-tropic Accumulation of Proteins and the Antitumor Agent Smancs. *Cancer Research* 46, 6387-6392.
- (49) Yuan, F., Dellian, M., *et al.* (1995), Vascular Permeability in a Human Tumor Xenograft: Molecular Size Dependence and Cutoff Size. *Cancer Research* 55, 3752-3756.
- (50) Moghimi, S. M., and Szebeni, J. (2003), Stealth liposomes and long circulating nanoparticles: critical issues in pharmacokinetics, opsonization and protein-binding properties. *Progress in Lipid Research* 42, 463-478.
- (51) Lasic, D. D. (1996), Doxorubicin in sterically stabilized liposomes. *Nature* 380, 561-562.
- (52) Lasic, D. D., and Needham, D. (1995), The "Stealth" Liposome A Prototypical Biomaterial. *Chemical Reviews* 95, 2601-2628.
- (53) Working, P. K., Newman, M. S., *et al.* (1999), Reduction of the cardiotoxicity of doxorubicin in rabbits and dogs by encapsulation in long-circulating, pegylated liposomes. *Pharmacology and Experimental Therapeutics* 289, 1128-1133.
- (54) Yuan, F., Quan, L.-d., *et al.* (2012), Development of macromolecular prodrug for rheumatoid arthritis. *Advanced Drug Delivery Reviews* 64, 1205-1219.
- (55) Schmidt, C., Lautenschlaeger, C., *et al.* (2013), Nano- and microscaled particles for drug targeting to inflamed intestinal mucosa—A first in vivo study in human patients. *Journal of Controlled Release* 165, 139-145.
- (56) Lamprecht, A., Schäfer, U., *et al.* (2001), Size-Dependent Bioadhesion of Micro- and Nanoparticulate Carriers to the Inflamed Colonic Mucosa. *Pharmaceutical Research* 18, 788-793.
- (57) Almeida, A., and Souto, E. (2007), Solid lipid nanoparticles as a drug delivery system for peptides and proteins. *Advanced Drug Delivery Reviews* 59, 478-490.
- (58) Etheridge, M. L., Campbell, S. A., *et al.* (2013), The big picture on nanomedicine: the state of investigational and approved nanomedicine products. *Nanomedicine: Nanotechnology, Biology and Medicine* 9, 1-14.
- (59) Cleland, J. L., Daugherty, A., *et al.* (2001), Emerging protein delivery methods. *Current Opinion in Biotechnology* 12, 212-219.
- (60) Landsiedel, R., Fabian, E., *et al.* (2012), Toxicokinetics of nanomaterials. *Archives of Toxicology* 86, 1021-1060.
- (61) Collnot, E.-M., Ali, H., *et al.* (2012), Nano- and microparticulate drug carriers for targeting of the inflamed intestinal mucosa. *Journal of Controlled Release* 161, 235-246.
- (62) Slütter, B., Plapied, L., *et al.* (2009), Mechanistic study of the adjuvant effect of biodegradable nanoparticles in mucosal vaccination. *Journal of Controlled Release* 138, 113-121.
- (63) Mönkäre, J., Reza Nejadnik, M., *et al.* (2015), IgG-loaded hyaluronan-based dissolving microneedles for intradermal protein delivery. *Journal of Controlled Release* 218, 53-62.
- (64) Mittal, A., Raber, A. S., *et al.* (2013), Non-invasive delivery of nanoparticles to hair follicles: A perspective for transcutaneous immunization. *Vaccine* 31, 3442-3451.
- (65) Shrewsbury, S. B., Cook, R. O., *et al.* (2008), Safety and Pharmacokinetics of Dihydroergotamine Mesylate Administered Via a Novel (Tempo™) Inhaler. *Headache: The Journal of Head and Face Pain* 48, 355-367.
- (66) Bur, M., and Lehr, C. M. (2008), Pulmonary cell culture models to study the safety and efficacy of innovative aerosol medicines. *Expert opinion on drug delivery* 5, 641-652.
- (67) <http://www.fda.gov/NewsEvents/Newsroom/PressAnnouncements/ucm403122.htm>. FDA News Release: FDA approves Afrezza to treat diabetes. (last access: 01.03.16)
- (68) Mahmud, A., and Discher, D. E. (2011), Lung vascular targeting through inhalation delivery: insight from filamentous viruses and other shapes. *IUBMB life* 63, 607-612.

- (69) Ruge, C. A., Kirch, J., *et al.* (2013), Pulmonary drug delivery: from generating aerosols to overcoming biological barriers-therapeutic possibilities and technological challenges. *The lancet. Respiratory medicine* 1, 402-13.
- (70) Geiser, M. (2010), Update on macrophage clearance of inhaled micro- and nanoparticles. *Journal of aerosol medicine and pulmonary drug delivery* 23, 207-217.
- (71) Antunes, M. B., and Cohen, N. A. (2007), Mucociliary clearance--a critical upper airway host defense mechanism and methods of assessment. *Curr Opin Allergy Clin Immunol* 7, 5-10.
- (72) Hofmann, W., and Asgharian, B. (2003), The effect of lung structure on mucociliary clearance and particle retention in human and rat lungs. *Toxicol Sci* 73, 448-56.
- (73) Olsson, B., Bondesson, E., *et al.* (2011), Pulmonary Drug Metabolism, Clearance, and Absorption, in *Advances in Delivery Science and Technology*, pp 21-50, Controlled Release Society.
- (74) Knowles, M. R., and Boucher, R. C. (2002), Mucus clearance as a primary innate defense mechanism for mammalian airways. *J Clin Invest* 109, 571-7.
- (75) Gumbiner, B. M. (1993), Breaking through the tight junction barrier. *The Journal of cell biology* 123, 1631-1633.
- (76) Rubin, B. K. (2002), Physiology of airway mucus clearance. *Respiratory care* 47, 761-768.
- (77) Schuster, B. S., Suk, J. S., *et al.* (2013), Nanoparticle diffusion in respiratory mucus from humans without lung disease. *Biomaterials* 34, 3439-3446.
- (78) Steimer, A., Haltner, E., *et al.* (2005), Cell culture models of the respiratory tract relevant to pulmonary drug delivery. *Journal of aerosol medicine : the official journal of the International Society for Aerosols in Medicine* 18, 137-182.
- (79) Lai, S. K., Wang, Y. Y., *et al.* (2009), Mucus-penetrating nanoparticles for drug and gene delivery to mucosal tissues. *Adv Drug Deliv Rev* 61, 158-171.
- (80) Sigurdsson, H. H., Kirch, J., *et al.* (2013), Mucus as a barrier to lipophilic drugs. *Int J Pharm* 453, 56-64.
- (81) Lillehoj, E. P., Kato, K., *et al.* (2013), Cellular and molecular biology of airway mucins. *International review of cell and molecular biology* 303, 139-202.
- (82) Zhu, Y., Chidekel, A., *et al.* (2010), Cultured human airway epithelial cells (calu-3): a model of human respiratory function, structure, and inflammatory responses. *Critical care research and practice* 10, 1-8.
- (83) Kirch, J., Ruge, C. A., *et al.* (2012), Nanostructures for Overcoming the Pulmonary Barriers: Physiological Considerations and Mechanistic Issues, in *Nanostructured Biomaterials for Overcoming Biological Barriers*, pp 239-271, Royal Society of Chemistry.
- (84) Kirch, J., Schneider, A., *et al.* (2012), Optical tweezers reveal relationship between microstructure and nanoparticle penetration of pulmonary mucus. *Proceedings of the National Academy of Sciences of the United States of America* 109, 18355-18360.
- (85) Ludwig, A. (2005), The use of mucoadhesive polymers in ocular drug delivery. *Adv Drug Deliv Rev* 57, 1595-639.
- (86) Creuwels, L. A., van Golde, L. M., *et al.* (1997), The pulmonary surfactant system: biochemical and clinical aspects. *Lung* 175, 1-39.
- (87) Dobbs, L. G. (1990), Isolation and culture of alveolar type II cells. *The American journal of physiology* 258, 134-147.
- (88) Frank, J. A. (2012), Claudins and alveolar epithelial barrier function in the lung. *Annals of the New York Academy of Sciences* 1257, 175-183.
- (89) Patton, J. S., and Byron, P. R. (2007), Inhaling medicines: delivering drugs to the body through the lungs. *Nature reviews. Drug discovery* 6, 67-74.
- (90) Geiser, M., Rothen-Rutishauser, B., *et al.* (2005), Ultrafine particles cross cellular membranes by nonphagocytic mechanisms in lungs and in cultured cells. *Environmental health perspectives* 113, 1555-1560.
- (91) Herd, H., Daum, N., *et al.* (2013), Nanoparticle geometry and surface orientation influence mode of cellular uptake. *ACS nano* 7, 1961-1973.

- (92) Ruge, C. A., Kirch, J., *et al.* (2011), Uptake of nanoparticles by alveolar macrophages is triggered by surfactant protein A. *Nanomedicine : nanotechnology, biology, and medicine* 7, 690-693.
- (93) Ruge, C. A., Schaefer, U. F., *et al.* (2012), The interplay of lung surfactant proteins and lipids assimilates the macrophage clearance of nanoparticles. *PloS one* 7, e40775.
- (94) Patton, J. S., Brain, J. D., *et al.* (2010), The particle has landed--characterizing the fate of inhaled pharmaceuticals. *Journal of aerosol medicine and pulmonary drug delivery* 23 Suppl 2, S71-87.
- (95) Lai, S. K., O'Hanlon, D. E., *et al.* (2007), Rapid transport of large polymeric nanoparticles in fresh undiluted human mucus. *Proceedings of the National Academy of Sciences of the United States of America* 104, 1482-1487.
- (96) Mura, S., Hillaireau, H., *et al.* (2011), Biodegradable Nanoparticles Meet the Bronchial Airway Barrier: How Surface Properties Affect Their Interaction with Mucus and Epithelial Cells. *Biomacromolecules* 12, 4136-4143.
- (97) Nordgård, C. T., Nonstad, U., *et al.* (2014), Alterations in Mucus Barrier Function and Matrix Structure Induced by Gyluronate Oligomers. *Biomacromolecules* 15, 2294-2300.
- (98) Hasenberg, M., Stegemann-Koniszewski, S., *et al.* (2013), Cellular immune reactions in the lung. *Immunol Rev* 251, 189-214.
- (99) Todoroff, J., and Vanbever, R. (2011), Fate of nanomedicines in the lungs. *Current Opinion in Colloid & Interface Science* 16, 246-254.
- (100) Brand, P., Schulte, M., *et al.* (2009), Lung deposition of inhaled alpha1-proteinase inhibitor in cystic fibrosis and alpha1-antitrypsin deficiency. *The European respiratory journal* 34, 354-360.
- (101) Heyder, J. (2004), Deposition of inhaled particles in the human respiratory tract and consequences for regional targeting in respiratory drug delivery. *Am Thorac Soc* 1, 315-320.
- (102) Ely, L., Roa, W., *et al.* (2007), Effervescent dry powder for respiratory drug delivery. *European Journal of Pharmaceutics and Biopharmaceutics* 65, 346-353.
- (103) Tsapis, N., Bennett, D., *et al.* (2002), Trojan particles: large porous carriers of nanoparticles for drug delivery. *Proceedings of the National Academy of Sciences of the United States of America* 99, 12001-5.
- (104) Pillai, O., and Panchagnula, R. (2001), Polymers in drug delivery. *Current Opinion in Chemical Biology* 5, 447-451.
- (105) Kumari, A., Yadav, S. K., *et al.* (2010), Biodegradable polymeric nanoparticles based drug delivery systems. *Colloids and Surfaces B: Biointerfaces* 75, 1-18.
- (106) Houchin, M. L., and Topp, E. M. (2008), Chemical degradation of peptides and proteins in PLGA: A review of reactions and mechanisms. *Journal of Pharmaceutical Sciences* 97, 2395-2404.
- (107) Germershaus, O., Lühmann, T., *et al.* (2015), Application of natural and semi-synthetic polymers for the delivery of sensitive drugs. *International Materials Reviews* 60, 101-131.
- (108) Dang, J., and Leong, K. (2006), Natural polymers for gene delivery and tissue engineering. *Advanced Drug Delivery Reviews* 58, 487-499.
- (109) Pereswtoff-Morath, L., and Edman, P. (1995), Dextran microspheres as a potential nasal drug delivery system for insulin - in vitro and in vivo properties. *International Journal of Pharmaceutics* 124, 37-44.
- (110) Chiu, H.-C., Hsiue, G.-H., *et al.* (1999), Synthesis and characterization of pH-sensitive dextran hydrogels as a potential colon-specific drug delivery system. *Journal of Biomaterials Science, Polymer Edition* 10, 591-608.
- (111) Hovgaard, L., and Bronsted, H. (1995), Dextran hydrogels for colon-specific drug delivery. *Journal of Controlled Release* 36, 159-166.
- (112) Rajaonarivony M., Vauthier C., *et al.* (1993), Development of a new drug carrier made from alginate. *Journal of Pharmaceutical Sciences* 82, 912-917.
- (113) Calvo, P., Remunan-Lopez, C., *et al.* (1997), Novel hydrophilic chitosan-polyethylene oxide nanoparticles as protein carriers. *Journal of Applied Polymer Science* 63, 125-132.

- (114) Grenha, A., Grainger, C. I., *et al.* (2007), Chitosan nanoparticles are compatible with respiratory epithelial cells in vitro. *European Journal of Pharmaceutical Sciences* 31, 73-84.
- (115) Coppi, G., Iannuccelli, V., *et al.* (2001), Chitosan-alginate microparticles as a protein carrier. *Drug Development and Industrial Pharmacy* 27, 393-400.
- (116) James, K. A., Fresneau, M. P., *et al.* (2001), Chitosan nanoparticles as delivery systems for doxorubicin. *Journal of Controlled Release* 73, 255-267.
- (117) Günbeyaz, M., Faraji, A., *et al.* (2010), Chitosan based delivery systems for mucosal immunization against bovine herpesvirus 1 (BHV-1). *European Journal of Pharmaceutical Sciences* 41, 531-545.
- (118) Ingram, J. T., and Lowenthal, W. (1966), Mechanism of Action of Starch as a Tablet Disintegrant I - Factors that Affect the Swelling of Starch Grains at 37°. *Journal of Pharmaceutical Sciences* 55, 614-617.
- (119) Patel, N. R., and Hopponen, R. E. (1966), Mechanism of Action of Starch as a Disintegrating Agent in Aspirin Tablets. *Journal of Pharmaceutical Sciences* 55, 1065-1068.
- (120) Kitamori, N., and Makino, T. (1982), Improvement in Pressure-Dependent Dissolution of Trepibutone Tablets by Using Intragranular Disintegrants. *Drug Development and Industrial Pharmacy* 8, 125-139.
- (121) Kottke, M. K., Chueh, H. R., *et al.* (1992), Comparison of Disintegrant and Binder Activity of Three Corn Starch Products. *Drug Development and Industrial Pharmacy* 18, 2207-2223.
- (122) Callens, C., Ceulemans, J., *et al.* (2003), Rheological study on mucoadhesivity of some nasal powder formulations. *European Journal of Pharmaceutics and Biopharmaceutics* 55, 323-328.
- (123) Clausen, A. E., and Bernkop-Schnürch, A. (2001), Direct compressible polymethacrylic acid-starch compositions for site-specific drug delivery. *Journal of Controlled Release* 75, 93-102.
- (124) Palviainen, P., Heinämäki, J., *et al.* (2001), Corn Starches as Film Formers in Aqueous-Based Film Coating. *Pharmaceutical Development and Technology* 6, 353-361.
- (125) (1974), Toxicological evaluation of certain food additives with a review of general principles and of specifications. Seventeenth report of the joint FAO-WHO Expert Committee on Food Additives. *World Health Organ Tech Rep Ser.* 539, 1-40.
- (126) Santander-Ortega, M. J., Stauner, T., *et al.* (2010), Nanoparticles made from novel starch derivatives for transdermal drug delivery. *Journal of Controlled Release* 141, 85-92.
- (127) Thiele, C., Auerbach, D., *et al.* (2011), Nanoparticles of anionic starch and cationic cyclodextrin derivatives for the targeted delivery of drugs. *Polym. Chem.* 2, 209-215.
- (128) Yamada, H., Loretz, B., *et al.* (2014), Design of Starch-graft-PEI Polymers: An Effective and Biodegradable Gene Delivery Platform. *Biomacromolecules* 15, 1753-1761.
- (129) Kunishima, M., Kitao, A., *et al.* (2002), A Racemization Test in Peptide Synthesis Using 4-(4,6-Dimethoxy-1,3,5-triazin-2-yl)-4-methylmorpholinium Chloride (DMT-MM). *Chem. Pharm. Bull.* 50, 549-550.
- (130) Blumenkrantz, N., and Asboe-Hansen, G. (1973), New Method for Quantitative Determination of Uronic Acids. *Analytical Biochemistry* 54, 484-489.
- (131) Bragd, P. L., Besemer, A. C., *et al.* (2000), Bromide-free TEMPO-mediated oxidation of primary alcohol groups in starch and methyl α -D-glucopyranoside. *Carbohydrate Research* 328, 355-363.
- (132) Thiele, C. (2010), Synthese von Cyclodextrin- und Stärkederivaten zum verbesserten Wirkstofftransport. *Organic Macromolecular Chemistry PhD*, Saarland University, 219.
- (133) Shiroza, T., Furihata, K., *et al.* (1982), The Structures of Diethylaminoethylated Glucose and Oligosaccharides Derived from Cationic Starch. *Agric. Biol. Chem.* 46, 1425-1427.
- (134) Paschall, E. F. (1959), Starch ethers containing nitrogen and process for making the same. *US2876217 A*.
- (135) Carlyle, G. C., and Wurzburg, O. B. (1957), Ungelatinized tertiary amino alkyl ethers of amylaceous materials. *US2813093 A*.

- (136) Sheehan, J. C., and Hess, G. P. (1955), A New Method of Forming Peptide Bonds. *Journal of American Chemical Society* 77, 1067-1068.
- (137) König, W., and Geiger, R. (1970), Eine neue Methode zur Synthese von Peptiden: Aktivierung der Carboxygruppe mit Dicyclohexylcarbodiimid unter Zusatz von 1-Hydroxy-benzotriazolen. *Chem. Ber.* 103, 788-789.
- (138) Kato, Y., Matsuo, R., *et al.* (2003), Oxidation process of water-soluble starch in TEMPO-mediated system. *Carbohydrate Polymers* 51, 69-75.
- (139) Le Corre, D., Bras, J., *et al.* (2010), Starch Nanoparticles: A Review. *Biomacromolecules* 11, 1139-1153.
- (140) Duncan, R. (2006), Polymer conjugates as anticancer nanomedicines. *Nature Reviews Cancer* 6, 688-701.
- (141) Desai, M. P., Labhasetwar, V., *et al.* (1996), Gastrointestinal Uptake of Biodegradable Microparticles: Effect of Particle Size. *Pharmaceutical Research* 13, 1838-1845.
- (142) Mijatovic, D., Eijkel, J. C. T., *et al.* (2005), Technologies for nanofluidic systems: top-down vs. bottom-up—a review. *Lab on a Chip* 5, 492.
- (143) Verma, S., Gokhale, R., *et al.* (2009), A comparative study of top-down and bottom-up approaches for the preparation of micro/nanosuspensions. *International Journal of Pharmaceutics* 380, 216-222.
- (144) Parrot, E. L. (1990), Encyclopedia of Pharmaceutical Technology, Marcel Dekker Inc.
- (145) Li, X., Anton, N., *et al.* (2010), Nanoparticles by spray drying using innovative new technology: The Büchi Nano Spray Dryer B-90. *Journal of Controlled Release* 147, 304-310.
- (146) Byrappa, K., Ohara, S., *et al.* (2008), Nanoparticles synthesis using supercritical fluid technology – towards biomedical applications. *Advanced Drug Delivery Reviews* 60, 299-327.
- (147) Hornig, S., Heinze, T., *et al.* (2009), Synthetic polymeric nanoparticles by nanoprecipitation. *Journal of Materials Chemistry* 19, 3838.
- (148) Govender, T., Stolnik, S., *et al.* (1999), PLGA nanoparticles prepared by nanoprecipitation: drug loading and release studies of a water soluble drug. *Journal of Controlled Release* 57, 171-185.
- (149) Nafee, N., Taetz, S., *et al.* (2007), Chitosan-coated PLGA nanoparticles for DNA/RNA delivery: effect of the formulation parameters on complexation and transfection of antisense oligonucleotides. *Nanomedicine: Nanotechnology, Biology and Medicine* 3, 173-183.
- (150) Cu, Y., LeMoëllic, C., *et al.* (2010), Ligand-modified gene carriers increased uptake in target cells but reduced DNA release and transfection efficiency. *Nanomedicine: Nanotechnology, Biology and Medicine* 6, 334-343.
- (151) Ravi Kumar, M. N. V., Bakowsky, U., *et al.* (2004), Preparation and characterization of cationic PLGA nanospheres as DNA carriers. *Biomaterials* 25, 1771-1777.
- (152) Calvo, P., Remunan-Lopez, C., *et al.* (1997), Chitosan and chitosan ethylene oxide propylene oxide block copolymer nanoparticles as novel carriers for proteins and vaccines. *Pharmaceutical Research* 14, 1431-1436.
- (153) Steel, R., Cowan, J., *et al.* (2012), Anti-inflammatory Effect of a Cell-Penetrating Peptide Targeting the Nrf2/Keap1 Interaction. *ACS Medicinal Chemistry Letters* 3, 407-410.
- (154) Monaghan, R. L., and Eveleigh, D. E. (1973), Chitosanase, a Novel Enzyme. *Nature New Biology* 245, 78-80.
- (155) Fenton, D. M., and Eveleigh, D. E. (1981), Purification and Mode of Action of a Chitosanase from *Penicillium islandicum*. *Journal of General Microbiology* 126, 151-165.
- (156) Sun, Y., Zhang, J., *et al.* (2013), Preparation of d-glucosamine by hydrolysis of chitosan with chitosanase and β -d-glucosaminidase. *International Journal of Biological Macromolecules* 61, 160-163.
- (157) GE Healthcare Bio-Sciences AB. (2014). *Cross flow filtration Method Handbook*.

- (158) Jiang, J., Oberdörster, G., *et al.* (2008), Characterization of size, surface charge, and agglomeration state of nanoparticle dispersions for toxicological studies. *Journal of Nanoparticle Research* 11, 77-89.
- (159) Zakowski, J. J., and Bruns, D. E. (1985), Biochemistry of human alpha amylase isoenzymes. *Crit Rev Clin Lab Sci* 21, 283-322.
- (160) Benedetti, G., Rastelli, F., *et al.* (2004), Challenging Problems in Malignancy. Case 1: Presentation of Small-Cell Lung Cancer With Marked Hyperamylasemia. *Journal of Clinical Oncology* 22, 3826-3828.
- (161) Selman, M. (2006), Role of Epithelial Cells in Idiopathic Pulmonary Fibrosis: From Innocent Targets to Serial Killers. *Proceedings of the American Thoracic Society* 3, 364-372.
- (162) Sakai, N., and Tager, A. M. (2013), Fibrosis of two: Epithelial cell-fibroblast interactions in pulmonary fibrosis. *Biochimica et Biophysica Acta (BBA) - Molecular Basis of Disease* 1832, 911-921.
- (163) Zoz, D. F., Lawson, W. E., *et al.* (2011), Idiopathic Pulmonary Fibrosis: A Disorder of Epithelial Cell Dysfunction. *The American Journal of the Medical Sciences* 341, 435-438.
- (164) Camelo, A., Dunmore, R., *et al.* (2014), The epithelium in idiopathic pulmonary fibrosis: breaking the barrier. *Frontiers in Pharmacology* 4, 1-11.
- (165) Sung, J. C., Pulliam, B. L., *et al.* (2007), Nanoparticles for drug delivery to the lungs. *Trends in Biotechnology* 25, 563-570.
- (166) Rytting, E., Nguyen, J., *et al.* (2008), Biodegradable polymeric nanocarriers for pulmonary drug delivery. *Expert opinion on drug delivery* 5, 629-639.
- (167) Schulz, H. (1998), Mechanisms and factors affecting intrapulmonary particle deposition: implications for efficient inhalation therapies. *PSTT* 1, 336-344.
- (168) Bosquillon, C., Lombry, C., *et al.* (2001), Influence of formulation excipients and physical characteristics of inhalation dry powders on their aerosolization performance. *Journal of Controlled Release* 70, 329-339.
- (169) Lippmann, M., and Albert, R. E. (1969), The effect of particle size on the regional deposition of inhaled aerosols in the human respiratory tract. *Am Ind Hyg Assoc J* 30, 257-275.
- (170) Snipes, M. B. (1994), Biokinetics of inhaled radionuclides, in *Internal Radiation Dosimetry*, pp 181-204, Health Physics Society.
- (171) Arakawa, T., Prestrelski, S. J., *et al.* (2001), Factors affecting short-term and long-term stabilities of proteins. *Advanced Drug Delivery Reviews* 46, 307-326.
- (172) Prime, D., Atkins, P. J., *et al.* (1997), Review of dry powder inhalers. *Advanced Drug Delivery Reviews* 26, 51-58.
- (173) Timsina, M. P., Martin, G. P., *et al.* (1994), Drug delivery to the respiratory tract using dry powder inhalers. *International Journal of Pharmaceutics* 101, 1-13.
- (174) Mackin, L. A., Rowley, G., *et al.* (1997), An Investigation of Carrier Particle Type, Electrostatic Charge and Relative Humidity on In-vitro Drug Deposition from Dry Powder Inhaler Formulations. *Pharmaceutical Sciences* 3, 583-586.
- (175) Kim, J.-C. K. J.-D. (2015), Preparation by Spray Drying of Amphotericin B-Phospholipid Composite Particles and Their Anticellular Activity. *Drug Delivery* 8, 143-147.
- (176) Maa, Y.-F., Zhao, L., *et al.* (2003), Stabilization of alum-adjuvanted vaccine dry powder formulations: Mechanism and application. *Journal of Pharmaceutical Sciences* 92, 319-332.
- (177) Millqvist-Fureby, A., Malmsten, M., *et al.* (1999), Spray-drying of trypsin - surface characterisation and activity preservation. *International Journal of Pharmaceutics* 188, 243-253.
- (178) Yang, L., Luo, J., *et al.* (2013), Development of a pulmonary peptide delivery system using porous nanoparticle-aggregate particles for systemic application. *International Journal of Pharmaceutics* 451, 104-111.

- (179) Ungaro, F., Giovino, C., *et al.* (2010), Engineering gas-foamed large porous particles for efficient local delivery of macromolecules to the lung. *European Journal of Pharmaceutical Sciences* 41, 60-70.
- (180) Sham, J. O. H., Zhang, Y., *et al.* (2004), Formulation and characterization of spray-dried powders containing nanoparticles for aerosol delivery to the lung. *International Journal of Pharmaceutics* 269, 457-467.
- (181) Grenha, A., Seijo, B., *et al.* (2007), Chitosan nanoparticle loaded mannitol microspheres - structure and surface characterization. *Biomacromolecules* 8, 2072-2079.
- (182) Massa, W. (2004), Crystal Structure Determination, Springer Verlag.
- (183) Hein, S., Bur, M., *et al.* (2010), The pharmaceutical aerosol deposition device on cell cultures (PADD OCC) in vitro system - design and experimental protocol. *ATLA* 38, 285-295.
- (184) Hein, S., Bur, M., *et al.* (2011), A new Pharmaceutical Aerosol Deposition Device on Cell Cultures (PADD OCC) to evaluate pulmonary drug absorption for metered dose dry powder formulations. *European Journal of Pharmaceutics and Biopharmaceutics* 77, 132-138.
- (185) Sletmoen, M., Maurstad, G., *et al.* (2012), Oligoguluronate induced competitive displacement of mucin-alginate interactions: relevance for mucolytic function. *Soft Matter* 8, 8413.
- (186) Chaubal, M. V., and Popescu, C. (2008), Conversion of Nanosuspensions into Dry Powders by Spray Drying: A Case Study. *Pharmaceutical Research* 25, 2302-2308.
- (187) Desai, M. P., Labhasetwar, V., *et al.* (1997), The Mechanism of Uptake of Biodegradable Microparticles in Caco-2 Cells Is Size Dependent. *Pharmaceutical Research* 14, 1568-1573.
- (188) Iskandar, F., Gradon, L., *et al.* (2003), Control of the morphology of nanostructured particles prepared by the spray drying of a nanoparticle sol. *Journal of Colloid and Interface Science* 265, 296-303.
- (189) Vehring, R. (2007), Pharmaceutical Particle Engineering via Spray Drying. *Pharmaceutical Research* 25, 999-1022.
- (190) Hulse, W. L., Forbes, R. T., *et al.* (2009), The characterization and comparison of spray-dried mannitol samples. *Drug Development and Industrial Pharmacy* 35, 712-718.
- (191) Hulse, W. L., Forbes, R. T., *et al.* (2009), Influence of protein on mannitol polymorphic form produced during co-spray drying. *International Journal of Pharmaceutics* 382, 67-72.
- (192) Finlay, W. H. (2001), The Mechanics of Inhaled Pharmaceutical Aerosols: An Introduction, Academic Press.
- (193) Rahimpour, Y., and Hamishehkar, H. (2012), Lactose Engineering for Better Performance in Dry Powder Inhalers. *Advanced Pharmaceutical Bulletin* 2, 183-187.
- (194) Zeng, X. M., Martin, G. P., *et al.* (2001), Lactose as a Carrier in Dry Powder Formulations: The Influence of Surface Characteristics on Drug Delivery. *Journal of Pharmaceutical Sciences* 90, 1424-1434.
- (195) Steckel, H., and Bolzen, N. (2004), Alternative sugars as potential carriers for dry powder inhalations. *International Journal of Pharmaceutics* 270, 297-306.
- (196) Larhrib, H., Martin, G. P., *et al.* (2003), The influence of carrier and drug morphology on drug delivery from dry powder formulations. *International Journal of Pharmaceutics* 257, 283-296.
- (197) Steckel, H., and Müller, B. W. (1997), In vitro evaluation of dry powder inhalers II: influence of carrier particle size and concentration on in vitro deposition. *International Journal of Pharmaceutics* 154, 31-37.
- (198) Forbes, B., and Ehrhardt, C. (2005), Human respiratory epithelial cell culture for drug delivery applications. *European Journal of Pharmaceutics and Biopharmaceutics* 60, 193-205.
- (199) Hermanns, M. I., Unger, R. E., *et al.* (2004), Lung epithelial cell lines in coculture with human pulmonary microvascular endothelial cells: development of an alveolo-capillary barrier in vitro. *Laboratory Investigation* 84, 736-752.

- (200) Casale, T. B., and Carolan, H. J. (1999), Cytokine-induced sequential migration of neutrophils through endothelium and epithelium. *Inflammation Research* 48, 22-27.
- (201) Rothen-Rutishauser, B. M., Kiama, S. G., *et al.* (2005), A Three-Dimensional Cellular Model of the Human Respiratory Tract to Study the Interaction with Particles. *American Journal of Respiratory Cell and Molecular Biology* 32, 281-289.
- (202) Blank, F., Wehrli, M., *et al.* (2011), Macrophages and dendritic cells express tight junction proteins and exchange particles in an in vitro model of the human airway wall. *Immunobiology* 216, 86-95.
- (203) Wottrich, R. (2003), Zur toxikologischen Untersuchung ultrafeiner Partikel: Entwicklung und Einsatz eines realitätsnahen in vitro Lungenmodells. *Institut für Toxikologie und Genetik*, Universität Karlsruhe.
- (204) <https://www.oecd.org/env/ehs/testing/TG%20413%20Revised%2016-OCT-2015.pdf>. *OECD GUIDELINE FOR THE TESTING OF CHEMICALS*. (last access: 30.03.16)
- (205) Zeng, X., de Groot, A. M., *et al.* (2015), Surface coating of siRNA-peptidomimetic nano-self-assemblies with anionic lipid bilayers: enhanced gene silencing and reduced adverse effects in vitro. *Nanoscale* 7, 19687-98.
- (206) Lutz, M. B., Kukutsch, N., *et al.* (1999), An advanced culture method for generating large quantities of highly pure dendritic cells from mouse bone marrow. *Journal of Immunological Methods* 223, 77-92.
- (207) Giard, D. J., Aaronson, S. A., *et al.* (1973), In vitro cultivation of human tumors: Establishment of cell lines derived from a series of solid tumors. *Journal of the National Cancer Institute* 51, 1417-1423.
- (208) Huang M., Khor E., *et al.* (2004), Uptake and Cytotoxicity of Chitosan Molecules and Nanoparticles: Effects of Molecular Weight and Degree of Deacetylation. *Pharmaceutical Research* 21, 344-352.
- (209) Huang, M., Khor, E., *et al.* (2004), Uptake and Cytotoxicity of Chitosan Molecules and Nanoparticles: Effects of Molecular Weight and Degree of Deacetylation. *Pharmaceutical Research* 21, 344-353.
- (210) Forbes, B., Shah, A., *et al.* (2003), The human bronchial epithelial cell line 16HBE14o- as a model system of the airways for studying drug transport. *International Journal of Pharmaceutics* 257, 161-167.
- (211) Ehrhardt, C., Kneuer, C., *et al.* (2002), Influence of apical fluid volume on the development of functional intercellular junctions in the human epithelial cell line 16HBE14o-: implications for the use of this cell line as an in vitro model for bronchial drug absorption studies. *Cell Tissue Res* 308, 391-400.

SCIENTIFIC OUTPUT

Publications

Sarah Barthold, Stephanie Kletting, Julian Taffner, Cristiane de Souza Carvalho-Wodarz, Elise Lepeltier, Brigitta Loretz and Claus-Michael Lehr; Preparation Of Nanosized Coacervates Of Positive And Negative Starch Derivatives Intended For Pulmonary Delivery Of Proteins, *J. Mater. Chem. B*, (2016), DOI:10.1039/c6tb00178e (*accepted*)

Sarah Barthold, Stephanie Kletting, Robert Haberkorn, Guido Kickelbick, Cristiane de Souza Carvalho-Wodarz, Elise Lepeltier, Brigitta Loretz and Claus-Michael Lehr; A carrier system for enhanced nanoparticle deposition in the deep lung – nanoparticles embedded in microparticles, *Pharm. Research* (*in preparation*)

ISAM Textbook of Aerosol Medicine

Publisher: International Society for Aerosols in Medicine

Editors: Barbara Rothen-Rutishauser and Rajiv Dhand

Chapter 8: Overview of inhaled nanopharmaceuticals

Sarah Barthold, Nicole Kunschke, Xabier Murgia, Brigitta Loretz, Cristiane de Souza Carvalho-Wodarz, Claus-Michael Lehr

ISBN: 978-1-4665-6786-3

Safety of Nanomaterials along their lifecycle – release, exposure & human hazards

Publisher: CRC Press Taylor & Francis Group NY

Editors: Wohlleben W., Kuhlbusch T.A.J., Schnekenburger J., Lehr C.-M.

Chapter 6: Lessons learnt from pharmaceutical nanomaterials

Emad Malaeksefat, **Sarah Barthold**, Brigitta Loretz, Claus-Michael Lehr

Presentations

02/2016: Scientific Meeting COMPACT
(Stevenage, England)

Poster presentation

Evaluating a Trojan Delivery System for its pulmonary applicability

- 07/2015: 42nd Meeting & Exposition of the Controlled Release Society
(Edinburgh, Scotland)
Poster presentation
Trojan starch-based nanoparticles for the deep lung delivery of IgG1
- 07/2015: 5th International HIPS Symposium
(Saarbrücken, Germany)
Poster presentation
Trojan polysaccharide-based nanoparticles for the deep lung delivery of proteins/peptides
- 02/2015: Scientific Meeting COMPACT
(Ludwigshafen, Germany)
Poster presentation
A Trojan Delivery System for pulmonary applications. Nanoparticles embedded into Microparticles
- 02/2015: CRS German Chapter Annual Meeting 2015
(Muttens, Switzerland)
Poster presentation
Spray drying of carbohydrate-based nanoparticles for pulmonary delivery
- 11/2014: 2. Doktorandentag der Naturwissenschaftlich-Technischen Fakultät III
(Saarbrücken, Germany)
Poster presentation
Chitosan nanoparticles for the deep lung delivery of Nr2
- 06/2014: 4th International HIPS Symposium
(Saarbrücken, Germany)
Poster presentation
COMPACT – a European Collaboration on the Optimization of Macromolecular Pharmaceutical Access to Cellular Targets
- 06/2014: F2F Meeting WP1 COMPACT
(Leiden, Netherlands)
Oral presentation
A nanotechnology enabled DDS for pulmonary protein/peptide delivery (update)

- 02/2014: Scientific Meeting COMPACT
(Stevenage, England)
Oral presentation
Chitosan nanoparticles as delivery system for Nrf2 to the lungs
Poster presentation
Chitosan nanoparticles for the deep lung delivery of Nrf2
- 11/2013: F2F Meeting WP1 COMPACT
(Copenhagen, Denmark)
Oral presentation
*A nanotechnology enabled DDS for pulmonary protein/peptide delivery
(update)*
- 04/2013: F2F Meeting WP6 COMPACT
(Saarbrücken, Germany)
Oral presentation
*Development of a nanotechnology enabled DDS for pulmonary protein/peptide
delivery*

CURRICULUM VITAE

Personal Information

Name	Sarah Sonja Barthold
Date / place of birth	04.12.86 in Marktredwitz
E-Mail	sarah.barthold@gmx.net
Nationality	German

Doctoral Thesis

10/2012 - 09/2015	Helmholtz Institute for Pharmaceutical Research Saarland; Institute for Biopharmacy and Pharmaceutical Technology, Saarland University, Saarbrücken
-------------------	---

Education & professional training

10/2012 – 03/2016	Professional training as <i>Fachapotheker for Pharm. Technology</i>
10/2012 - 09/2015	Doctoral thesis
09/2012	Certification as Pharmacist (Apotheker)
04/2011	2 nd section of the pharmaceutical examination
10/2006 - 04/2011	Pharmaceutical Studies, University of Regensburg
06/2006	Graduation at the Luisenburg - Gymnasium Wunsiedel (Abitur)
1997 - 2006	Luisenburg - Gymnasium Wunsiedel, Germany

Practical Experience

10/2015 – now	<u>Scientific assistant</u> Saarland University, Biopharmacy and Pharmaceutical Technology, Germany
10/2012 – 09/2015	<u>PhD student</u> Helmholtz Institute for Pharmaceutical Research Saarland, Germany
01/2013 - 12/2015	<u>Pharmacy emergency services</u> Glückauf Apotheke Saarbrücken, Germany

01/2012 - 06/2012	<u>Practical training for pharmacists</u> Hirsch Apotheke Konstanz, Germany
07/2011 - 12/2011	<u>Research Internship</u> Pharmaceutical Sciences, University of Otago, New Zealand <i>Dispersing amorphous drug particles into a carrier matrix – Effect of spatial separation and carrier properties on recrystallization behavior of amorphous indomethacin</i> Supervision: Prof. Dr. Rades
09/2009 - 02/2010	<u>Research internship</u> Drug Formulation & Delivery, ETH Zurich, Switzerland <i>Preparation of PLGA microspheres and microencapsulation of ovalbumin by spray drying using the Nano Spray Dryer B-90 and Mini Spray Dryer B-191</i> Supervision: Prof. Dr. Leroux, Prof. Dr. Gander
04/2009 - 08/2009	<u>Student Research Assistant</u> Pharmaceutical Biology, University of Regensburg, Germany <i>Fractionation and characterization of extracts from R. aculeatus</i> Supervision: Prof. Dr. Heilmann
02/2008 - 03/2008	<u>Internship: Quality Control</u> Streuli Pharma AG, Uznach, Switzerland
08/2007	<u>Practical training for pharmacists</u> Apotheke Sana-Klinikum Hof, Germany
02/2007 - 03/2007	<u>Practical training for pharmacists</u> Neue Apotheke, Wunsiedel, Germany

ACKNOWLEDGMENTS

Meine Danksagung möchte ich unüblicher Weise nicht mit dem Doktorvater beginnen – er möge es mir verzeihen – sondern mit meiner Familie. Ihr habt mein neugieriges Wesen durch eure Erziehung geprägt und euer Interesse an der Welt wurde ebenso zu meinem. Ihr habt mich gelehrt immer nach dem *warum* zu fragen. Darüber hinaus konnte ich immer auf eure uneingeschränkte Unterstützung und Zuneigung bauen. Liebe Oma, lieber Opa, ich kann euch leider keine Lasten abnehmen, aber ich möchte euch, als Zeichen meiner Hochachtung, meine Doktorarbeit widmen. Ich hab euch lieb!

Herrn Prof. Dr. Claus-Michael Lehr möchte ich – direkt an zweiter Stelle! - für die herausfordernde und interessante Themenstellung danken. Seine exquisiten und einmaligen Kommentare machen ihn zu einem außerordentlich herzlichen Chef!

Weiterer Dank gebührt Herrn Prof. Dr. Thorsten Lehr für die Übernahme des Zweitgutachtens. Des Weiteren möchte ich mich bei allen weiteren Mitgliedern der Prüfungskommission bedanken.

Frau Dr. Brigitta Loretz, der guten Seele des Hauses, gebührt besonderer Dank für Ihre immer offenstehende Tür und die hilfreichen Diskussionen - egal wie voll der Schreibtisch auch war/ist.

Dear Dr. Elise Lepeltier, thank you so much for everything: from discussing NMR spectra to “good job” comments in a moment of need!

Dem COMPACT (und hier v.a. WP1) Team möchte ich meinen Dank aussprechen für die gut strukturierte Zusammenarbeit und die im Gedächtnis bleibenden F2F Meetings. Besonders hervorheben möchte ich Herrn Dr. Stefan Bassarab, der als Leiter von WP1 neben der fachlichen Expertise zusätzlich immer für gute Stimmung sorgte.

I would also like to express my gratitude to Sarah Gordon for proof reading.

Zusätzlich möchte ich meinen Dank gegenüber den Technikern aussprechen, dem Rückgrat des Instituts. Von Petra König, über Dr. Chiara De Rossi, hin zu Jana Westhues, Peter Meiers oder Marijas Jurisic. Egal welches (manchmal noch so dumme) Problem man hatte, es gab immer jemanden, der einem gerne! weiterhalf.

Julian Taffner, Charlotte Steinmetz und Greta Magnano danke ich für ihre experimentellen Arbeiten im Labor als studentische Hilfskräfte. Ich hoffe, ihr musstet nicht nur schuften, sondern konntet auch einiges lernen und hattet auch noch Spaß dabei. Ich wünsche euch auf eurem Weg alles Gute!

Natürlich möchte ich mich auch bei allen Mitdoktoranden und Kollegen (hier v.a. 0.17 für die Lach- oder Heulflashes) bedanken, die für ein unglaublich positives Arbeitsklima gesorgt haben. Die ausufernden Gespräche/Situationen in manch harter Zeit waren echt klasse und die Zusammenarbeit mit euch hat mich sehr viel Spaß gemacht.

Auch Chrisso möchte ich an dieser Stelle erwähnen. Du bist (fast) vom allerersten Anfang an mit dabei gewesen und bist wie eine Schwester für mich. Ich bin froh, dass es dich gibt!

Manchmal begegnet man Menschen, die man so in der Situation gar nicht erwartet hätte: Erster Arbeitstag, total unerfahren und dann sitzt da ein ebenso verlorener Mensch gegenüber und man kommt ins Gespräch, fängt zusammen Mäuse, isst voller Bedauern viel zu viel Ofenkäse, geht in die Therme, arbeitet fächerübergreifend, betreut Studenten und hat einfach nur eine sau gute Zeit, obwohl es eigentlich miserabel läuft und man eigentlich nur weinen möchte. Dies tut man auch, aber meist dann doch eher vor Lachen. Danke Steffi!!!

Auch möchte ich mich bei dir Simon bedanken, für die abenteuerliche Zeit, die langweiligen Fernsehabende, deine Fähigkeit alles zu Reparieren was kaputt geht, und deine nicht-lustigen Sprüche. =) Danke für den Ausgleich zu dieser stressigen Doktorandenzeit!

Da steh ich nun ich armer Thor und bin – mehr oder minder - so klug als wie zuvor. Was bleibt ist das Kennenlernen von – damals – Menschen die zu – heute - Freunden wurden und die Weiterentwicklung der eigenen Persönlichkeit. Es sind die Menschen die uns zu dem machen was wir sind.